ADVANCED MATERIALS
www.advmat.de

Advanced Multifunctional Aqueous Rechargeable Batteries Design: From Materials and Devices to Systems

Lei Li, Qichong Zhang, Bing He, Rui Pan, Zhixun Wang, Mengxiao Chen, Zhe Wang, Kuibo Yin, Yagang Yao,* Lei Wei,* and Litao Sun**

Multifunctional aqueous rechargeable batteries (MARBs) are regarded as safe, cost-effective, and scalable electrochemical energy storage devices, which offer additional functionalities that conventional batteries cannot achieve, which ideally leads to unprecedented applications. Although MARBs are among the most exciting and rapidly growing topics in scientific research and industrial development nowadays, a systematic summary of the evolution and advances in the field of MARBs is still not available. Therefore, the review presented comprehensively and systematically summarizes the design principles and the recent advances of MARBs by categories of smart ARBs and integrated systems, together with an analysis of their device design and configuration, electrochemical performance, and diverse smart functions. The two most promising strategies to construct novel MARBs may be A) the introduction of functional materials into ARB components, and B) integration of ARBs with other functional devices. The ongoing challenges and future perspectives in this research and development field are outlined to foster the future development of MARBs. Finally, the most important upcoming research directions in this rapidly developing field are highlighted that may be most promising to lead to the commercialization of MARBs and to a further broadening of their range of applications.

1. Introduction

The increasing energy consumption and ever-growing environmental concerns of greenhouse gas emissions require safe, environmentally friendly, and cost-efficient energy storage technologies. Since renewable and green energy sources such as solar, wind, and tide are available only intermittently, batteries are an exceptionally promising technology to store electricity generated from such sources for later use at the peak consumption times in large scale networks.[1–4] Commercial lithium-ion batteries (LIBs) with high energy density, cycle stability, and energy efficiency have dominated the energy storage field, and they provide a great convenience for our modern lives.[5,6] However, their further applications are hindered by safety concerns involving the use of harmful organic electrolytes and by the high cost of the appropriate electrode materials.[7,8] Lately, abundant sodium and potassium resources in nature have attracted much attention because of their similar chemical properties to lithium, where sodium-ion batteries and potassium-ion batteries have, thus, become promising alternatives for LIBs.[9–12] Although the issue of high cost can be solved using such novel battery materials, the usage of conventional organic electrolytes that are toxic and flammable still affects the safety of battery operation. Therefore, in recent years, large research

L. Li, Q. C. Zhang, R. Pan, K. B. Yin, L. T. Sun
SEU-FEI Nano-Pico Center
Key Laboratory of MEMS of Ministry of Education
Southeast University
Nanjing 210096, China
E-mail: qczhang2016@sinano.ac.cn; slt@seu.edu.cn

Q. C. Zhang
Key Laboratory of Multifunctional Nanomaterials and Smart Systems
Suzhou Institute of Nano-Tech and Nano-Bionics
Chinese Academy of Sciences
Suzhou 215123, China

Q. C. Zhang
Division of Nanomaterials and Jiangxi Key Lab of Carbonene Materials
Suzhou Institute of Nano-Tech and Nano-Bionics
Nanchang
Chinese Academy of Sciences
Nanchang 330200, China

B. He, Z. X. Wang, M. X. Chen, Z. Wang, L. Wei
School of Electrical and Electronic Engineering
Nanyang Technological University
50 Nanyang Avenue, Singapore 639798, Singapore
E-mail: wei.lei@ntu.edu.sg

Y. G. Yao
National Laboratory of Solid State Microstructures
College of Engineering and Applied Sciences
and Collaborative Innovation Center of Advanced Microstructures
Nanjing University
Nanjing 210093, China
E-mail: ygyao2018@nju.edu.cn

The ORCID identification number(s) for the author(s) of this article can be found under https://doi.org/10.1002/adma.202104327.

DOI: 10.1002/adma.202104327

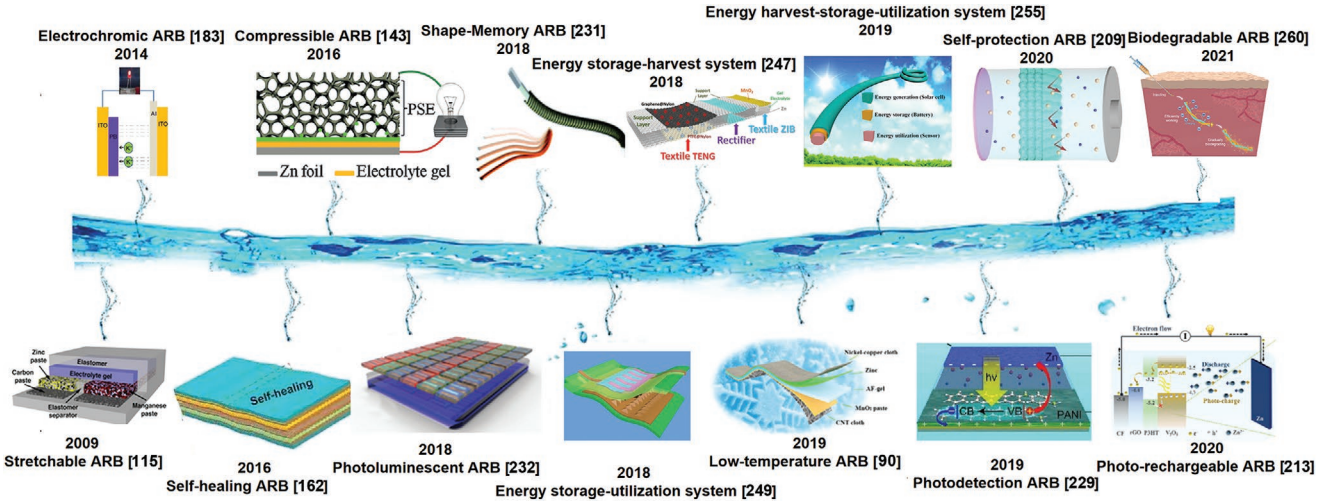

Figure 1. Brief development history of the smart ARBs and integrated systems for MARBs. From left to right: Reproduced with permission.[115] Copyright 2009, Wiley-VCH. Reproduced with permission.[183] Copyright 2014, the Authors, published by Springer Nature. Reproduced with permission.[162] Copyright 2016, Wiley-VCH. Reproduced with permission.[143] Copyright 2016, Wiley-VCH. Reproduced with permission.[232] Copyright 2018, Royal Society of Chemistry. Reproduced with permission.[231] Copyright 2018, Royal Society of Chemistry. Reproduced with permission.[249] Copyright 2018, Royal Society of Chemistry. Reproduced with permission.[247] Copyright 2018, Wiley-VCH. Reproduced with permission.[90] Copyright 2019, Royal Society of Chemistry. Reproduced with permission.[255] Copyright 2019, Elsevier. Reproduced with permission.[229] Copyright 2019, Wiley-VCH. Reproduced with permission.[209] Copyright 2020, Wiley-VCH. Reproduced with permission.[213] Copyright 2020, Royal Society of Chemistry. Reproduced with permission.[260] Copyright 2021, Royal Society of Chemistry.

and development efforts have been made to explore alternative concepts for the design of batteries with high safety of operation and low cost.

Compared with organic electrolytes, aqueous electrolytes offer low-cost, high safety, easy fabrication, and high ionic conductivity and have, thus, been a recent focus in both scientific research and industrial development.[13–16] Inspired by the attractive advantages of aqueous electrolytes, aqueous rechargeable batteries (ARBs) have been considered a promising candidate for large-scale energy storage devices. To date, massive efforts have been devoted to electrode materials, electrolyte, and energy storage mechanisms to achieve high-performance ARBs.[17–20] The main ARBs currently reported are based on quite different charge carriers such as non-metallic ions (e.g., H^+, NH_4^+),[16] monovalent metal ions (e.g., Li^+, Na^+, K^+),[21,22] and multivalent metal ions (e.g., Zn^{2+}, Ca^{2+}, Mg^{2+}, Al^{3+}),[23] where the latter have the advantage of one ion carrying two charges. It is worth noting that ARBs may be divided into four categories according to the energy storage mechanisms of the electroactive materials: Systems with i) conventional ion insertion, ii) dual ion co-insertion, iii) conversion reaction, and iv) coordination reaction.[24,25] As expected, a considerable number of ARBs with low cost, high safety, and outstanding electrochemical performance have been developed.[9–28]

As a result of the emergence of the Internet of Things and the rapid development in biomimetics and artificial intelligence, a new class of multifunctional energy-storage devices has emerged. Besides the continuous efforts to increase the energy-storage capability of ARBs, considerable efforts have been made to develop multifunctional ARBs (MARBs) to expand their applications to new fields that conventional ARBs cannot normally achieve.[29,30] MARBs bring together several diverse research fields, which leads to numerous unprecedented applications. The successful construction of novel high-performance MARBs depends mainly on three aspects. In particular, i) the progress in functional materials, ii) the structure design, and iii) the device integration.[31–34] The development of MARBs in recent years may be regarded an interdisciplinary effort driven by the materials chemistry, energy chemistry, and device chemistry scientific communities. To date, an extensive amount of studies have published concerning the development of MARBs, which have reported on massive advancements in this emerging interdisciplinary area of research. A comprehensive overview over the history of MARBs is illustrated in **Figure 1**. To understand the conceptual framework and to better guide future research in this area, we present a comprehensive review on the latest advances in research and development in the field of MARBs.

From a point of view that concerns the design principles, the latest advances and further challenges and opportunities of MARBs are outlined. First, the design principles of MARBs consisting of functional materials and integrated systems are presented. We focus on the functional material design of current collectors, electrode materials, electrolytes, separators, gel electrolytes, substrates, packaging materials, and novel integrated systems for both plane and fiber-shaped devices. Following, the latest advances and practical applications of MARBs are summarized, ranging from smart ARBs to integrated systems. Finally, based on the current developments, we provide an assessment of the major challenges and the prospective solutions in this field, offering guidance on the future development of this highly exciting research and technology field. Although the development of MARBs may be regarded to still be in its infancy, we expect that the rapid progress of integration techniques in materials science will pave new ways for their broad commercial applications in the near future.

2. Design Principles of MARBs

As the name implies, MARBs can be employed not only for energy storage but also for other simultaneous tasks such as energy harvesting and utilization, a concept that may well be applicable in some of the next generation electronic devices, as listed in the following: 1) Flexible or wearable electronic products may be at the forefront of the next generation of consumer electronics, so it is essential that they exhibit an energy storage system with additional mechanical properties such as stretchability, compressibility, self-healing, and shape-memory effects to maintain their excellent electrochemical performance after high-strength deformation.[35–37] 2) ARBs can selfterminate their working cycle in timely manner to avoid damage of the device or the occurrence of fire when the internal temperature of the battery exceeds the operating value under harsh working conditions, where such self-protection function may expand the range of applications of ARBs.[38] 3) Solar energy is a typical natural renewable energy source. It is expected that solar cells may increasingly be used for the versatile configuration of converting solar energy into electricity, where ARBs may help addressing the intermittent issue and improve utilization efficiency.[39] 4) Sensors and nanogenerators may be integrated into portable MARBs in a single device.[40,41] Accordingly, MARBs may be a better choice in terms of safety, convenience, and practicality, since they may lead to new functionalities without increasing the size of the energy storage section. The MARBs design principles reported previously in terms of the functional materials used, and in terms of the respective integrated devices are summarized in **Figure 2**. The conventional electrode materials and structures, electrolyte components, separator types, and device conformations cannot match the requirements of MARBs. To achieve better versatility, each MARB device component and device configuration need to be re-explored. The following sections systematically introduce these development processes.

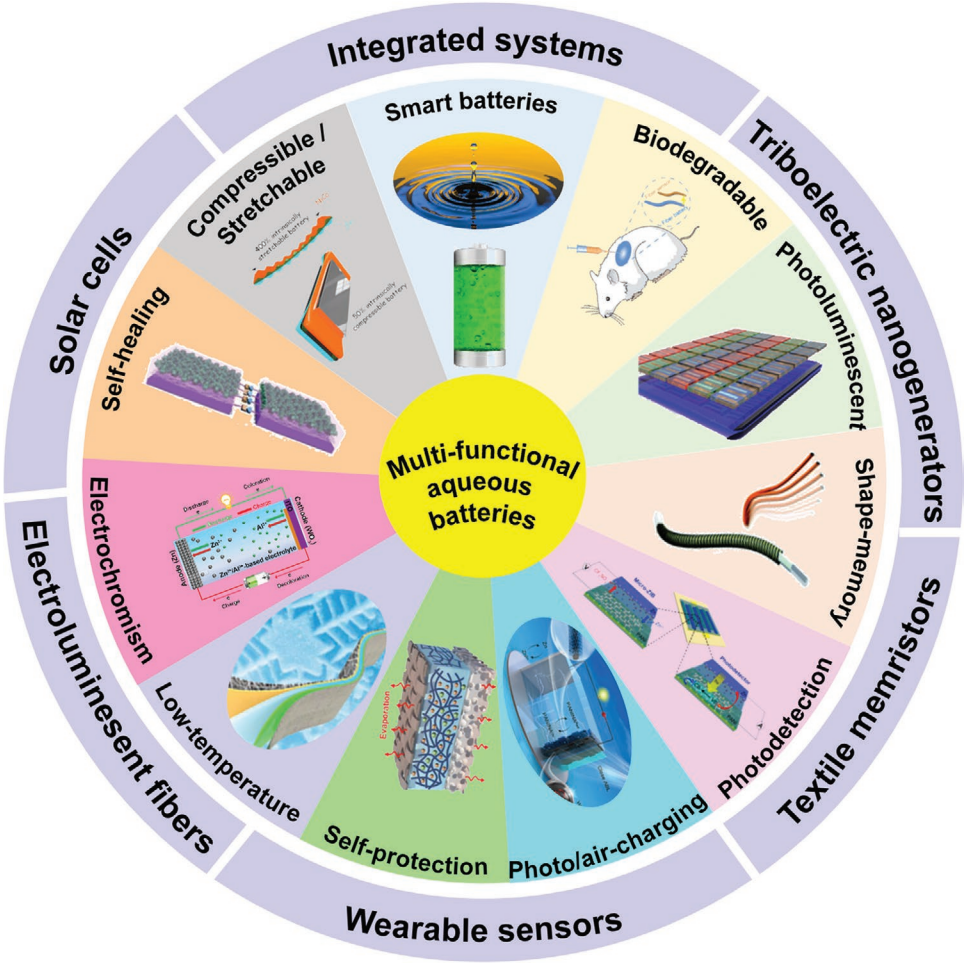

Figure 2. Design principles of MARBs. Counterclockwise, from compressible/stretchable to biodegradable: Reproduced with permission.[155] Copyright 2019, Elsevier. Reproduced with permission.[93] Copyright 2019, Wiley-VCH. Reproduced with permission.[181] Copyright 2019, Elsevier. Reproduced with permission.[90] Copyright 2019, Royal Society of Chemistry. Reproduced with permission.[210] Copyright 2020, Wiley-VCH. Reproduced with permission.[221] Copyright 2021, Wiley-VCH. Reproduced with permission.[229] Copyright 2019, Wiley-VCH. Reproduced with permission.[231] Copyright 2018, Royal Society of Chemistry. Reproduced with permission.[232] Copyright 2018, Royal Society of Chemistry. Reproduced with permission.[260] Copyright 2021, Royal Society of Chemistry.

2.1. Functional Battery Components

One of the most direct and effective strategies to employ functional materials is the process of preparing ARBs with additional functionalities beyond their energy storage capability. More specifically, different functionalities can be achieved by replacing the conventional materials in the corresponding components of the ARB with alternative functional materials. It should be noted that these functional materials may be divided into seven main categories, including: 1) active materials, 2) current collectors, 3) electrolytes, 4) separators, 5) gel electrolytes, 6) substrates, and 7) package materials, which can, respectively, realize the aforementioned ten kinds of smart characteristics for ARBs. This section systematically summarizes their concepts, mechanisms, the choice of material, and the performance or significance of using them as ARB components.

2.1.1. Active Materials

Active materials are one of the key components in rechargeable batteries and the essence of energy storage, because the occurrence of their reversible electrochemical reactions results in electronic transfer and ionic diffusion. Thus, they may immediately affect the specific capacity, working voltage, cycle stability, and rate capability of the battery. Two main examples of A) electrochromic and B) photoelectric responsive materials will be discussed, which both add functionalities to ARBs involving the substitution of the active materials by various dopants. This concept requires as a prerequisite to develop electrochromic and photoelectric responsive materials that can be integrated into ARBs to add the electrochromic or photoelectric responsive functionality.

A. Substances whose color changes when a voltage is applied are called electrochromic materials. This effect can be related to the reversible insertion/extraction of charges during the electrochemical reduction/oxidation of the material, which leads to the phenomenon of their color changing at different redox states.[42–44] At present, electrochromic materials that can be used as active materials in energy storage devices are roughly grouped into three categories. Inorganic oxides are considered to be the most typical electrochromic cathode/anode materials, commonly including WO_3,[45] V_2O_5,[46] TiO_2,[47] NiO,[48] and MnO_x.[49] Organic materials, based on polydiacetylene[50] and conducting polymers,[51] have also been found to provide electrochromic functionality. Among these examples, conducting polymers may be the most promising class of materials owing to their low cost, facile fabrication, and excellent electrochemical properties. It is worth noting that some metal coordination complexes such as Prussian blue[52] and viologen-based[53] complexes are also utilized in electrochromic devices as electrochemically active materials. The configuration of electrochromic ARBs is similar to that of the conventional sandwich-like ARBs, except that the conductive substrate needs to be transparent to visualize the color changes. The resulting ARBs can monitor their power in real-time by color changes and are able to beautify electronics (**Figure 3**a).[54]

B. Photoelectric responsive materials can convert light into detectable electrical signals. Their working mechanism is based on photonic activation of electrons from a lower energy level to a higher one due to the absorption of photons, thereby yielding electrical signals.[55] Such materials can exhibit both electrochemical activity and photoelectric response when employed as active materials in batteries. Up to now, most known materials such as metal oxides (Co_3O_4, Fe_2O_3), nitrides (C_3N_4) conducting polymers (PPy), graphene, and silicon-based semiconductors exhibit photoelectric response and have been used in photodetectors.[56–59] As shown in Figure 3b, a flexible fiber-shaped supercapacitor was assembled using Co_3O_4 as a cathode and graphene as an anode material.[60] As a result, the device exhibited both photoelectric response and charge storage functionality for potential applications in the fields of environmental monitoring and sensors.[61,62] Furthermore, certain photodetecting capacitors may harvest solar energy to directly charge themselves (Figure 3c), which would entail higher energy efficiency and easier preparation compared to indirect self-charging capacitors that need to have a separate energy harvesting system integrated.[63]

2.1.2. Current Collectors

Current collectors possess high electronic conductivity, large specific surface area, and superior stability in the operating voltage window. Therefore, they exhibit the necessary conditions to be used in ARBs, which may lead to outstanding energy storage capability. At present, commonly used current collector in ARBs mainly include stainless steel mesh,[64] carbon cloth,[65] polyester cloth,[66] and conductive paper.[67] However, such materials are inherently rigid and stiff, and compressible and stretchable ARBs cannot be obtained. Common squeezable current collectors for fabricating compressible energy storage devices mainly rely on four possible classes of materials (Figure 3d): 1) The use of carbon nano-sponges leads to good electrical conductivity but high mechanical strength, where applications are limited due to poor compressibility.[68] 2) Sponge-like woods can be carbonized in Ar to produce squeezable carbonated sponges featuring good compressibility, excellent conductivity, but also undesired mechanical strength.[69] 3) Sponges may be directly immersed in a carbon nanotube solution several times until saturated. Such sponges then possess excellent compressibility, strong mechanical strength, but unsatisfactory conductivity.[70] 4) Vertically aligned Ni or Ti nanowire arrays can be grown on Ni or Ti sheets through a modified magnetic-field-driven process, which creates a current collector with high conductivity and mechanical strength, acceptable compressibility, and heavy.[71] Given these considerations, by the selection of a suitable compressible current collector, it may become increasingly feasible to build ARBs with robust compressibility for withstanding various ambient pressures, but without sacrificing the excellent electrochemical performance.

Similarly, with respect to tensile properties, conventional current collectors cannot meet the requirements of deformation and stretching in ARBs, because they usually fail to reach strain values beyond 10%. Consequently, many strategies for preparing stretchable current collectors in ARBs have

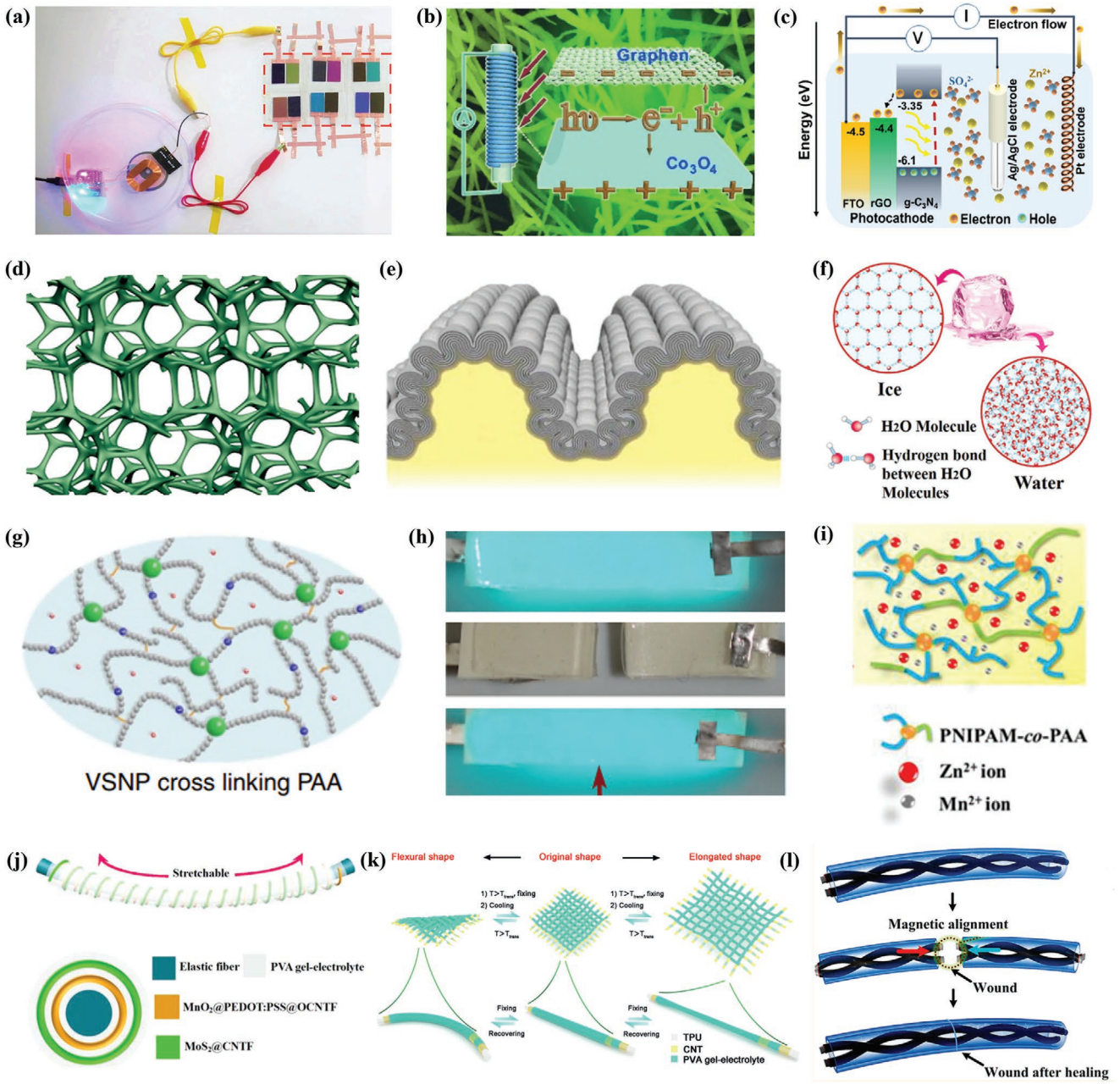

Figure 3. a) Wireless charging was used to charge full electrochromic supercapacitor devices. Reproduced with permission.[54] Copyright 2020, American Chemical Society. b) Current response of the photodetector powered by the flexible asymmetric fiber supercapacitor. Reproduced with permission.[60] Copyright 2014, Wiley-VCH. c) Schematic representation of a three-electrode experiment of g-C_3N_4@rGO/FTO electrodes. Reproduced with permission.[63] Copyright 2020, American Chemical Society. d) Schematic structure of the PANI-SWCNT-sponge. Reproduced with permission.[68] Copyright 2019, Royal Society of Chemistry. e) Illustration of the structure of a longitudinal section of an NTS_m sheath, showing 2D hierarchical buckling. Reproduced with permission.[73] Copyright 2015, American Association for the Advancement of Science. f) The crystal structures of water and ice with hydrogen bonds inside. Reproduced with permission.[88] Copyright 2021, Wiley-VCH. g) Preparation of the vinyl hybrid silica nanoparticles electrolyte. Reproduced with permission.[99] Copyright 2015, Springer Nature. h) Demonstration of cutting-healing process of the healable electrochromic device. Reproduced with permission.[100] Copyright 2018, the Authors, published by Springer Nature. i) Schematic of reversible sol–gel transition electrolyte. Reproduced with permission.[104] Copyright 2018, Elsevier. j) The structure of the stretchable fiber-shaped asymmetric supercapacitor (SFSC, up) and its cross-sectional structure (down). Reproduced with permission.[107] Copyright 2017, Elsevier. k) Schematic of the SFSC and the resulting textile that are reversibly transformed into flexural or elongated states and recovered to the original shape. Reproduced with permission.[114] Copyright 2015, Wiley-VCH. l) Schematic self-healing process of the supercapacitor by packaging materials. Reproduced with permission.[117] Copyright 2015, American Chemical Society.

been proposed in recent years to improve their overall stretchability.[72,73] So far, elastic current collectors usually have the following major conformations. The most representative stretchable collectors are based on wavy structures, which have been pioneered by Bowden and Whitesides and have been widely utilized in stretchable electrodes.[74] As sketched in Figure 3e, such periodic wavy structures are formed by attaching the active materials onto a pre-stretched elastic substrate and then release the applied tension.[75] In addition, rigid island materials can be interconnected to elastic linkers such as retractable metal chains, which construct island bridge structures with stretch capability.[76] Other efficient strategies such as 3D porous and helically coiled spring structures can also achieve good stretchability of the current collector.[77,78] Certainly, whichever aforementioned current collector is employed in ARBs, it can add tensile functionality to obtain stretchable ARB components.

2.1.3. Electrolytes

As a vital component of rechargeable batteries, the electrolyte also plays a significant role in their electrochemical performance. Usually, the electronically insulating electrolyte is made up of solvents and solutes, whose main function is to transfer ions between the cathode and anode when electrochemical reactions occur. The water, needless to say, is selected as the solvent to prepare an aqueous electrolyte for fabricating ARBs. As a main drawback, the water often freezes in cold environments, which usually results in lower ionic conductivity and insufficient wettability of the electrolytes, where the respective ARB encounters serious degradation of the electrochemical performance as a consequence. To deal with this problem, enormous research efforts have been made to optimize the composition of electrolytes, such that they would withstand operation without performance decline at subzero temperature.

To develop electrolytes for ARBs that can retain their electrochemical performance and can operate in frigid conditions, the following strategies may be most promising: 1) using a supersaturated aqueous electrolyte, and 2) introducing additives into the electrolyte. Such supersaturated electrolytes may be called "water-in-salt" electrolytes, as proposed by Wang et al.[79] Some common solutes such as LiCl, KOH, bis(trifluoromethane sulfonyl) imide (LiTFSI), and ($Zn(CF_3SO_3)_2$) have been applied in diverse aqueous batteries systems, achieving normal operation of the battery at cold conditions.[80–82] This was attributed to the following two factors: 1) The freezing point of a "water-in-salt" electrolyte can be significantly reduced due to the thermodynamics of mixed solutions, and 2) the formation of conductive solid-electrolyte interphases (SEI) decreases the charge transfer resistance.[83] Furthermore, useful additives including H_2SO_4, HBF_4, $Zn(BF_4)_2$, and acetonitrile, may be mixed into the electrolyte to effectively reduce the freezing point.[84–87] This reduction may well be caused by strong interactions between the additive molecules and the water, where the hydrogen bonds between the water molecules may break or weaken to inhibit freezing (Figure 3f).[88] Thus, the resultant electrolyte can maintain low interfacial charge transfer resistance and high ionic diffusivity even in subzero environments. It is worth noting that non-toxic and safe additives should be chosen in general, which is of great significance for the construction of ARBs with high operational safety that function correctly even at low temperature. Moreover, antifreezing hydrogel electrolytes can also contribute to batteries working at low temperatures, which will be discussed in more detail in the next section.

2.1.4. Gel Electrolytes

The most widely used electrolytes for constructing conventional ARBs are usually based on liquids. However, liquid electrolytes seem unsuitable to be used in multifunctionality smart ARBs. This is because the devices undergo deformations of bending, twisting, and stretching, which can easily lead to short-circuiting and leakage despite effective encapsulation. Accordingly, a sound strategy may be the use of gel electrolytes consisting of ionically conductive substance and gel polymer matrixes (e.g., poly(vinyl alcohol) [PVA], polyacrylamide [PAM], and poly(ethylene oxide) [PEO]), that have the potential to substitute liquid electrolytes in smart ARBs.[89,90] Gel electrolytes are generally good ionic conductors and electronic insulators. More interestingly, they exhibit properties that may be of great significance for other smart functionalities such as antifreezing, self-healing, and photoluminescence.[91–93] As stated above, a hydrogel with antifreezing properties can alleviate the deterioration of the battery performance at subzero temperature. Such hydrogels can be prepared by adding cryo-protectants with high evaporation enthalpies such as glycerol, sorbitol, and oil into the hydrogel, which is similar to the mechanisms of introducing cosolvents or additives to effectively inhibit water freezing.[94,95]

The energy storage devices may inevitably be damaged by accidental mechanical forces in the course of daily use. Self-healing polymers can heal and recover physical breaks in the materials. Inspiration of this extraordinary material functionality originates from the commonplace self-healing capacity of biological systems. Thereby, energy storage devices with self-healing functionality can be achieved by utilizing self-healing materials for the respective device components. These functional materials are separated into two categories, including intrinsically and extrinsically self-healing materials, according to whether external stimulation is needed to complete the self-recovery.[96–98] Intrinsically self-healing materials are based on the mechanism of molecular non-covalent and covalent cross-linking, and have already been applied in energy storage devices. A typical strategy for realizing the intrinsic self-healing ability of devices is adopted by the use of gel electrolytes with self-healing ability. To date, most self-healing gel electrolyte are based on polyacrylic acid (PAA, Figure 3g), PAM, and their derivatives, where the polymer matrices can be prepared by diverse methods to add self-healing functionality to energy storage devices.[99] In addition to the self-healing capability, a phosphor self-healable PAA hydrogel modified by polyurethane has been demonstrated to exhibit luminescence, which even further increases the ARB functionalities, as shown in Figure 3h.[100] When such hydrogels are employed in ARBs, the resulting luminescent smart ARBs may hold tremendous potential to be integrated into self-powered colorful display screens.

2.1.5. Separators

Commonly, porous and non-conductive polymeric membranes are selected as separators, located between the positive and negative electrodes, to prevent short circuits and provide ionic channels. They mainly play a protective role, in particular they assure the thermal safety of the battery. Due to the occurrence of generated heat from the increase of the external temperature or the accumulation of internal reaction heat, the battery may damage or even explode. Therefore, fast and reversible thermally responsive materials may be incorporated into separators, which can address the calamitous issue of thermal runway, leading to ARBs with self-protective functionality. The thermal response mechanism is based on phase-transitions, which can be encountered in materials like poly-peptides, poly(*N*-isopropyl acrylamide), poly(phosphazene)s, and polyethers.[101–103] Additionally, separators containing the appropriate thermally responsive materials may quickly close or reopen holes along with increasing or decreasing temperature, to reversibly interrupt ionic transfer pathways. It should be noticed that gel electrolytes can not only act as a medium for ionic transport to promote electrochemical reactions, but also serve as a separator at the same time to avoid short circuits. Therefore, gel electrolytes composed of thermally responsive materials may be applied to improve the thermal safety of ARBs working at high temperature, as shown in Figure 3i.[104] To conclude, it is of avail to construct smart separators and electrolytes that can respond to changes in temperature, which would enable the development of ARBs with self-protective functionality to expand their range of applications to higher temperature.

2.1.6. Substrates

Although ARB substrates are not directly involved in the electrochemical performance, they have also attracted growing research interest due to the possibility to add additional functionalities to ARBs, such as the ability to stretch or shape memory effects. In contrast to the current collectors, stretchable substrates can be electrically insulating. Currently, there are three major types of stretchable substrates based on papers, fibers, and polymers. Non-conductive paper has been explored as substrate material owing to the low cost and easy customization. For example, techniques like origami and kirigami can provide high linear and areal deformability of paper that have inspired designing foldable stretchable paper-based substrates.[105,106] Elastic fibers offer properties like lightweight, good mechanical strength, and stretchability, and they are, therefore, widely adopted for stretchable energy storage devices. As depicted in Figure 3j, fiber-based substrates are first pre-stretched, followed by twisting them into a yarn-shaped electrode and wrapping them with gel electrolyte, and finally releasing it to the relaxed state to form a stretchable fiber-shaped energy storage device.[107] As for the polymer-based substrates, poly-dimethylsiloxane (PDMS) may be regarded the most promising candidate due to its excellent elasticity, transparency, mechanical strength, and chemical stability. Thus, the resulting devices would be stretchable when the conductive active materials are coated onto the surface of the PDMS substrate.[108]

In addition to stretchability, another interesting smart property for energy storage devices is the shape memory effect, which can also be realized via the substrates. In general, shape-memory materials can be classified into two categories: alloys and polymers.[109] Alloys as shape memory substrates are mainly based on Cu-, Fe-, NiTi-, and intermetallic compounds.[110] Among them, by considering the virtue of superior mechanical and electrical properties, NiTi-based compounds are the most popular alloy material to achieve shape memory effects. The mechanism of shape memory for alloy materials relies on the reversible martensitic transformation by the actuation of external stimuli such as heat, pressure, or magnetic field.[111] For polymeric materials, the shape memory effect is mainly derived from the cooperation of elastic segments and transition segments responding to various external stimuli.[112] At present, the reported polymer-based shape-memory materials include polyurethane (PU), trans-isopolyprene, polynorbornene, and styrene-butadiene copolymers.[113] Owing to their lightweight, they are more suitable for portable and wearable electronics in comparison with the alloy-based shape-memory materials. As shown in Figure 3k, supercapacitors can be assembled by sequentially coating PU fibers with thin layers of CNTs, PVA gel electrolyte, CNTs, and PVA gel electrolyte, leading to a device with excellent shape memory capability that can recover the original shape even after flexural or elongated deformation.[114]

2.1.7. Packaging Materials

Encapsulation procedures are indispensable for the protection and integrity of assembled energy storage devices. They can act as a barrier to prevent the evaporation of the water in ARGs in form of moisture, and to resist the entry of external moisture and air. Therefore, the packaging maybe regarded as an effective way to reduce external and internal changes to the electrochemical performance of the device. Some polymers are commonly applied as packaging materials such as PMDS, ecoflex, PU, PET, and silicone rubber.[78–38] By the selection of polymers with smart properties to encapsulate the devices, additional functionalities can be obtained. For instance, both PMDS and ecoflex as packaging materials enable the device to hold stretchable functionality to some extent.[116] In addition, the aforementioned PU material not only exhibits the shape memory effect, but also forms a protective shell when it is used as a packaging material, and has the capability of self-healing (Figure 3l).[117] In the future design of MARBs, the use polymers that possess multiple smart properties as packaging materials may have massive potential to achieve multi-functional energy storage devices. It should be noted at this point that the use of diverse functional materials for fabricating MARBs have their own merits and flaws. The selection of various functional materials is not independent, but the synergies and compatibility of each battery component have to be considered. Furthermore, it is necessary to evaluate the trade-off between the electrochemical performance and the added smart characteristics for the development of optimal MARBs.

2.2. Integrated Systems

Apart from the strategies described above that focus on the introduction of functional materials, another straightforward and effective method is the integration of ARBs with other devices to bring more functional characteristics to the ARB. It is therefore indicated to investigate the most cutting-edge technologies to achieve integration and assembly of such systems. The most frequently reported devices by far to be integrated into ARBs are energy harvesting devices with the prospect of achieving intelligent and immediate storage of harvested energy in a single device. Among this type of integrated devices, two types of configurations have been successfully employed, that are plane-shaped and fiber-shaped configurations.[118–120] In the following section, the design principles for these integrated systems will be discussed in detail.

2.2.1. Plane Integrated System

The most common plane-shaped configurations of energy storage devices adopt the sandwich-like structure owing to the low cost and simple fabrication procedures. This typical configuration can readily integrate with other devices to assemble single-unit and multifunctional sandwich structures. In the literature, plenty of coverage can be found that is devoted to such configurations of integrated devices. It is important to point out though that integrated devices using ARBs are still rare and in their infancy to date. Therefore, it may be useful and helpful for future developments to refer to a similar but already more mature research and development field like the assembly of supercapacitor (SC)-based integrated devices. By learning from this more advanced research field, the design of the equivalent ARBs-based integrated systems may well benefit, especially since the architectures of these two types of energy storage devices are similar.[121–122]

Generally, for plane-shaped configurations, various components are stacked layer by layer to form the plane sandwich-like integrated device, featuring ultrathin thickness and good flexibility. For example, two SWCNT films with energy storage or photodetector functions were separated by a printing paper, obtaining a foldable all-solid-state paper-like bifunctional integrated device (**Figure 4**a).[123] In addition to the integration of only one functional device into an energy storage device, it has been demonstrated that it is also possible to integrate two devices. For example, two kinds of sensing elements have been integrated on both sides of a supercapacitor to develop a highly integrated supercapacitor-sensor (HISS) system that provides a strain sensor, power supply, and photodetector functions, as shown in Figure 4b.[124] Enlightened by this, synchronized integration of two different mechanisms (e.g., solar cell and sensor) into ARBs for an all-in-one device will be desirable and advantageous. Another strategy for designing sandwich-like integrated devices is to integrate or better to say to share a part of the energy storage devices with another functional device. For example, one electrode of an ARB or SC may act as the counter electrode of a solar cell.[125] An example is the incorporation of piezo-nanogenerators into SC, assembling an integrated device with supercapacitor and piezoelectric-driven self-charging functionality (Figure 4c).[126] This example may well guide future research on the integration of more functional devices into energy storage components. It should be noted that these sandwich-like integrated devices may need to be sealed by the use of PDMS or PET packaging materials to prevent each component from separating.[39,127] As for plane-shaped configurations, the design of micro-integrated structures is also regarded a promising assembly method. This is mainly attributed to the merit of a short ion diffusion distance in electrolytes, which would then suffer less from strain during deformation. Such a device may have application in easy-to-use wearable or miniaturized electronics.[128–130] Usually, interdigitated energy storage systems are employed for fabricating micro-integrated configurations to further reduce the size and weight of the whole device, which is also conducive to improve their energy density. In addition, compared with other architectures, the interdigitated design can be more readily integrated with other miniaturized functional devices onto a chip, while being more compatible with other components in the resultant micro integrated devices. For example, Figure 4d depicts an electrochemically active interdigitated on-chip SC with integrated thin-film transistors (TFTs) and rectifiers to fabricate a micro-integrated monolith rectifier–storage unit.[131] Similarly, an all-flexible self-powered micro integrated system, which consists of a tandem Si-solar cell, a lithium-ion micro-battery, and an MXene hydrogel pressure sensor (Figure 4e), has been built by using the combination of plasma-enhanced chemical vapor deposition and screen-printing processes.[132] Moreover, such micro-integrated configurations can be sculpted into stylish patterns, which gives them an eye-catching design, which may be especially attractive in wearable electronics.

2.2.2. Fiber-Shaped Integrated System

Compared with the conventional plane-shaped configurations, the fiber-shaped configurations represent superiority in terms of their higher flexibility, omni-directional deformability, and outstanding stretchability, displaying tremendous potential for the manufacturing of large-scale wearable electronics.[133–136] Accordingly, integrated devices based on fiber-shaped configurations have been widely explored in terms of three main configurations, which are twisted, coaxial, and all-in-one configurations. The twisted configuration is easily fabricated by twisting two fiber devices with different functionalities. So far, this configuration of fiber-shaped integrated devices may be the most popular because their unique structure is similar to that of fabric filaments and can thus be woven into electronic textiles readily. As shown in Figure 4f, a twisted fiber-shaped integrated device may be assembled by twisting a fiber-shaped SC and photodetector together with PVA gel.[137] Although coaxial configurations are more complicated to fabricate as compared to twisted configurations, they could offer a more stable architecture against multiple mechanical deformations. Coaxial fiber-shaped integrated devices are generally obtained by the layer-by-layer assembly of two or more fiber-shaped energy modules with different functionalities. Figure 4g illustrates a good example of this configuration with a core–shell structure,

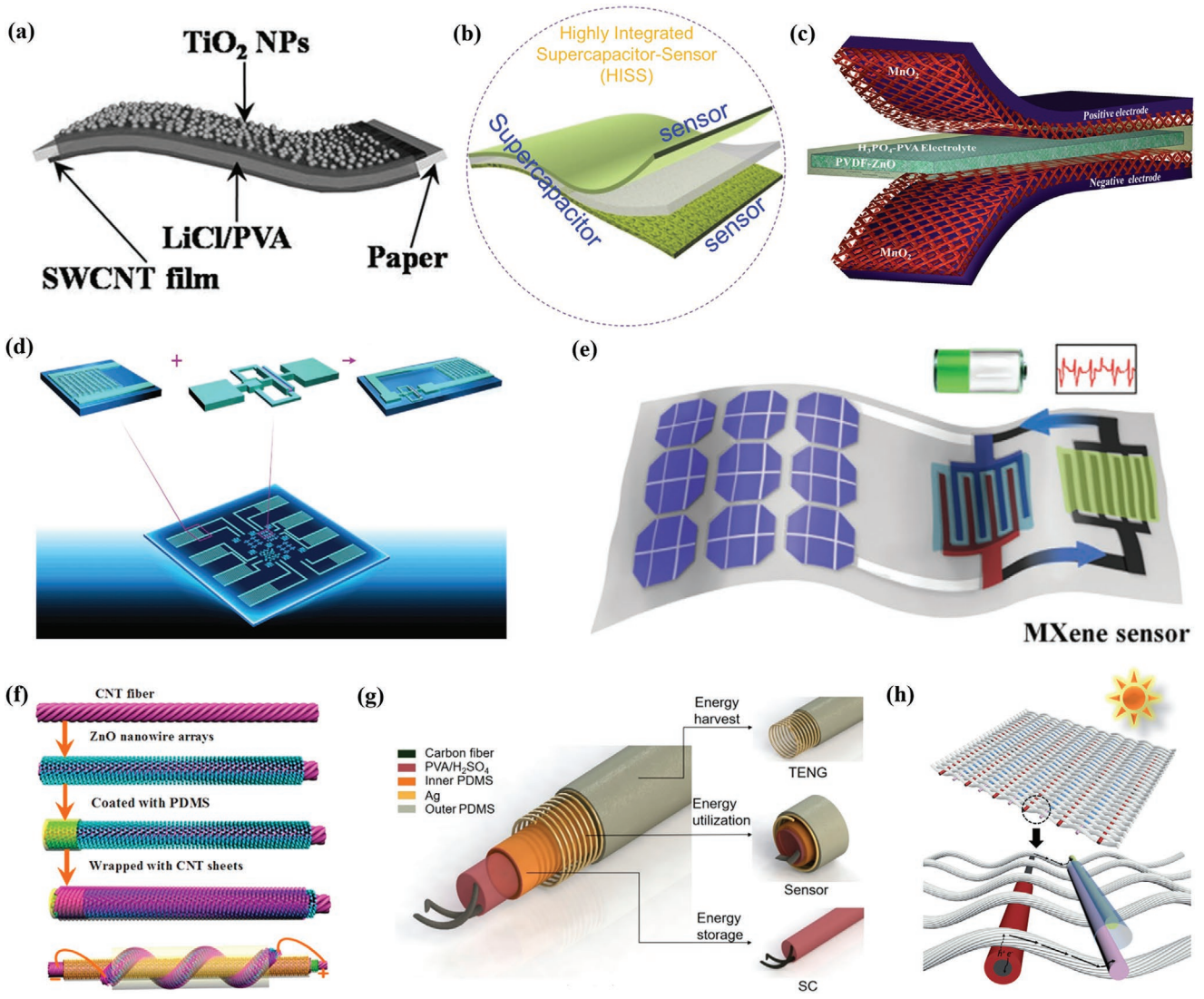

Figure 4. a) Schematic structure of the supercapacitor-photodetector integrated system. Reproduced with permission.[123] Copyright 2017, Wiley-VCH. b) Structural illustration of photodetection-supercapacitor-strain sensing integrated system. Reproduced with permission.[124] Copyright 2016, Wiley-VCH. c) Schematic diagram of the fabricated self-charging supercapacitor with PVDF-ZnO film as a separator and piezoelectric. Reproduced with permission.[125] Copyright 2015, American Chemical Society. d) Schematic diagram of the rigid microsupercapacitors–thin film rectifier circuits integrated system. Reproduced with permission.[131] Copyright 2018, Wiley-VCH. e) Schematic illustration of the flexible microbatteries-sensor integrated system. Reproduced with permission.[132] Copyright 2021, Wiley-VCH. f) Synthesis scheme of the twisted-fiber supercapacitor-UV photodetector integrated system. Reproduced with permission.[137] Copyright 2017, American Chemical Society. g) Schematic structure diagrams of the coaxial-fiber triboelectric nanogenerator-supercapacitor-pressure sensor integrated system. Reproduced with permission.[138] Copyright 2021, American Chemical Society. h) Schematic illustration of the flexible self-powered textile by weaving photoactive and electrochemically active fibers. Reproduced with permission.[139] Copyright 2021, Royal Society of Chemistry.

sharing the same axis for all the modules.[138] As stated above, owing to the excellent knitting and weaving properties, fiber-shaped devices with diverse functionalities can be simultaneously woven into all-in-one integrated electronic fabrics or textiles. Recently, using an industrial loom technology, a flexible self-charging integrated electronic textile has been manufactured by bridging energy harvesting fibers and energy-storing fibers (Figure 4h).[139] Such electronic textiles possess the characteristics of flexibility, and they are breathable and light weight. Such properties not only open an avenue for the development of fiber-shaped integrated devices, but also provide a preliminary exploration pathway for future portable and wearable electronics.

3. Recent Advances in Smart ARBs

The development of an ideal power source is a key challenge to the realization of multifunctional electronic devices. As one of the most potential power storage and supply systems, conventional ARBs with rigid and single-functionality are unlikely to satisfy the manifold requirements of the next-generation

electronic products. Accordingly, it is particularly urgent to explore novel batteries with outstanding energy storage capability and simultaneous multifunctionality. To incorporate additional functions into ARBs, two main effective strategies may be adopted, which are the integration of functional materials into ARBs or the integration of ARBs with other functional devices. For the former strategy, the additional functionalities acquired from specific functional materials can be divided into ten main themes, including 1) compressible/stretchable functions, 2) shape-memory effects, 3) self-healing, 4) self-protection, 5) low-temperature resistance and antifreezing, 6) photodetection, 7) electrochromic activity, 8) photo/air-charging, 9) photoluminescence, and 10) biodegradable properties. A functional material exhibiting any of these functionalities can be integrated into the respective component of the ARB to obtain smart ARBs. In the following section, these functions are systematically reviewed to demonstrate the recent progress in the development of versatile smart ARBs.

3.1. Compressible/Stretchable ARBs

The rapid development of wearable and other smart electronic products has put forward extra requirements on energy storage components with strong mechanical endurance against shape deformation apart from providing power output. Inspired by the recent successful fabrication of flexible LIBs and SCs,[140–142] ARBs as another promising energy storage technology have great potential to accommodate deformations such as compressing and stretching. The electrode and electrolyte materials with squeezing and stretching tolerance are generally considered to be the key factors in achieving compressible ARBs that can withstand large mechanical stresses. Some studies have demonstrated that various types of highly compressible ARBs can be manufactured without sacrificing the electrochemical performance by employing carbon-based sponges, foams, and aerogels as substrates, and hydrogels as electrolytes. Such recent research efforts focusing on different approaches to make battery materials stretchable, may be classified into five categories, including: 1) depositing the active materials onto a stretchable substrate, 2) bridging rigid components through elastic interconnections, 3) wrapping the active materials onto an elastic fiber-shaped substrate, 4) forming spring-like structure, and 5) utilizing intrinsically stretchable electrolyte materials.

Qu et al.[143] reported the construction of a tactile sensing Zn-air battery (TSZAB) that consists of a graphene-coated pressure-sensitive sponge (PSE) cathode, a KOH-based hydrogel electrolyte, and a Zn foil as an anode. The graphene-coated PSE was fabricated by di-coating a conductive graphene sheet solution onto the backbones of a commercial polyurethane sponge, as displayed in **Figure 5**a. Up to a compression of about 80%, the TSZAB still exhibited highly reversible compressibility (Figure 5b), which may be ascribed to the spongy structure of the electrode in a sandwich-like configuration. The PSE plays the role of both a power controller and an air cathode in the TSZABs. As illustrated in Figure 5d, the contact area between the electrode and the electrolyte may be changed with variable pressure loading, which would affect the reaction sites and concentration of oxygen, so that the power output of the TSZAB would be self-controlled. This ability of the TSZAB has been demonstrated by illuminating them with LED lamps (Figure 5c). Additionally, the TSZAB offered impressive electrochemical performance including the desired areal capacity of 1.25 mAh cm^{-2}, a stable discharge voltage of 1.3 V, and an energy density of up to 1200 Wh L^{-1}. However, physical electrode preparation methods (e.g., drop-casting, slurry-coating, and dip-coating) for the fabrication of ZABs may result in a weak bond between the catalyst and the spongy substrates, making them prone to detachment under severe deformation conditions. To address this limitation, an effective and scalable electrodeposition method was employed by Wang et al.[37] to build an air-cathode by directly attaching Fe-doped Co_3O_4 nanowires onto spongy nitrogen-doped carbon foams. This configuration shows a high open circuit potential of 1.51 V and a specific capacity of 867.2 mAh g^{-1}. More importantly, even under a compressive strain of 40%, the ZAB can still light up a red LED and effectively self-drive water-splitting. To expand the application of sponge-like electrodes in ARBs, the concept was further applied to zinc-ion batteries (ZIBs). It was shown that the ZIBs displayed high compressibility without degradation of the electrochemical performance exhibiting specific capacity retention rates of up to 98.4% after 1500 cycles, even at a compressive strain of 60%. It has been further reported that spongy electrodes with a unique 3D porous structure can strengthen the compression tolerance and facilitate electron and ion transfer, features that are likely to contribute to the stability of the electrochemical performance.[144] As an alternative, 3D printing technologies are a facile approach to obtain 3D substrates with a coplanar layout.[145] Such 3D printing technologies offer promising potential for the manufacturing processes because of their inherent advantages such as simple, controllable, and scalable operation. As a proof-of-concept, the 3D-printed rGO/CNTs@$Ni(OH)_2$ cathode and rGO/CNTs@α-Fe_2O_3 anode of a quasi-solid-state Ni-Fe battery (QSS-NFB) were fabricated by Yang's group via layer-by-layer stacking using a 3D printing method, as illustrated in Figure 5e.[146] Evidently, the mass of 3D-printed rGO/CNT micro-lattices is lightweight, and their thickness can be well controlled by adjusting the printing layers, which may be favorable for the manufacture and practical application of portable batteries (Figures 5f,g). Moreover, the SEM image clearly demonstrated that their configurations were interconnected by open-pore framework structures (Figures 5h,i). It is also encouraging that QSS-NFB, that was 3D-printed onto a PVA/KOH gel electrolyte, provided well-maintained electrochemical performance even under the condition of high strength compression. Specifically, at a compression rate of up to 60%, the capacity retention was 84.5% after 500 cycles at each different strain. The capacity retention could then be restored to 89.1% after 500 cycles, when the compression was removed and the device returned to the original state, as shown in Figure 5j. Furthermore, layer-by-layer self-assembly can also be used for the construction of 3D compressible and elastic substrates. Nevertheless, the compressibility of the aforementioned ARBs is usually derived from the electrode substrates, rather than the electrolyte. Apparently, the conventional liquid electrolytes have no elastic characteristics. It is usually required to combine them with a polymer matrix to form a gel electrolyte. Hydrogels are desired electrolyte materials for elastic Zn-based batteries.

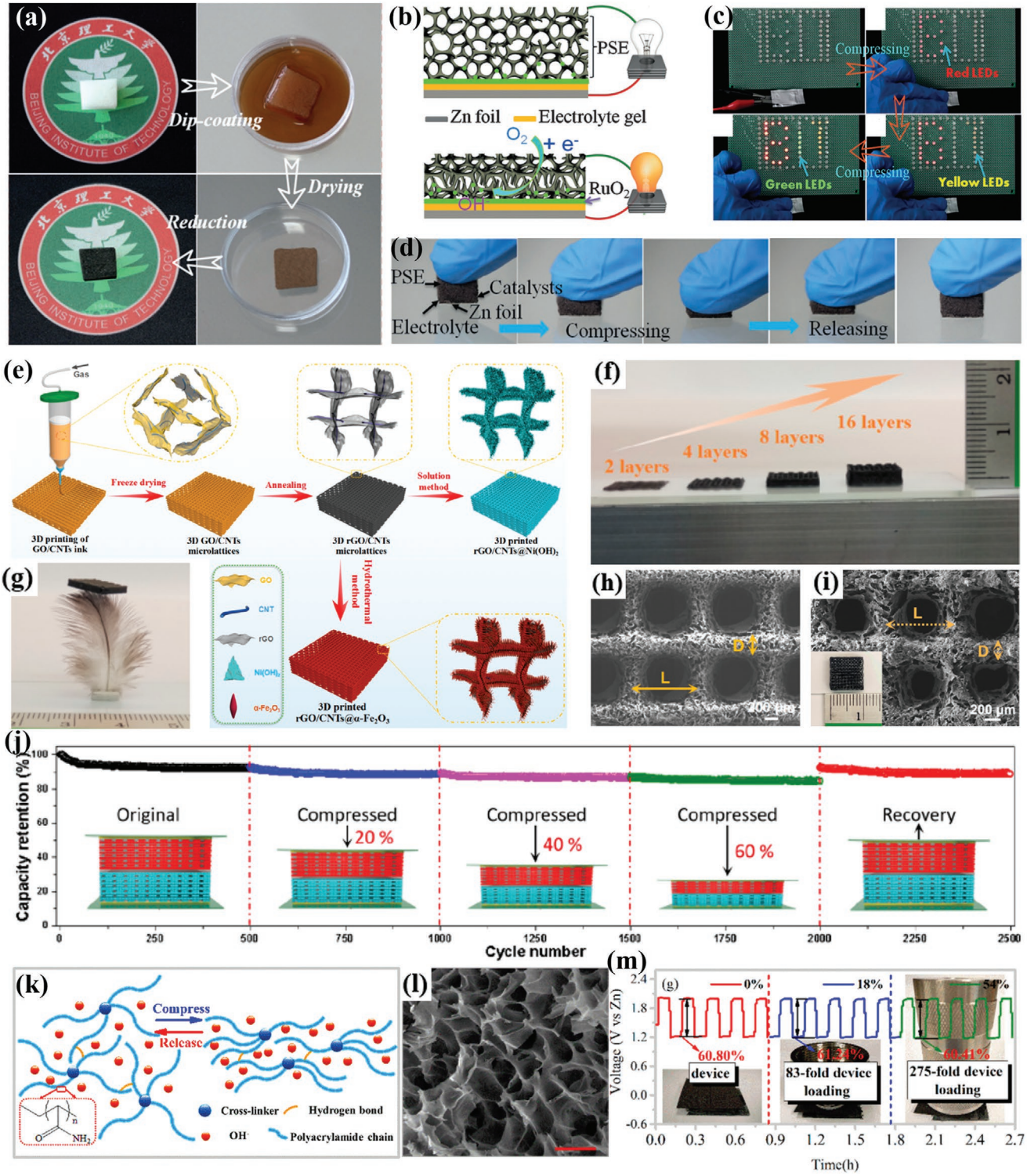

Figure 5. a) Fabrication procedure of the PSE. b) Schematic illustration showing the structure and working principle of TSB. c) Red, yellow, and green LEDs illuminated by TSBs with increase of applied pressure. d) Photos of the structure and the compression-recovery process for TSB. Reproduced with permission.[143] Copyright 2016, Wiley-VCH. e) Schematic fabrication process of 3D-printed cathode and anode. f) Photos of 3D-printed rGO/CNT microlattices samples. g) Photo showing a 3D-printed rGO/CNT sample can be rested on a light feather. h,i) SEM images of the 3D-printed rGO/CNT and rGO/CNTs@$Ni(OH)_2$ microlattices. j) Cycling performance of 3D-printed Ni–Fe battery at 200 mA cm^{-2}. Reproduced with permission.[146] Copyright 2020, American Chemical Society. k) High compressibility illustration of the PAM hydrogel electrolyte. l) SEM image of the freeze-dried PAM hydrogel. m) Discharge polarization curves of zinc–air battery. Reproduced with permission.[147] Copyright 2018, American Chemical Society.

Zhi et al.[147] applied compressible polyacrylamide (PAM) as a polymer matrix to build a compressible hydrogel electrolyte for rechargeable ZABs. The mechanism behind the compressibility of hydrogels is described in Figure 5k. The cross-linkers in the PAM structure can effectively prevent the formation and extension of cracks, thus enhancing the mechanical strength of the electrolyte even under largely compressive strain. It can be clearly seen from the SEM image in Figure 5l that the PAM has large pores, which is beneficial for the diffusion of ions. Accordingly, the assembled ZAB exhibited stable charge-discharge capacity even when compressed to a strain of 54% (Figure 5m) and bending to an angle of 90°. By similar procedures, an intrinsically compressible chargeable Zn-MnO_2 battery was assembled using a PAM electrolyte, MnO_2@graphite paper as a cathode, and Zn@graphite paper as an anode, where a high compressive strain of 77.8% and good battery performance was achieved.[40]

Furthermore, Park and co-workers fabricated a bioinspired Jabuticaba-like hybrid carbon/polymer (HCP) composite with better electronic conductivity than composites, where single fillers were injected into a stretchable ecoflex substrate.[148] The HCP has been shown to be capable of withstanding 1000 stretching and releasing cycles at a tension of 200%. As depicted in **Figure 6**a, a stretchable aqueous rechargeable lithium-ion battery (ARLB) was manufactured using a $LiMnO_4$@CNT cathode, a polyimide@AC anode, 1 M of Li_2SO_4 aqueous electrolytes, and the strucuture was sealed using ecoflex as a packaging material to extend the tensile life-span owing to the fact that each component would be more compact. However, it is worth noting that the configuration of this battery is an all-in-one layout, which is different from that of the sandwich-type layout. The ARLBs exhibited extremely stable electrochemical properties under tensile conditions, which is mainly manifested in a capacity retention of 80% even under 100% strain, and the capacity restored to the initial level when the tension was reduced to 0% (Figure 6b). To verify its practical application under tensile conditions, a red LED can be successfully illuminated by the fully charged ARLB even at a strain of up to ≈100% (Figure 6c). Significantly, the ARLBs presented good electrochemical and mechanical properties, indicating that the use of a stretchable ecoflex substrate as a packaging material is promising for the construction of stretchable ARLBs. Apart from ecoflex, other elastomers such as polydimethylsiloxane (PDMS) are also promising candidates for use as an elastic substrate. For example, Lee's[149] group embedded Ag nanowires (AgNW) into an elastic PDMS substrate by employing a lithographic filtration method to build AgNW/PDMS as a cathode and elastic substrate for silver-zinc (Zn-Ag) batteries that could be stretched to up to 80%. Similar to the 3D printing of compressible ARBs, stretchable ARBs can also be made using printing technologies. Recently, Wang et al.[150] introduced polystyrene-*block*-polyisoprene-*block* polystyrene as a hyperelastic binder (≈1300% strain), which was mixed with the active materials to form an electrode ink, and a conductive substrate was employed. The electrode ink was then screen printed onto the surface of stretchable thermoplastic polyurethane (TPU) textile to fabricate all-printed stretchable zinc-silver oxide (Zn-Ag_2O) ARBs (Figure 6d). The Zn-Ag_2O batteries possessed optimized electrochemical performance and strong mechanical endurance, which may be associated with the highly elastic SIS that can prohibit delamination between the conductive substrate and the active materials when the batteries are stretched. Interestingly, the areal capacity of the stretched battery (3.94 mAh cm^{-2}) was higher than that in the pristine state (3.78 mAh cm^{-2}), which can be explained by the expansion of the active surface area from the cracks formed during the tensile process (Figure 6e). Additionally, in both pristine states and after elongating to 100% repeatedly ten times, the batteries exhibited stability of up to 30 cycles at a current density of 3 mA cm^{-2} (Figure 6f). In addition to planar stretchable ARBs, 1D fiber-shaped stretchable batteries including ZABs,[151] ZIBs,[152] Zn-Ag batteries,[153] and aluminum-air batteries[154] can also be successfully fabricated. As illustrated in Figure 6g, Arias et al.[155] designed a wire-shaped Zn-Ag battery based on an inherently stretchable helical band spring as the conductive substrate. Then, a zinc electrode, a PVA electrolyte, a sacrificial barrier film, and a silver electrode were successively electro-deposited or wrapped onto the surface of the helical band spring, yielding wire-shaped stretchable Ag-Zn batteries. A high capacity of 1.2 mAh cm^{-1} and repeated bending for up to 1700 cycles where encountered with a bending radius of 0.5 cm, but also with an undesirable degree of stretching. Thus, Ag-Zn wire batteries with serpentine ribbon geometry were constructed to further control the degree and direction of the elongation. Moreover, such serpentine-like batteries were packaged into stretchable elastomers to obtain adequate space and warrant uniform deformations when the batteries were stretched. Indeed, the as-fabricated serpentine-like batteries could be stretched to up to 100% (Figure 6h). Even after 500 stretch cycles at the same strain, it still yielded stable capacity as high as 3.5 mAh cm^{-2} (Figure 6i). Based on the above results, the serpentine-like unique design is considered as an effective strategy, although its 100% stretching is still far away from being sufficient for practical applications of stretchable fiber-shaped ARBs as the power source for wearable electronics. Therefore, Zhi et al. further expanded the stretching degree of fiber-shaped ARBs, where a double-helix yarn was applied as a conductive substrate to fabricate high-performance yarn ZIBs, which would be elastic, waterproof, and tailorable.[154] More specifically, the cathode of this elastic ZIBs was prepared by roll-dip-coating of conventional MnO_2 onto the surface of pristine carbon nanotube (CNT) yarn, while the Zn electro-plating method was adopted to fabricate the anode via roll-electrodeposition of zinc onto the surface of the pristine CNT yarn. The yarn cathode and anode were wrapped by PAM-based gel that acted as electrolyte and separator, followed by winding it onto 300% stretchable elastic fiber. Finally, the fabrication of quasi-solid-state yarn ZIB was accomplished after an ecoflex packaging was wrapped onto the elastic fiber, as shown in Figure 6j. As expected, the resulting ZIB exhibited superior electrochemical performance, including a high specific capacity of 302.1 mAh g^{-1}, a volumetric energy density of 53.8 mWh cm^{-3}, and an excellent capacity retention rate of up to 98.5% at a current density of 2 A g^{-1} after 500 cycles. Additionally, this yarn ZIB could be stretched up to 300% (Figure 6k) and was continuously operated for 12 h under deionized water, proving superior stretchability and waterproofing, respectively. In particular, the specific capacity retention rate was still reasonable even under different deformation states such as straight, bent,

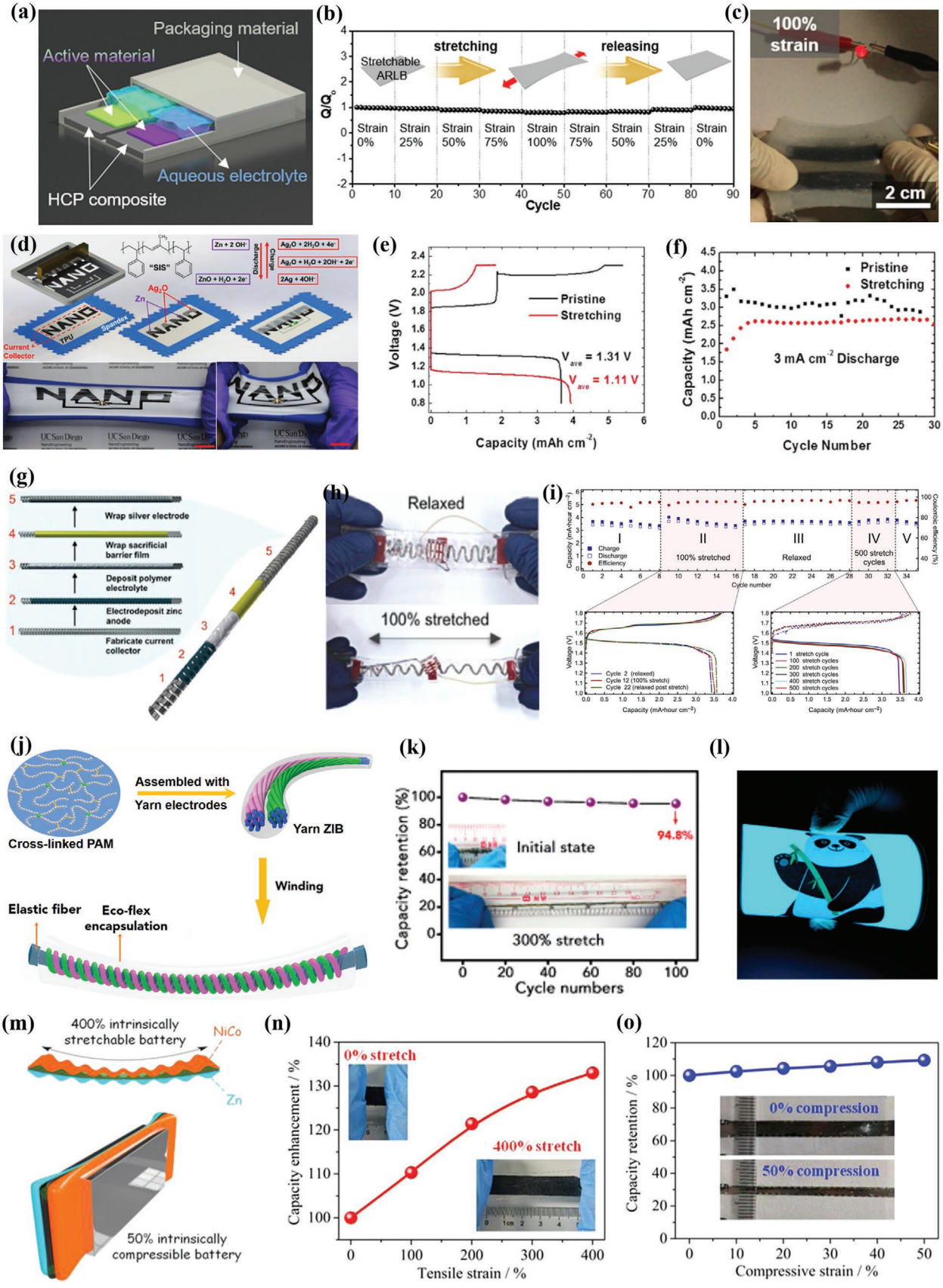

knotted, twisted, and straight, which may be likely due to the employment of double-helix CNT as a substrate. More importantly, the yarn ZIB could power a light-emitting diode (LED) and a 100 cm^2 electroluminescent panel, even when it was cut short and woven into textile, as shown in Figure 6l. This work reveals that the quasi-solid-state yarn ZIB with excellent stretchability, knittability, and waterproofing capability is promising as a power supply in the next generation of flexible and wearable electronic devices.

It is important to note though that the application of only compressed or stretched ARBs is not sufficient to power flexible wearable devices. Compression and stretching are common phenomena in the practical application of wearable electronics in daily life, and thus energy storage devices that offer such dual functionality are indispensable. In recent years, several strategies have been developed to achieve highly compressible and stretchable ARBs with outstanding electrochemical performance. As displayed in Figure 6m, Huang et al.[155] reported on a smart NiCo//Zn ARB exhibiting these two functions based on the use of sodium polyacrylate (PANa) and CNT paper as an electrolyte matrix, whereas Au-coated conductive substrates were used. The satisfactory electrochemical and mechanical performance of the assembled compressible and stretchable NiCo//Zn ARB may be attributed mainly to the following factors. On the one hand, the high ionic conductivity and good alkaline compatibility with PANa hydrogel, as well as the enhanced conductivity of Au@CNT paper, can facilitate excellent electrochemical performance, especially the rate capability was rather high. A stable capacity of 79 mAh g^{-1} at a high current rate of 113 C was detected. On the other hand, the use of PANa hydrogel with inherent stretchability and compressibility is one of the critical factors for the successful fabrication of such smart ARBs. Furthermore, a novel arched electrode structure with a wavy shape was assembled by paving NiCo@Au@CNT and Zn@Au@CNT to each side of a pre-stretched PANa poly-electrolyte, followed by the release of the strain in PANa (Figure 6n). By employing this unique NiCo//Zn ARB structure, an inherent 400% strain with an enhanced 1.3-fold capacity could be obtained. Interestingly, the battery could also be compressed up to 50% of strain with well-maintained capacity, by exerting a force on both sides of the PANa polyelectrolyte (Figure 6o). Moreover, these smart NiCo//Zn ARBs can operate steadily under 500 stretching cycles and 1500 compression cycles, providing an initial specific capacity of 87% and 97%, respectively. This universal feasibility of PANa as an electrolyte matrix for applications in ZABs with both stretchable and compressible functions may in fact be rather promising.[156,157] Thus, PANa hydrogel electrolyte-based smart ARBs with mechanical strength are expected to be applied as effective power supplies in the next-generation of wearable electronics.

In short, there may be several strategies available to develop compressible and/or stretchable functionalities in ARBs. From the current point of view, none of these strategies can be generally regarded to be the best. Due to the different materials used or the various applications envisaged, each specific strategy may have its advantages and disadvantages. Therefore, the construction of such electrochemical energy systems requires careful consideration of several factors simultaneously.

3.2. Self-Healing ARBs

Mechanical damage under strong internal or external deformation is a serious problem for any electronic device. This is particularly relevant in the application of flexible and wearable ARBs because they are subjected to varying extents of body movements. Accordingly, it is desirable that the ARBs can automatically heal any mechanical damage can automatically recover to the normal operation conditions. In other words, smart ARBs with self-healing functionality can repair their injuries to a certain extent, similar to living organisms. In general, self-healing smart ARBs can be fabricated by introducing self-healing polymers into certain components of the battery. These self-healing polymers can be applied to modify any of the ARB components, mainly the electrodes and electrolytes. Once damaged, the modified electrodes or electrolytes can be restored based on the reconstruction of the fracture surface with or without external stimuli such as light or heat. Both such stimuli give rise to mechanisms based on molecular interdiffusion or reversible (non)covalent bond cross-linking.[158–161] Up to now, several self-healing ARBs have been studied, which significantly prolongs the service lifespan of the respective ARBs, as well as further reduces e-waste and economic costs.

Peng et al.[162] reported a self-healing aqueous LIB by the use of polymer substrates with self-healing properties. More specifically, aligned carbon nanotubes containing $LiMn_2O_4$ or $LiTi_2(PO_4)_3$ nanoparticles were attached to a self-healing polymer substrate as cathode or anode material (**Figure 7**a). Next, aqueous lithium sulfate/sodium carboxymethylcellulose was selected to serve as both electrolyte and separator to assemble highly flexible smart aqueous LIBs with self-healing functionality. In a subsequent experiment, the aqueous LIB was cut into pieces, but the simplest contact between the separates parts could re-connect them within seconds. This interesting phenomenon is attributed to the fact that the broken hydrogen bond networks in the polymer substrate can reconstruct at the

Figure 6. a) Schematic illustration of the stretchable ARLB configuration. b) Normalized discharge capacity of the stretchable ARLB at different strains. c) Photograph showing an LED illuminated by the stretchable ARLB at 100% strain. Reproduced with permission.[148] Copyright 2018, Wiley-VCH. d) Screen-printing process of a stretchable Zn-Ag_2O battery. e) The first cycle voltage curve of the stretchable Zn-Ag_2O battery at 2 mA h cm^{-2}. f) The discharge capacity of stretchable Zn-Ag_2O battery. Reproduced with permission.[150] Copyright 2016, Wiley-VCH. g) Schematic illustration of the assembly process of the flexible fiber-shaped Zn-Ag batteries. h) Photos of serpentine-shaped Zn-Ag batteries. i) Areal capacity and coulombic efficiency of the assembled battery. Reproduced with permission under the terms and conditions of the Creative Commons Attribution Non-Commercial License 4.0.[153] Copyright 2017, the Authors, published by American Association for the Advancement of Science. j) Schematic diagram of fabrication and encapsulation of the yarn ZIB. k) Normalized capacities of the as-prepared stretchable yarn ZIB. l) Photograph of a electroluminescent panel illuminated by yarn batteries. Reproduced with permission[152] Copyright 2018, American Chemical Society. m) Schematic of the stretchable and compressible battery. n) Capacity enhancement ratio of the battery at different tensile strain. o) Normalized capacity of the battery at different compressive strain. Reproduced with permission.[155] Copyright 2019, Elsevier.

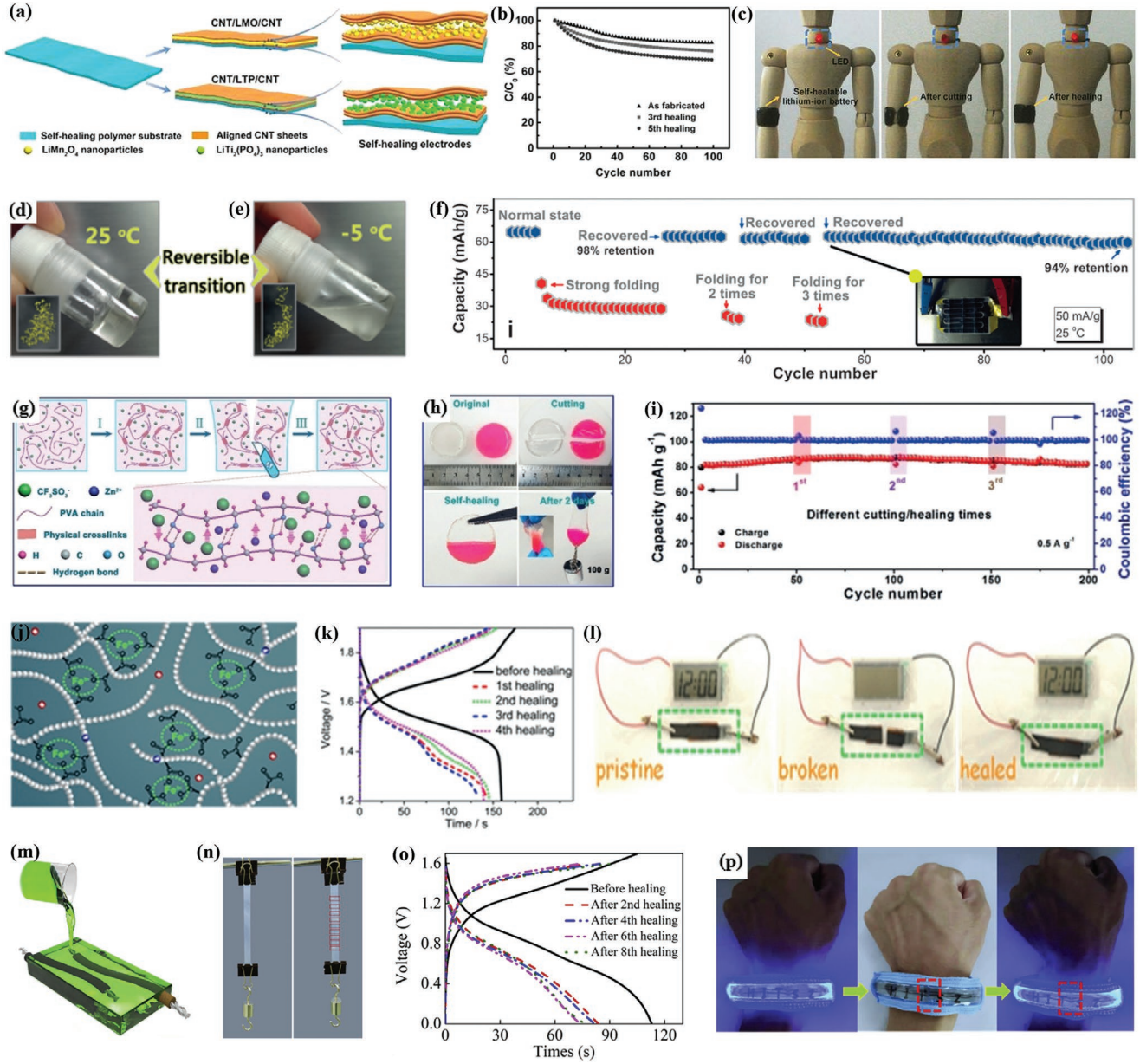

Figure 7. a) Fabrication procedure of the self-healing electrodes. b) Cycling performance of ALIBs at different self-healing numbers. c) Photographs of the self-healing process of the ALIB. Reproduced with permission.[162] Copyright 2016, Wiley-VCH. d–e) Photographs of electrolyte and corresponding polymer chain configurations (insets). f) Cycling capability of the battery with strong folding interrupts and recovery after folding for 3 times. Reproduced with permission.[164] Copyright 2017, Wiley-VCH. g) Schematic fabrication and mechanism of self-healing electrolyte. h) Photographs of the self-healing behavior of the hydrogel electrolyte. i) Cycle performance of the self-healing ZIBs. Reproduced with permission.[94] Copyright 2019, Wiley-VCH. j) Schematic mechanism of self-healability for PANa-Fe^{3+} hydrogel. k) GCD curves of self-healing battery. l) Photographs showing the self-healing battery powered clock. Reproduced with permission.[167] Copyright 2018, Wiley-VCH. m) Filling the precursor solution into the mold. n) Loading test of original hydrogel and hydrogel after being cut for nine times. o) GCD curves before and after multiple cutting/self-healing cycles. p) Photographs of a light strip powered the self-healing ARLB. Reproduced with permission.[168] Copyright 2020, Elsevier.

cracked surface. Furthermore, the electrochemical performance of this battery was maintained well even after multiple cutting and self-healing. This may be regarded a good example of stable cycling performance, as depicted in Figure 7b. To demonstrate the proof-of principle, a self-healing LIB was wrapped around the elbow of a puppet to power a red LED, which continued to light up after the self-healing (Figure 7c). Similarly, by employing self-healing carboxylated-polyurethane (CPU) as a substrate, Zhi's[37] group fabricated a self-healing aqueous Zn-MnO_2 battery for a safe wearable power system. Since electrolytes are critical components in any battery, it is clear that the self-healing electrolytes may be extraordinarily effective. However, such electrolytes may require additional stimulation to achieve their self-healing functionality such as temperature. For example, a thermo-reversible polymer hydrogel was adopted to serve as a self-healing electrolyte, relying on a

temperature-sensitive sol–gel transition mechanism. Interestingly, there are sol–gels available that adopt the form of a gel at room temperature while transforming to a liquid at lower temperature, as shown in Figures 7d,e.[163] This specific phase transition allows the damaged electrolyte to recover by rewetting at low temperatures. Based on these findings, Cui and co-workers[164] proposed a new cooling-recovery concept for the fabrication of smart ARBs with self-healing functionality. They prepared flexible Zn-based batteries using thermoreversible Pluronic hydrogel as an electrolyte. The Zn-based batteries exhibited superior rate capacity and stable cycling performance over 300 cycles, which may be due to the high ionic conductivity of this electrolyte. More importantly, the self-healing efficiency of the cracked electrolyte-electrode area can reach 98% in 5 minutes at −5 °C, while the leakage of the electrolytes during the self-healing process could be prevented by the capillary effect in the cellulose support. As shown in Figure 7f, the reproducibility and reliability of the self-healable function at cold temperature were fully manifested by the cycling test with folding interrupts.

To simplify the self-healing complexity of batteries, it is expected that certain gel electrolytes may be used that can achieve self-healing without external stimulation. Niu et al.[94] reported that PVA/$Zn(CF_3SO_3)_2$ may be such a hydrogel electrolyte that can spontaneously self-recover by forming hydrogen bonding. As shown in Figure 7g, a freeze/thaw method was applied to synthesize PVA/$Zn(CF_3SO_3)_2$ electrolyte and to further assemble an integrated all-in-one ZIB, based on the fact that this method allowed converting the liquid into a hydrogel. The electrolyte showed ideal ionic conductivity and exhibited strong self-healing capability without external stimulation (Figure 7h). Therefore, such integrated all-in-one ZIBs displayed excellent rate capability and stable cycle performance. In addition, the repeatability of the self-healing capability was proven after multiple cutting and self-healing cycles, which was mainly demonstrated by the ability to recover the discharge specific capacity of 81.4 mAh g^{-1} and maintain stable cyclability up to 200 cycles (Figure 7i). In addition to hydrogen bonding, coordination bonding is an alternative form to reconnect networks by reversible non-covalent crosslinking. The coordination bonding through multivalent metal-ligand interactions is widely found in certain supramolecular coordination polymers.[165,166] Recently, a PANa-based hydrogel with self-healing ability was prepared by Huang et al.,[167] where ferric ions (Fe^{3+}) as cross-linkers were used to achieve reversible cross-linked PANa hydrogel chains (Figure 7j), exhibiting self-healing functionality. The network of such Fe^{3+} cross-linking PANa hydrogels exhibits both sufficient stability and dynamics. Therefore, a NiCo||Zn battery was fabricated using a PANa-Fe^{3+} hydrogel as an electrolyte, and inherently autonomic self-healing features were observed. As depicted in Figure 7k, even after 4 cutting and self-healing cycles, a capacity retention rate of 87% was achieved for such NiCo||Zn battery. As shown in Figure 7l, a clock can be turned on again within a few seconds when contact is made between pieces of a cut-up battery, which fully illustrates its excellent self-healing capability and practicality. As mentioned before, the ability of self-healing is particularly critical for wearable batteries. Therefore, fiber-shaped batteries possess great potential since they are easier to weave into energy storage fabrics or textiles and are thus, more suitable for wearable electronics. Therefore, it is imperative to develop such fiber-shaped batteries with self-healing functionality for the development of the next-generation wearable electronics.

In this context, Huang et al.[168] reported that a self-healable hydrogel electrolyte was prepared using PANa and sodium alginate chains that were cross-linked through a calcium ion matrix. This electrolyte was then coated onto two parallel yarn electrodes (Figure 7m), using $LiMn_2O_4$ as an anode and LiV_3O_8 as a cathode, to assemble an aqueous lithium-ion yarn battery with intrinsic self-healing functionality. This electrolyte showed excellent self-healing capability, which was still able to recover its integrity after being cut 9 times (Figure 7n). Consequently, the corresponding yarn battery, after cutting and self-healing up to 8 cycles, retained its initial capacity to 68% (Figure 7o). The wearable and self-healing features in the yarn battery were well demonstrated by continuing to power a light strip around the wrist after cutting and self-healing. Such structure may therefore be highly relevant for practical applications (Figure 7p).

However, obtaining self-healing capability of a whole device by modifying all its components to improve their durability and service lifespan remains a challenge for ARBs since they constitutes a multicomponent structure. Accordingly, all the components may be integrated together in an all-in-one configuration, which may be again highly promising for self-healing ARBs. Such seamless configuration can effectively improve the self-healing capability of the whole devices, and has, thus, great significance to extend the service life of wearable electronics in the future.

3.3. Electrochromic ARBs

Electrochromic devices using amorphous WO_3 films were first manufactured by Deb in 1969.[169] The electrochromic phenomenon refers to the reversible color change of electroactive materials caused by electrochemical oxidation/reduction under the condition of an external voltage or current. Conventional electrochromic devices are a multilayer structures that are usually composed of two conductive substrate layers, an electrochromic electrode layer, an electrolyte layer, and a counter electrode layer.[43] Since electrochromic devices share similar materials as compared to batteries, electrochemical mechanisms and similar configurations may be feasible. Such devices would be applicable in the field of energy storage and conversion, with the aim to obtain electrochromic ARBs with visual functionality. However, unlike in conventional opaque batteries, these materials need to be transparent when constructing electrochromic ARBs, so that the reversible changes of color can be clearly visualized. Accordingly, the energy storage level of the transparent battery can be visually displayed by the change of color in real-time, which can enhance the user-friendliness based on the visual output.[170,171] So far, much research and development efforts have focused on the improvement of electrochromic materials and technologies to obtain advanced electrochromic ARBs.[34–176] The following section systematically summarizes such recent research efforts like the improvement of electrode materials, the optimization of electrolyte composition, and the exploration of self-charging technology.

In terms of the selection criteria for suitable electrochromic materials for ARBs, it is required that the electroactive compound shows different color after charging and discharging, and possesses an ideal potential difference with the counter electrode materials. Nanomaterials based on metal oxides have been proven to be a promising class of materials for high-performance electrochromic electrodes due to their merit of unique electronic structure characteristics, fast charge transfer rates, and optical- and electro-chemical stability. Recently, Elezzabi and co-workers[177] reported that an electrochromic ARB can be fabricated by adopting a Ti-substituted tungsten molybdenum oxide (MTWO) colloid as a cathode material. As illustrated in **Figure 8**a, rigid channels occur as a result of the Ti-doping that produce cationic vacancies as active sites in the MTWO lattice. This mechanism is beneficial for Zn^{2+} intercalation during the charging and discharging processes in electrochromic ARBs. Astonishingly, the MTWO colloids exhibit preeminent electrochromic properties, including low light-scattering and high optical transmittance, which is mainly due to the inhibition of the formation of larger nanowire clusters during the deposition of solution-treated films. Therefore, the obtained electrochromic batteries showed satisfactory open-circuit voltage of more than 1.2 V (Figure 8b) and an optical contrast of 62% can be observed after fully charging and discharging (Figure 8c). It takes about 17 s for such a battery to complete the in situ self-coloring process, and an areal specific capacity of 150 mAh m^{-2} was retained after 300 s (Figure 8d). It is extremely critical to further reduce the self-coloring time, and enhance the specific capacity and switching speed for practical application of electrochromic ARBs. As mentioned above, the electrochromic mechanism is mainly related to the valence states and kinetics of reversibly ionic insertion and extraction.[178] Multivalent ions (e.g., Al^{3+}, Zn^{2+}, or Mg^{2+}) can provide more charges than those of the commonly used monovalent ions (e.g., Li^+, Na^+, or H^+). Moreover, compared with Zn^{2+} ions, Al^{3+} ions as charge carriers showed better kinetics in electrochromic materials.[179,180] To this end, it is necessary to optimize the electrolytes containing such ions in terms of Elezzabi's[181] group obtained a hybrid Zn^{2+}/Al^{3+}-based electrolyte by mixing $ZnSO_4$ with $AlCl_3$ in distilled water. Subsequently, a novel electrochromic ARB was assembled using Zn foil as an anode, electrodeposited WO_3 as a cathode, and a hybrid 1 M $ZnSO_4$-$AlCl_3$ electrolyte (Figure 8e). For the WO_3 cathode used with the hybrid $ZnSO_4$-$AlCl_3$-based electrolyte, the discharge specific capacity can reach 185.6 mAh cm^{-2} at a current rate of 0.5 mA cm^{-2}, which is much higher than the value reached in the $ZnSO_4$ -based electrolyte (Figure 8f). Moreover, an obvious optical contrast of 88% and fast switching times of 3.9 and 5.1 s for coloration and bleaching processes, respectively, were observed (Figure 8g). More importantly, the obtained electrochromic ARBs had an open-circuit voltage of about 1.15 V, which can power a 0.5 V LED for up to 80 minutes (Figure 8h) with a high optical contrast value of 77%. In short, the fast switching speed, capacity, and optical contrast of such electrochromic ARBs achieved constitute significant improvements owing to the use of hybrid $ZnSO_4$-$AlCl_3$-based electrolytes. Optimizing the composition of cathode materials and electrolytes has been confirmed to enable the fine-tuning of the performance of electrochromic batteries, but opaque anode materials such as Zn foil are still an obstacle. This may lead to the nonuniformity of the spatial distribution of the electric field, which in turn restricts coloration uniformity and compromises the switching times. Therefore, Elezzabi et al.[182] adopted an electrodeposition method for depositing Zn onto a stainless-steel mesh to form a transparent Zn mesh anode. Additionally, to endow the electrochromic ARB with energy retrieval functionality, a photovoltaic (PV) solar cell was integrated into the electrochromic ARB with the objective of recharging during the daytime., as shown in Figure 8i, Prussian blue (PB) was chosen as the cathode material to fabricate transparent electrochromic ARBs with self-charging functionality. As expected, the transparent Zn mesh presented high optical transmittance of 87.8%, which is only slightly lower than that of bare stainless-steel mesh (89.3%, Figure 8j). Consequently, such a battery showed uniform coloration and decoloration processes with switching times of 3.6 and 2.5 s respectively, and a coloration efficiency of up to 131.5 cm^2 C^{-1}. As depicted in Figure 8k, a high optical contrast of 67.2% can be observed before and after charge and discharge. Most importantly, Figure 8i illustrates that the obtained batteries can self-charge over the PV solar panel during the day, taking about 10 s with an optical contrast of 63% for coloration processes. At night or during sunlight intermittency, the batteries that have enough electrical energy available can light up an LED, which corresponds to the decoloration process (see inset in Figure 8i). These results clearly demonstrate the practicability of electrochromic ARBs with self-charging functionality. On the other hand, both external power supply and integrated solar cells increase the complexity of the manufacturing process for self-charging electrochromic ARBs to a certain extent. To simplify the production steps and decrease the additional energy consumed, inherent self-charging electrochromic ARBs were developed by Sun et al.[183] As illustrated schematically in Figure 8m, these electrochromic ARBs were mainly composed of PB electrodeposited onto the surface of ITO glass as the cathode, Al attached to another ITO glass as the anode and aqueous KCl as the electrolyte. These batteries exhibited self-powered and self-charging bi-functional features. More specifically, as shown in Figure 8n, two PB‖Al batteries in series can light up a red LED. When the PB was reduced by Al to Prussian white (PW, colorless), the connected LED fails to light up, indicating the discharged state of the bleached battery. Interestingly, the batteries can be recolored after a disconnection time of 1 h, which is attributed to the oxidation of PW to PB by the presence of dissolved oxygen in the electrolyte. Once reconnected, the LED was turned on again, proving that such batteries possess a self-charging function. Figure 8o indicates that the switching times of the bleaching and coloration processes amounted to 10 and 590 s, respectively, where the bleaching and coloration processes correspond to the discharging and self-charging processes. It should be noted that the switching times could be measured in situ. Although such electrochromic ARBs exhibit an inherent self-charging functionality, the rather slow charging rates can be further improved (Figure 8p). To address this problem, Zhao et al.[175] assembled electrochromic ARBs based on aluminum–tungsten oxides (Al–$W_{18}O_{49}$) to achieve ultrafast self-charging in a few seconds by adding a tiny amount of H_2O_2 (Figure 8q). The utilization of H_2O_2 can apparently enhance the specific

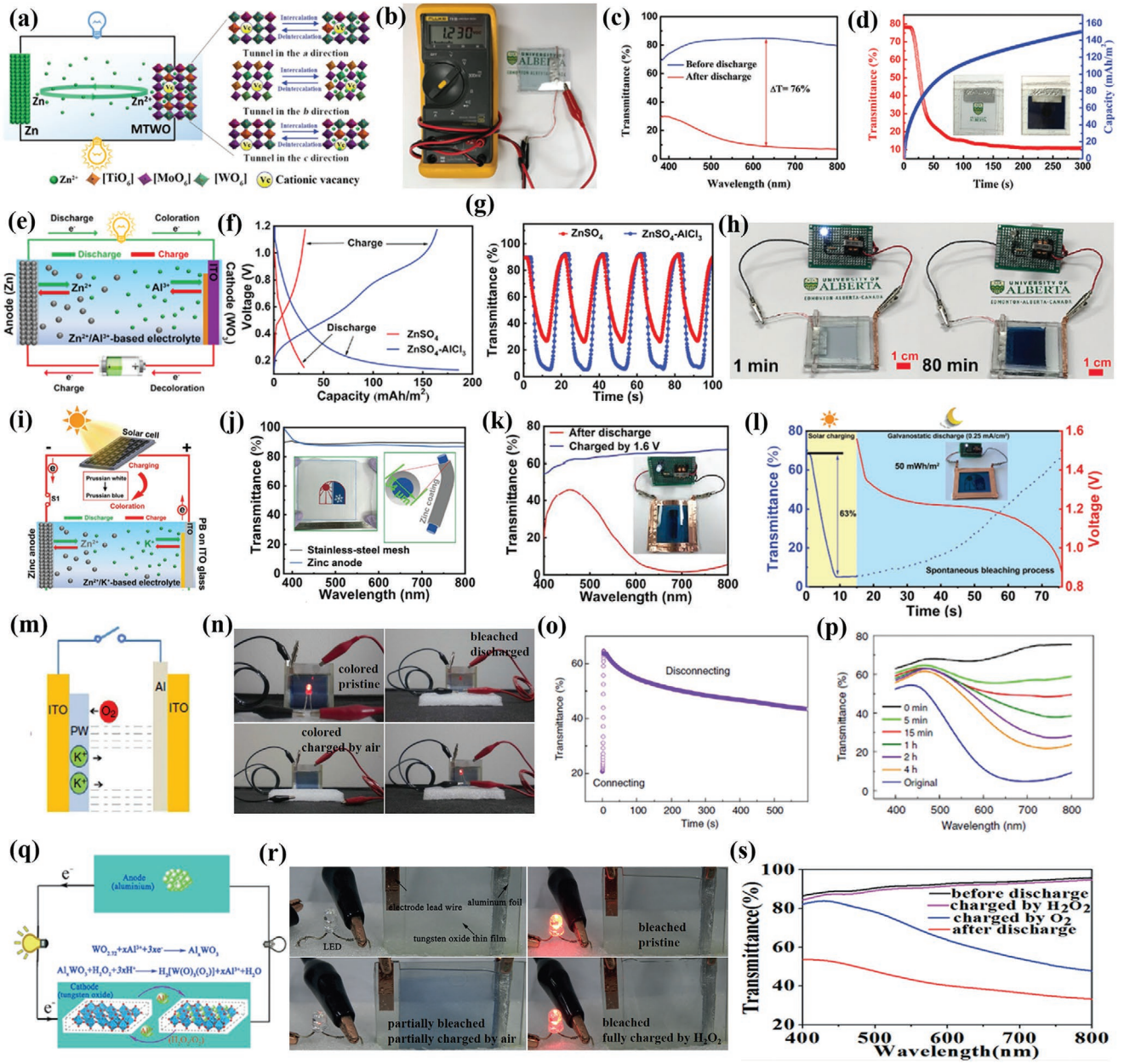

Figure 8. a) Schematic diagram of the Zn||MTWO battery. b) Photograph of the electrochromic ARBs with an open-circuit potential of 1.23 V. c) Transmittance spectra of the MTWO cathode. d) In situ self-coloring process of the electrochromic ARBs[177] Copyright 2019, Wiley-VCH. e) Schematic mechanism of the aqueous hybrid electrochromic battery. f) Dynamic optical transmittance tests of WO_3 cathodes. g) GCD curves of the WO_3 cathode. h) Photographs of electrochromic batteries lit up a LED. Reproduced with permission.[181] Copyright 2019, Elsevier. i) Architecture and mechanism of the electrochromic ARBs. j) Transmittance spectra of a bare stainless-steel mesh and transparent zinc anode. k) Transmittance spectra of a flexible smart window. l) In situ transmittance spectra of electrochromic devices. Reproduced with permission.[182] Copyright 2020, Wiley-VCH. m) Schematic mechanisms for the bifunctional device. n) Photographs of the two devices connected in series as self-charging batteries. o) In situ transmittance test of the electrochromic device connected and then disconnected. p) Transmittance spectra of the original self-powered electrochromic device. Reproduced with permission.[183] Copyright 2014, the Authors, published by Springer Nature. q) The mechanism of the battery to power LED. r) Bifunctional electrochromic batteries with self-powered and self-charging abilities. s) The transmittance spectra of electrochromic batteries. Reproduced with permission.[175] Copyright 2016, Wiley-VCH.

capacity up to 429 mAh g^{-1} of the Al–$W_{18}O_{49}$ batteries, which probably originates from the complicated combination of structure and valence state changes in tungsten oxide. As displayed in Figure 8r, the freshly prepared batteries in a transparent state light up the LED, indicating that the ARB is fully charged at this state. The exhausted batteries show deep blue color and the LED was relit after leaving it in ambient air for 24 h under faint light for recharging. Surprisingly, the blue batteries became transparent within only 8 s when a tiny amount of H_2O_2 was added and the brightness of the LED returned to its initial level.

The above results and the transmittance of such batteries under different states (Figure 8s) fully demonstrate the H_2O_2-assisted ultrafast self-charging and decoloration rates. In a nutshell, numerous studies have revealed the mechanism underlying the discoloring of electrochromic material and the energy storage/conversion. However, it should be noted that the simultaneous operation of electrochromic and energy storage/conversion processes needs to be balanced carefully, because low current density is of great importance to warrant a high coloring efficiency and fast response, whereas a high current density is required to obtain a high power density of electrochromic ARBs.

3.4. Low-Temperature Resistive ARBs

It is well established that aqueous electrolytes exhibit plenty of virtues that none of their counterparts in non-aqueous electrolytes possess. Nonetheless, their application is severely hampered because their high solidifying point is prone to freezing at subzero temperatures, which is still a subject in current research and development of ARBs. This unwanted phenomenon of freezing may be a critical factor in the performance deterioration and failure of ARBs, which severely limits their practicality under frosty weather and in cold regions. To tackle this problem, numerous articles concerning various strategies of modifying aqueous electrolytes have been published already to extend the low-temperature operational range of ARBs.[184–193] In the following section, several of these effective strategies to build smart ARBs with the capability to resist low temperature will be described in detail.

It is inspiring that the use of water-in-salt electrolytes can facilitate the production of high-voltage ARBs,[79,194] where solutions of extremely high concentrations may possess extremely low solidifying points to inhibit freezing. As a typical example, a 22 м KCF_3SO_3 was selected as the electrolyte in an aqueous K-ion battery (AKIB) by Hu and co-authors.[195] As demonstrated in **Figure 9**a, the 3,4,9,10-perylene tetracarboxylic diimide (PDCDI) anode used with the 22 м KCF_3SO_3 aqueous electrolyte presented a wider voltage range than it does using a 1 м KCF_3SO_3 electrolyte, which coincides with some pioneering reports in the literature. Moreover, KCF_3SO_3 has the highest ionic conductivity between –20 and 25 °C compared with other salts such as $NaCF_3SO_3$ and $LiCF_3SO_3$, which is shown in Figure 9b. Accordingly, a 22 м KCF_3SO_3 water-in-salt electrolyte enabled a superior-performance of KIBs with a Fe-substituted Mn-rich Prussian blue $K_xFeyMn_{1-y}[Fe(CN)_6]_w \cdot zH_2O$ cathode and a PDCDI anode. Particularly, pouch AKIBs can operate over a wide temperature range from –20 to 60 °C at a current density of 0.1 to 0.5 C (Figure 9c), showing satisfactory capacity and voltage plateaus. Surprisingly, the pouch AKIB showed stable cycling capability even at a low temperature of –20 °C (Figure 9d). It needs to be pointed out that other types of high concentration electrolytes were also confirmed to be effective, including $Zn(CF_3SO_3)_2$, Li_2SO_4, $NaClO_4$, and LiTFSI. However, the utilization of large amounts of salt may partly increase the costs, as well as hinder the ion diffusion due to the lack of free water. Therefore, another facile and effective strategy to be considered for the further reduction of costs and bringing down the freezing points is the mixing of organic additives into the electrolytes. As depicted in Figure 9e, a water-based electrolyte solvent (salt-free) containing dimethyl sulfoxide (DMSO) with a molar ratio of 0.3 ($\chi_{DMSO} = 0.3$) exhibits a freezing point as low as –130 °C. The mechanism of this antifreezing solvent was explored through nuclear magnetic resonance (NMR) technology.[196] It was argued that the hydrogen bonds between water molecules were weakened with the addition of DMSO, but strong hydrogen bonds between DMSO and water molecules were formed, which inhibited the icing of the solvents. Based on these considerations, Tao et al.[197] employed 2 м $NaClO_4$ with $\chi_{DMSO} = 0.3$ as electrolyte (2 м-0.3 electrolyte) with reasonable ionic conductivity of 0.11 mS cm^{-1} under –50 °C (Figure 9f). By molecular dynamic simulations, the composition of the 2 м-0.3 electrolyte is mainly in the form of free water molecules and molecules aggregated to 1DMSO-2Water via hydrogen bonds (Figure 9g). $NaTi_2(PO_4)_3$@C||activated carbon ARBs based on 2 м-0.3 electrolytes were thus assembled, where the resulting device showed better discharge capacity and cycle stability than those of the corresponding battery without $\chi_{DMSO} = 0.3$ at –50 °C (Figure 9h). It should be noted that other common organic additives such as acetonitrile[198] and ethylene glycol[199] give rise to the same effect. However, it is expected that organic solvents may not be involved in aqueous electrolytes in future developments because this would sacrifice inherent merits of the aqueous electrolyte. Thus, another effective strategy has been developed to modulate the structure of the electrolyte, where certain concentrations of salt in the electrolyte may break the hydrogen bonds between water molecules. $ZnCl_2$ was chosen to explore the effect of its concentration on the freezing point by Chen and co-workers.[200] With the addition of $ZnCl_2$ in the concentration range of 1 to 7.5 м, hydrogen bonds between water molecules are broken (Figure 9i) and the solidification temperature of the electrolyte is reduced to –114 °C. This rise of the solidification temperature when the $ZnCl_2$ concentration exceeds 7.5 м may be ascribed to the enhanced ionic interactions in the electrolyte. Astonishingly, this 7.5 м $ZnCl_2$ electrolyte can achieve an ionic conductivity of 1.79 mS cm^{-1} at –114 °C, as well as being able to operate in an ultra-wide temperature range of –100 °C to +60 °C. As schematically illustrated in Figure 9j, PANI || Zn ARBs were successfully fabricated using 7.5 м $ZnCl_2$ electrolytes. The capability of the PANI || Zn ARBs to withstand low temperature was proven by demonstrating a superior capacity retention of almost 100% after 2000 cycles at –70 °C (Figure 9k). Evidence for the functionality of the PANI || Zn ARBs was obtained by lighting up a red LED at –70 °C (Figure 9l). Another approach to address the inherent issue of sluggish ionic migration kinetics in aqueous electrolytes in the cold environment is the construction of ARBs with proton (hydronium) based acidic electrolytes. Very recently, common acids such as H_2SO_4, H_3PO_4, and HBF_4,[85,201–203] have been shown to serve as an acid aqueous electrolyte with well-controlled ionic diffusion and reduced icing point. For example, Wang et al.[204] reported that the utilization of H_2SO_4 mixed with $MnSO_4$ as a hybrid acidic electrolyte is useful for the fabrication of hydronium ARBs with anti-that can be operated at low temperature. Ex-situ characterizations clearly demonstrated reversible hydronium insertion/extraction reactions in a pyrene-4,5,9,10-tetraone (PTO) anode and reversible Mn^{2+}/MnO_2 conversion reactions in a MnO_2 cathode (Figure 9m).

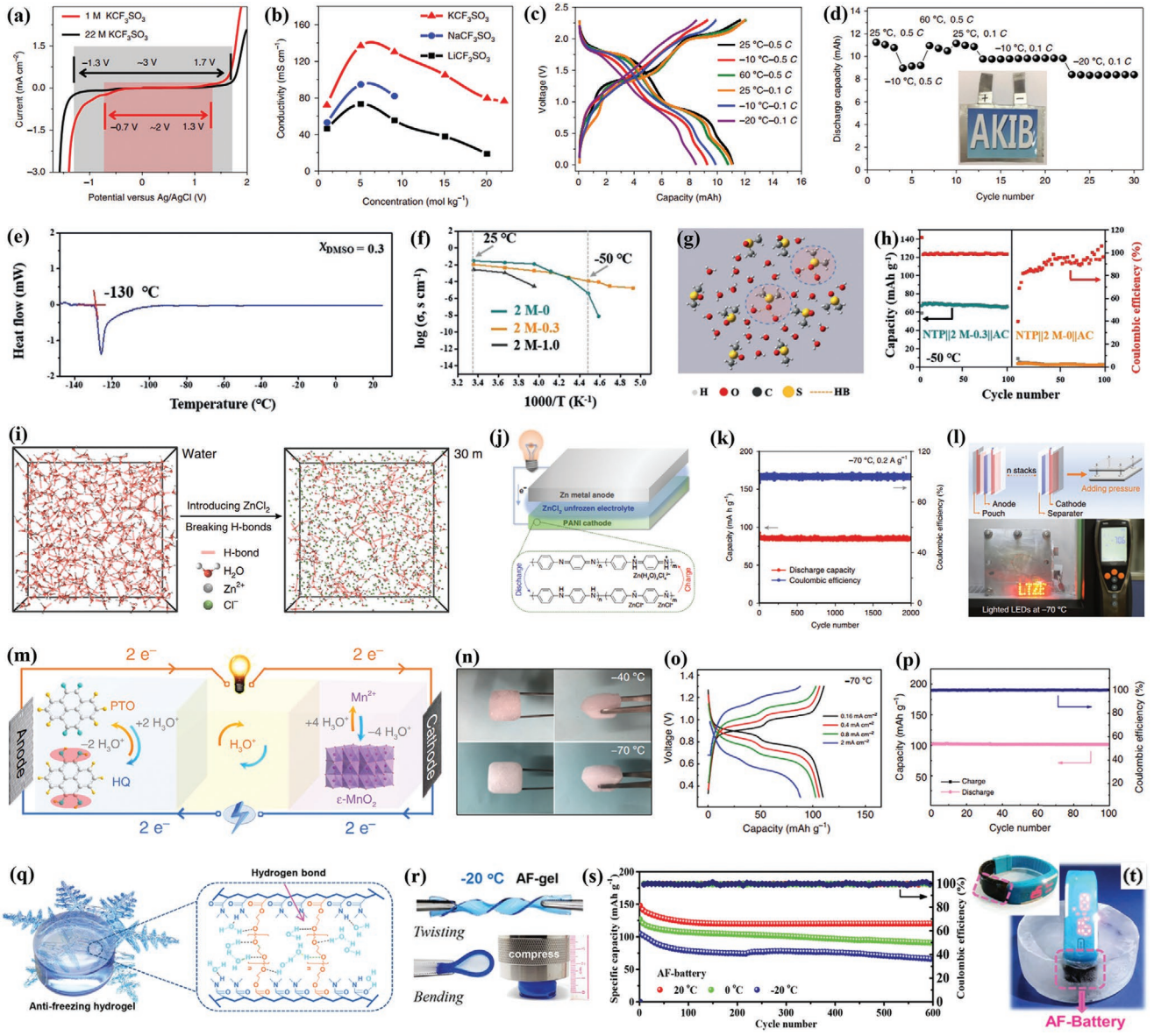

Figure 9. a) Linear sweep voltammetry profiles recorded on titanium mesh at 10 mV s^{-1}. b) The change of ionic conductivity upon increasing concentration for various aqueous electrolytes at 25 °C. c) GCD curves and d) cycling performance of pouch cell. Reproduced with permission.[195] Copyright 2019, Springer Nature. e) DSC of χ_{DMSO} = 0.3 electrolyte solvent. f) Temperature-dependent ionic conductivity research. g) Local structure of the χ_{DMSO} = 0.3 system from MD simulations. h) Cycling stability of batteries measured at −50 °C. Reproduced with permission.[197] Copyright 2019, Wiley-VCH. i) The snapshot of MD simulational. j) The configurations and redox mechanism of batteries. k) Cycling performance at −70 °C and 0.2 A g^{-1}. l) The schematic of fabricated pouch cell and the lighted LEDs. Reproduced with permission.[200] Copyright 2020, the Authors, published by Springer Nature. m) Working mechanism for the hydronium-ion battery. n) Optical photographs of the hybrid electrolyte after remaining at different temperature for several hours. o) Rate capability of the hydronium-ion battery described at −70 °C. p) Cycling stability of the hydronium-ion battery at −70 °C. Reproduced with permission.[204] Copyright 2020, the Authors, published by Springer Nature. q) Schematic of the strong hydrogen bonds in the AF-gel. r) Elastic stability of the AF-gel. s) Cycling capability of the AF-battery at different temperatures. t) The practicality of AF-batteries by powering a wristband electrical watch in solid ice. Reproduced with permission.[91] Copyright 2019, Royal Society of Chemistry.

Interestingly, although such hybrid acid electrolytes freeze at temperatures between −40 and −70 °C (Figure 9n), the formed solid-state hydronium ARB can still operate well. As shown in Figure 9o, such a battery yielded a discharge specific capacity of 110 mAh g^{-1} at a current rate of 0.4 even under an ultra-low temperature of −70 °C. Furthermore, excellent cycling stability with capacity retention of up to 99% after 100 cycles under 0.8 mA cm^{-2} was observed for this battery at −70 °C (Figure 9p). In addition, other acidic electrolytes such as H_3PO_4 and HBF_4 were shown to also exhibit satisfactory performance at low temperatures.

Considering the drawbacks of liquid electrolytes for application in flexible and wearable electronics, it is imperative to develop flexible solid-state ARBs that are capable of operating

normally in cold environments. Hydrogel electrolytes are regarded an ideal alternative for the preparation of elastic ARBs. Several efforts towards the fabrication of hydrogel-based ARBs that can operate at low temperature have been made to date.[205,206] For example, an anti-freezing hydrogel (AF-gel) electrolyte was designed by Zhi et al.[91] Such dual cross-linked AF-gel was obtained by the polymerization of EG-based water-borne anionic polyurethane acrylates (EG-waPUA) and acrylamide (AM). EG-waPUA/AM forms strong hydrogen bonds with water molecules (Figure 6q), which leads to excellent flexibility, a low freezing point, and high ionic conductivity. It was found that EG-waPUA/AM exhibited excellent mechanical strength even at a low temperature of –20 °C (Figure 9r). Given the above advantages, a flexible Zn-MnO_2 AF-ARB was built by the use of EG-waPUA/AM to serve as both electrolyte and separator. Figure 9s demonstrates that even at –20 °C, the discharge specific capacity can still retain 74.54% after 600 cycles at 2.4 A g^{-1} with Coulombic efficiencies close to 100%. Two batteries were connected in series to power a wristband electrical watch in solid ice (Figure 9t), which provides evidence for the practicality of such AF-ARBs at low temperature. Although the above-mentioned improvements could enable ARBs to operate at low temperature, some of these studies involve organic species, which may in fact not be practical, because they may undermine the inherent safety and low cost of aqueous systems.

In addition, most reports are only limited to the optimization of the electrolyte, although suitable electrode materials with high electron conductivity and fast ion transport at low temperatures are also indispensable prerequisites for the excellent low temperature tolerance of ARBs.

3.5. Self-Protecting ARBs

In addition to the pursuit of high electrochemical performance, thermal safety is also a crucial issue that must be considered in the manufacture and practical application of ARBs.[207] In general, thermal safety issues occur when batteries are operated at constantly rising external temperature or they accumulate internal heat.[208] This can lead to performance deterioration, damage, and even explosion of the batteries. Therefore, ARBs with self-controlled electrochemical performance are desirable, but they need to comply with security concerns, especially at high temperatures. The changing temperature need to automatically trigger the on-off switch of the batteries. Such functionality may be achieved by the use of thermo-responsive polymers. At present, self-protection smart ARBs were mainly explored based on modified polymer separators, namely developing novel hydrogel-based separators with reversible thermo-responsive capability.

Having porous structures is a basic feature of separators for their application in ARBs, to provide ionic transport channels for the redox reactions of the active electrode materials.[187] If the pores in the separators can reversibly open and close with temperature changes, the ionic migrations can be controlled to achieve self-protection of the device. Therefore, Niu et al.[209] recently prepared poly(N-isopropyl acrylamide) (PNIPAM) hydrogel with thermo-responsive and porous networks. The acrylamide (AM) containing hydrophilic acylamino groups were uniformly mixed with PNIPAM hydrogel to obtain the PNIPAM/AM hydrogel copolymer that can be applied over a wider temperature window. These PNIPAM/AM-based hydrogel was shown to exhibit disappearing and recovering pores during heating and cooling processes, respectively (**Figure 10**a). This interesting phenomenon was confirmed by SEM, as shown in Figure 10b. In addition, the surface wettability shifts reversibly between hydrophobic and hydrophilic, which allows further tuning the ionic migration rates. Therefore, PNIPAM/AM-based thermal-gated separators were employed to assemble smart ZIBs with self-protecting functionality. The discharge specific capacity of this ZIB is almost zero at room temperature up to 60 °C. While cooled to 25°C, the capacity returns to the initial level. Such excellent thermal self-protection capability was also reflected even after multiple heating/cooling cycles (Figure 10c). The reversible dimming and lighting of an LED as the temperature changes demonstrates the self-protection capability of ZIBs at high temperatures (Figure 10d). For the ARBs, another method to achieve self-protection is the use of smart hygroscopic hydrogel electrolytes. Recently, Fan and co-workers[210] employed polyacrylamide (PAAm) hydrogel as a matrix to synthesize hygroscopic hydrogel electrolyte. The water inside such electrolytes can reversibly be evaporated and reabsorbed during the heating and cooling processes and thus, the transport of ions is efficiently improved to allow stand-by and reactivation of such ARBs (Figure 10e). In general, the mass and ionic diffusion coefficients of such electrolytes display a reversible decrease or increase correlated with the rise or fall of the temperature (Figures 10f,g). A smart Zn/MnO_2 battery was fabricated based on these hygroscopic hydrogel electrolytes, yielding superior cyclic stability beyond 500 cycles under a current rate of 10 mA cm^{-2} at room temperature (Figure 10h). This was demonstrated by considering the impedance value that barely changed after 500 cycles. This smart Zn/MnO_2 battery can provide power to light up an orange LED. More importantly, the ARB shut itself down automatically at 50 °C. When the temperature drops to 25 °C, the battery was returned to normal operation (Figure 10i). This may be regarded strong evidence for the reversible self-protection capability at high temperatures. Inspired by this and combined with the mechanism of polymers withstanding low temperature, future research may focus on the preparation of polymers that have both low temperature resistance and thermal response, which not only will potentially widen the operation temperature range of the respective ARB but also increase the number of functionalities.

3.6. Photo/Air-Charging ARBs

The rechargeability and potential reuse are desirable features of aqueous secondary batteries. In both academic research and commercial applications, this is achieved by connecting external power systems to recharge depleted ARBs. However, this may increase the inconvenience and energy loss during the use of such ARBs to a certain extent, but they may not operate under harsh environmental conditions. ARBs that can recharge themselves through ambient light after running out of power are desirable. Therefore, the development of smart ARBs with self-charging functionality has attracted large research attention

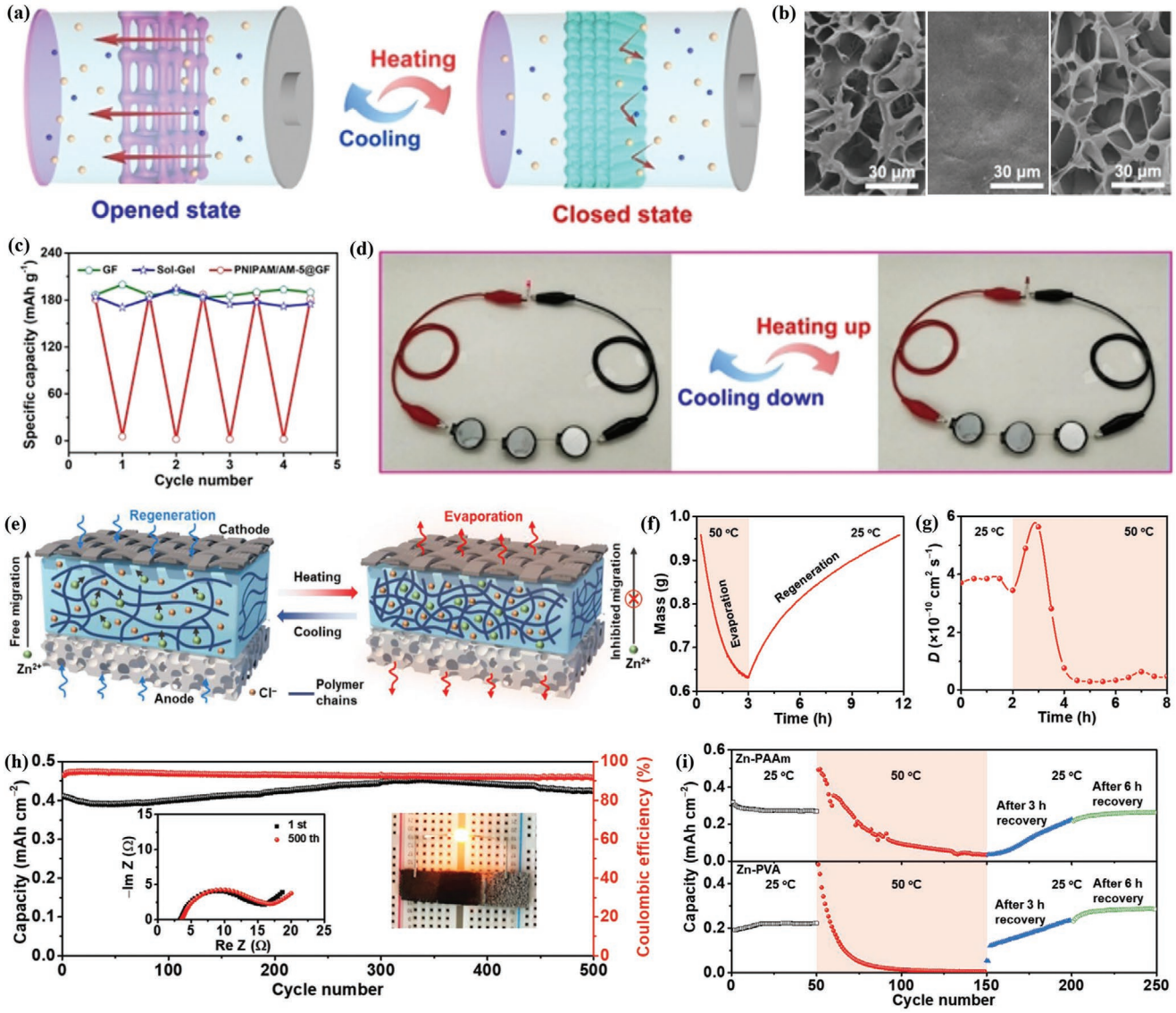

Figure 10. a) Schematic illustration of the thermal self-protective ZIBs. b) The SEM images of separators at diverse temperatures: 25 °C, 60 °C, and down to 25 °C. c) Reversibility of thermal response of ZIBs during heating/cooling cycles. d) The photographs of the ZIBs in series powering a LED under heating and cooling conditions. Reproduced with permission.[209] Copyright 2020, Wiley-VCH. e) The mechanism of the thermal self-protective ZIBs. f) Mass change curves of the hydrogel at 50 and 25 °C. g) Coefficient of ionic diffusion of the hydrogel electrolyte upon increasing from 25 to 50 °C. h) Cycling capability test at 10 mA cm^{-2} (insets: the impedance spectra of the battery and a photo of a battery powering a LED). i) The thermal-responsive reversibility of two types of the ZIBs. Reproduced with permission.[210] Copyright 2020, Wiley-VCH.

from energy scientists. Numerous very recent research efforts have focused on exploring the design of self-charging electrode materials to build the corresponding smart ARBs.[211,212] Such smart ARBs may be regarded promising candidates for future energy storage devices given that ordinary manufacturing procedures would be feasible and the self-charging performance is expected to be acceptable.

It is well known that sunlight is a renewable energy source that offers inexhaustible and pollution-free energy harvesting. Sunlight has been widely used as an energy source, including in photocatalysts and solar cells. Furthermore, self-charging smart ARBs using sunlight have already been explored. As a representative example, an aqueous photo-ZIB that can be directly self-charged via illumination without using solar cells was fabricated by Volder and co-authors.[213] They designed photo-active cathodes based on a mixture of vanadium pentoxide (V_2O_5) nanofibers, poly(3-hexylthiophene-2,5-diyl) (P3HT), and reduced graphene oxide (rGO). This cathode allows both solar energy harvesting and energy storage, achieving a light charging process (**Figure 11**a). Under concurrent actions of photo-charging and discharging, such photo-ZIB exhibited a discharge specific capacity of ≈190 and ≈370 mAh g^{-1} under dark and illuminated conditions, respectively. Moreover, the discharge voltage drops slower under illuminated conditions as compared to dark conditions (Figure 11b). Surprisingly, the light-conversion efficiencies can

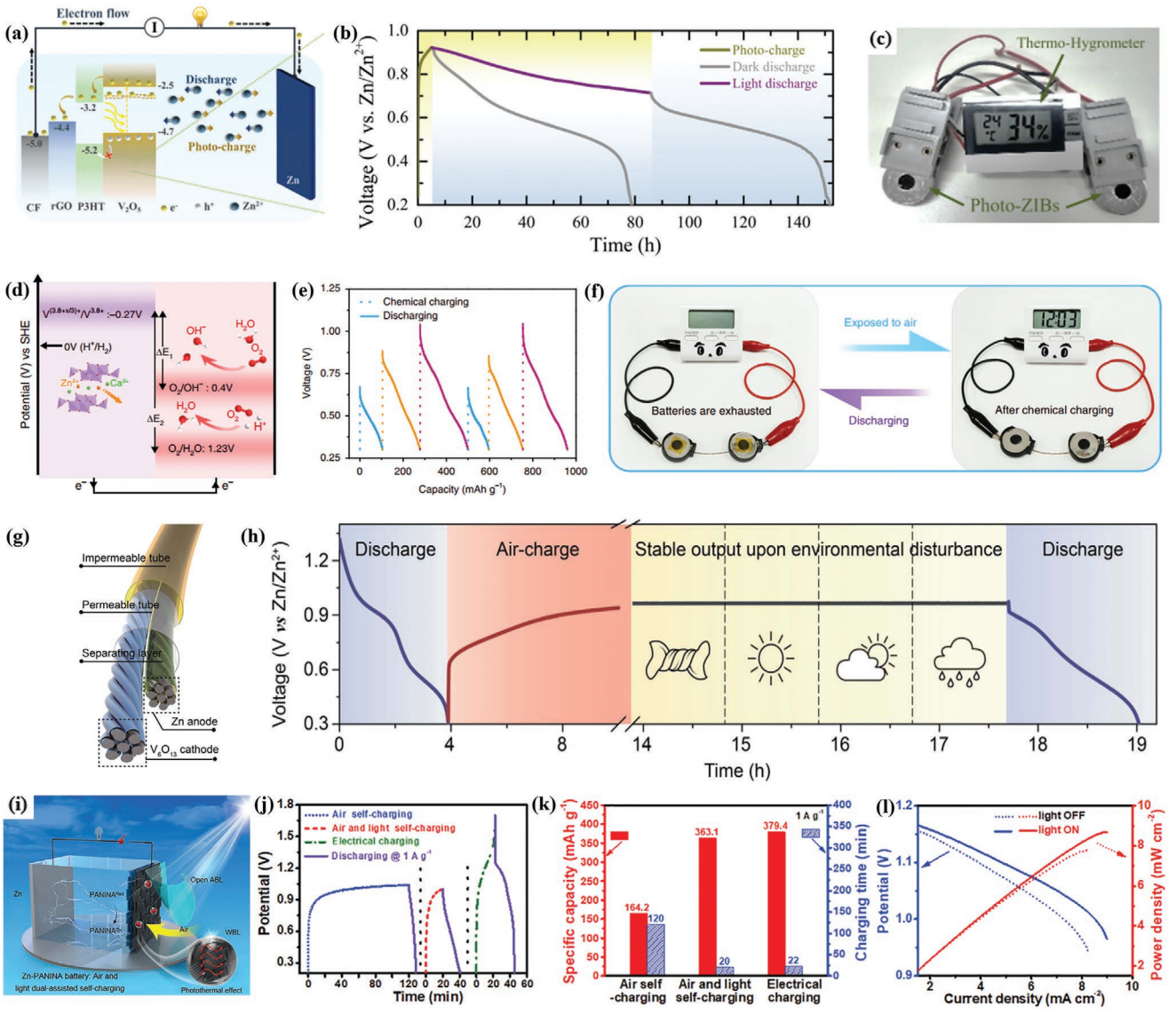

Figure 11. a) Schematic diagram of the photo-charging mechanism of photo-ZIBs. b) Photo-charge and galvanostatic discharge curves of the photo-ZIB in dark and light states. c) Two photo-ZIBs powering thermo-hygrometer under light conditions. Reproduced with permission.[213] Copyright 2020, Royal Society of Chemistry. d) Energy level transition diagram of $CaZn_{3.6}VO$ and O_2. e) Voltage–capacity curves of the batteries after being chemically charged to different states. f) Two self-charging ZIBs in series powering a timer. Reproduced with permission.[216] Copyright 2020, the Authors, published by Springer Nature. g) An illustration of the VCF/Zn battery fiber. h) The stable voltage output of VCF/Zn battery fiber under different environment. Reproduced with permission.[220] Copyright 2021, Royal Society of Chemistry. i) The Zn–PANINA battery self-charged process by air and light dual-assisted. j) Charging curves under three diverse charging modes and the their galvanostatic discharging curves at current rate of 1 A g^{-1}. k) Charging time and discharge capacity under three diverse charging ways. l) Power density and polarization curves without and with sunlight. Reproduced with permission.[221] Copyright 2021, Wiley-VCH.

reach ≈1.2%, which is significantly higher than that of previously reported photo-charging LIB systems.[214,215] As shown in Figure 11c, the self-charging capability of this photo-ZIB under illuminated conditions was further confirmed by its capability to operate as a commercial sensor. The photo-active cathodes-based pouch cells with an optical window of ≈64 cm^2 also exhibited satisfactory self-charging capability under illumination. However, sunlight intensity depends on weather conditions, locations and times, leading to fluctuation and intermittence. These undesired features limit the self-charging functionality of ARBs relying on sunlight. To tackle this problem, Niu et al.[216] developed a novel cathode material ($CaV_6O_{16}{\cdot}3H_2O$) that can be oxidized in ambient air oxygen (Figure 11d). Subsequently, an aqueous ZIB was assembled that could be successfully self-charged in air using a $CaV_6O_{16}{\cdot}3H_2O$ cathode. As expected, such ZIB offered excellent electrochemical performance in terms of a high initial discharge capacity of 300 mAh g^{-1} at 0.1 A g^{-1}, superior rate capability of up to 30 A g^{-1} (62 mAh g^{-1}), and stable capacity retention of 100% after 10000 cycles at 10 A g^{-1}. More importantly, after 30 h of self-charging by directly exposing the cathodes to ambient air, the discharge capacity of such ZIBs can still reach 221.4 mAh g^{-1} (Figure 11e). It is worth

noting that this self-charging process requires the presence of H_2O because the electron-acceptor O_2 may react with H_2O to form OH^-, which is conducive to the self-charging operation.[217–219] By powering a liquid crystal display, the feasibility and practicality of the ZIB after self-charging through ambient air is illustrated in Figure 11f.

As mentioned before, fiber-shaped batteries are easier to be woven into textiles or fabric for future wearable electronics because of their lightweight, flexibility, and durability. Therefore, it is indicated to develop fiber-shaped batteries with self-charging functionality. Very recently, Peng and co-workers[220] developed fiber-shaped aqueous ZIBs that can be self-charged by ambient air. They developed a double-layer tubular encapsulation for such ZIBs based on V_6O_{13} for integration into aligned CNT fiber as a cathode (Figure 11g). It should be noted that the diffusion of oxygen can be effectively controlled by installing or removing the outer tube, and electrolyte evaporation and moisture corrosion were prevented by the inner tube, which is conducive to the discharging and self-charging process of the fiber-shaped aqueous ZIBs. Such ZIBs exhibited a high discharge capacity of 371 mAh g^{-1} at 0.2 A g^{-1} and a capacity retention of 91% after 5000 cycles at 5 A g^{-1}. As shown in Figure 11h, after the exhausted fiber-shaped ZIB was air-charged, it exhibited an extremely stable voltage under deformation and adverse weather conditions. It has been proven that both sunlight and air can be harvested separately in the electrode to yield ARBs with self-charging functionality. If one single electrode reacts with both sunlight and air for self-charging simultaneously, the electrochemical performance and self-charging capability of the battery may be further enhanced due to their synergistic effect. To implement this bifunctional electrode, Yu et al.[221] reported recently that an "all-in-one" cathode made of an active layer of PANI can be deposited onto a carbon cloth, a waterproof breathable layer, and an air barrier layer. Such cathodes give rise to versatility, including redox reactions, oxygen catalytic reductions, and photothermal response. Furthermore, a smart aqueous ZIB that can harvest and exploit concurrently air and light from the ambient environment to achieve energy storage and conversion was assembled based on the "all-in-one" cathode concept (Figure 11i). Such ZIBs exhibited an extremely high capacity of 379.4 mAh g^{-1} at a current rate of 1 A g^{-1}. As depicted in Figure 11j, the self-charging capability of exhausted ZIBs under dual light and air exposure is considerably better than under air exposure alone and close to electron assisted self-charging. An impressively fast 20 min self-charging was achieved by dual light and air exposure to offer a satisfactory discharging capacity of 363.1 mAh g^{-1}. This excellent performance may be ascribed to photothermal effects during light illumination (Figure 11k). Interestingly, this self-charging ZIB can be converted into a primary ZAB due to its unique structural configuration. The ZAB also performs better with light rather than without, in terms of voltage and power density, as indicated in Figure 11l. This strategy utilizes dual light and air exposure, which facilitate the application of such self-charging ARBs in various environments. Therefore, such batteries that self-recharge through air and light open up an efficient way to make full utilization of several kinds of energy, while also providing greater convenience for applications in wearable electronics.

3.7. Photodetecting ARBs

The mechanism of converting light into electrical signals is termed photodetection and the respective devices may be called photodetectors, which are of great significance in numerous fields such as automatic control, sensors, and infrared thermal imaging.[222–224] However, the power supplies of conventional photodetectors are mainly through a connection to batteries or supercapacitors in series. This complex interconnection can reduce the energy density of the entire system and severely restrict their employment in portable and wearable electronics because of the increase in weight and volume.[225,226] To solve this obstacle, it is indicated to develop novel technologies to integrate energy storage and photodetection functionality into one simple and compact device. This requires bifunctional materials that are electroactive and photosensitive.

Polyaniline (PANI) as electrode materials are widely used in the field of ARBs owing to their high electrical conductivity, good redox reversibility, and low cost.[227] Moreover, PANI is also a p-type semiconductor that has been successfully applied in photodetectors before.[228] Relying on these characteristics, Niu et al.[229] employed PANI to assemble a flexible bifunctional device. As illustrated in **Figure 12**a, the PANI cathode and Zn anode materials were electrodeposited onto Au arrays and onto the polyethylene terephthalate (PET) film electrolyte, respectively, to obtain an interdigitated smart micro-ZIB with photodetection functionality. In fact, this microdevice exhibits dual functionality, where the PANI serves as both the cathode of the ZIB and the working electrode of the photodetector. This device offered a good energy density of 49.2 mWh cm^{-3} at 130 mA cm^{-3} in terms of energy storage, and simultaneously possesses photodetection functionality with a sensitivity of 2.85 to white light (Figure 12b,c). The performances can still be maintained or even enhanced when the microdevice was designed to various sizes and shapes. More importantly, because of the ultrathin all-in-one configuration, the photocurrent response strength shows no obvious decline even in the bended state (Figure 12d). Although this work has successfully integrated a photodetector into an ARB single device, its photodetection performance was not ideal compared to that of conventional photodetectors. This limitation may be caused by the electroactive materials that serve as both the working electrode of photodetector and the ARB. Therefore, it is necessary to optimize the working electrode or even to reconsider the configuration of the whole device to further improve energy storage and photodetection performances.

3.8. Shape-Memory ARBs

The use of ARBs in wearable electronics is hampered by irreversible deformations caused by long-term mechanical stress, which can lead to performance degradation and even structural damage. Integrating shape memory functionality into ARBs may effectively prolong their service life.[230] Smart ARBs with shape-memory functionality have the capability to remember the original shape and restore after the release of temporary stress while retaining the initial energy storage capacity.

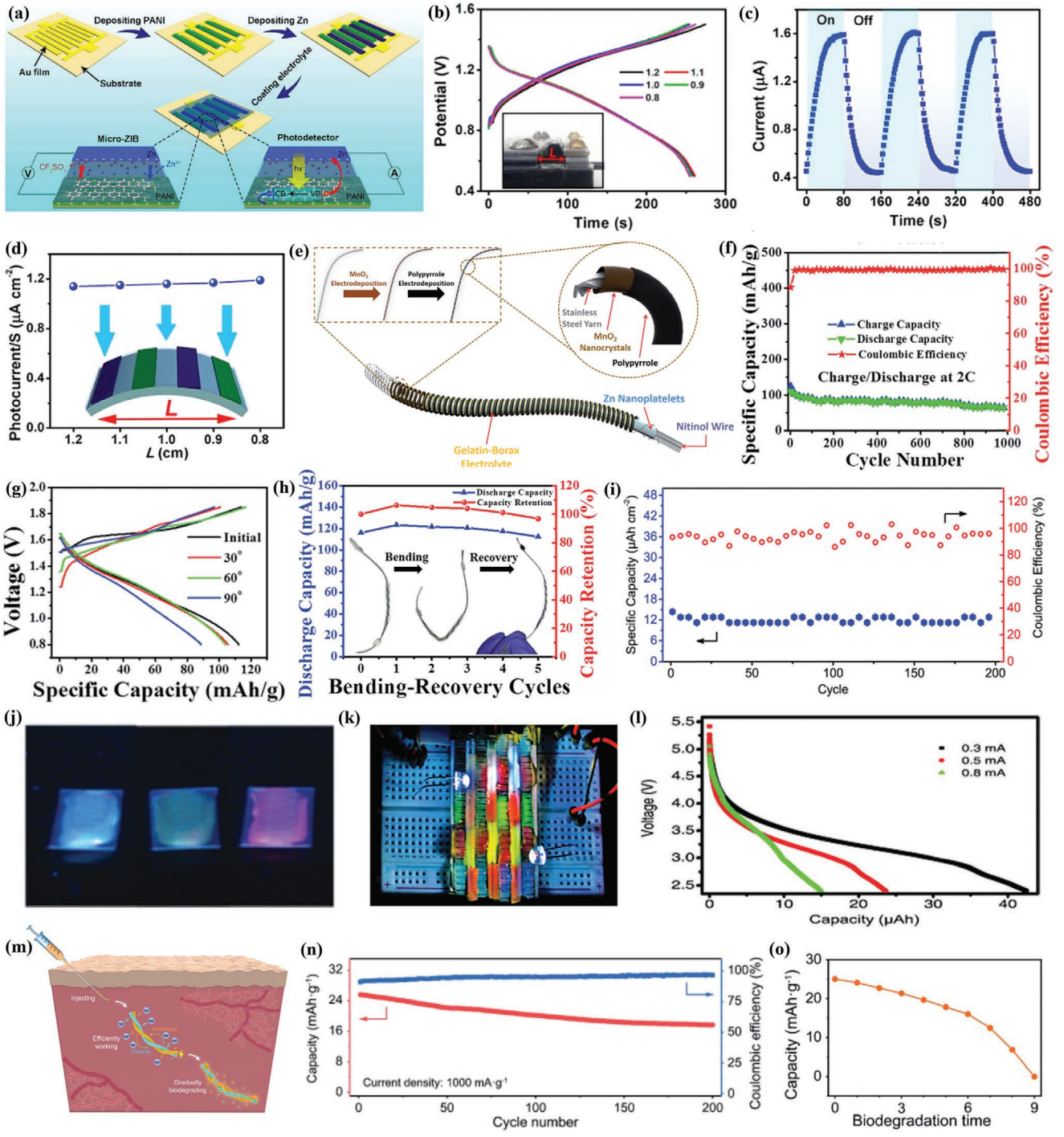

Figure 12. a) Schematic diagram of assembling a micro-ZIB or a photodetector. b) GCD curves of the bifunctional devices at diverse bending conditions. c) Its hotoresponsive curves at 10 mW cm^{-2}. d) Its ihotocurrent per unit area at diverse bending conditions.Reproduced with permission.[229] Copyright 2019, Wiley-VCH. e) Schematic diagram of the shape memory wire battery. f) Its cycling capability at 2 C. g) Its GCD curves under different angles tested at 2C. h) Its discharge capacity and capacity retention tested at 2 C. Reproduced with permission.[231] Copyright 2018, Royal Society of Chemistry. i) Cycling performance of the μZMB. j) Digital photographs of the μZMB. k) The μZMB array under UV light illumination. l) Galvanostatic discharge curves of the μZMB array tested at 0.3, 0.5, and 0.8 mA. Reproduced with permission.[232] Copyright 2018, Royal Society of Chemistry. m) Schematic of the direct implantation process, working process and biodegradation after the use in the body. n) Cycling performance of the fiber battery in vivo. o) Evolution of specific capacity upon increasing biodegradation time of the fiber battery in vivo. Reproduced with permission.[260] Copyright 2021, Royal Society of Chemistry.

A flexible fiber-shaped aqueous ZIB exhibiting shape memory effects was recently reported by Zhi et al.[231] As depicted in Figure 12e, they utilized Nitinol wire as a substrate, stainless steel yarn as an anode, a polypyrrole coating on MnO_2 as a cathode and gelatin-borax as a substrate. Such ZIBs exhibited a discharge specific capacity of 135.2 mA h g^{-1} at 1 C and stable cyclability beyond 1000 cycles (Figure 12f), which is superior to ZIBs using liquid electrolyte due to the enhanced ionic conductivity and moisturizing retention. When the battery was bent at different angles, it did not significantly loose discharge specific capacity, which indicates good mechanical flexibility (Figure 12g). More surprisingly, after bending this fiber-shaped ZIB, it responds to temperature changes to recover its original shape, that is, within 6 s of immersion in 45 °C water the original shape is recovered. Moreover, even after five reversible bending cycles, the specific capacity was barely lost (Figure 12h). However, it should be pointed out that the thermally responsive substrate may well lead to fluctuations in the electrochemical performance after repeated bending. The development of ARB components such as electrodes and electrolytes with shape memory effects are expected to be further pursued in future research to better maintain the inherent performance after bending.

3.9. Photoluminescent ARBs

More functional materials have been incorporated into electronic products to improve their functionality and versatility, but their bulky size often restricts a wider range of applications, at least to a certain extent. Among them, power supply and screen systems usually occupy the largest volume in a large range of electronic products. Therefore, for the manufacturing of miniaturized devices, several integration strategies are commonly used. For example, integrating power supplies into the screen will greatly reduce the device size. To achieve such goal, it is necessary to obtain a small and transparent power supply that emits light in response to external stimuli.

Encouragingly, a smart aqueous Zn–MnO_x-based microbattery (μZMB) was developed successfully by Zhi and coworkers.[232] By using PET as a substrate and gelatin containing CdTe quantum dots (QDs) as the electrolyte, such μZMB exhibited light hazing and photoluminescent capabilities. Furthermore, the addition of borax enhanced the stability of the photoluminescent functionality of the QDs and the ionic conductivity of the electrolyte throughout the electrochemical reaction processes. As shown in Figure 12i, the μZMB displayed stable capacity over 200 cycles and an energy density of 21 mWh cm^{-3}, which constitutes a powerful feature in favor of its practical application. As expected, μZMB with or without QDs exhibited different colors of photoluminescence when exposed to ultraviolet light (Figure 12j). Based on this phenomenon, its array can replace the color filter that is integrated into the screen to build a miniaturized battery-in-screen configuration. Diverse colors (red-green-blue) of luminescence could be observed on the μZMB array under ultraviolet light illumination, where the μZMB array was directly powered by itself (Figure 12k). It is important to note that the μZMB array retained high energy storage capacity under different current densities (Figure 12l). From these results, it can be concluded that an embedded strategy may pave the way for the future design of small-scale multifunctional electronics.

3.10. Biodegradable ARBs

It is well known that implantability and biocompatibility are essential functionalities for ARBs to be applicable in medical electronics. In addition, ARBs with biodegradable ability exhibit extremely attractive application potential, where they may lead to improved convenience for disease diagnosis and treatment. The biodegradable capacity of such ARBs may be explained by the fact that they automatically fuse with the surrounding biological tissue after finishing their task. To endow the ARBs with biodegradable functionality, they must not damage the surrounding tissue and, thus, they are supposed to display high flexibility and miniaturization.

Very recently, a biodegradable fiber was fabricated by Peng and co-workers.[260] The resultant MARBs consist of a polydopamine/polypyrrole anode, MnO_2 cathode, biodegradable chitosan, and body fluid as the electrolyte and separator, respectively. As illustrated in Figure 12m, they can relatively easily be integrated into biological tissue without producing a response from the immune system, after they had been injected directly into the body. As expected, a gradual biodegradable phenomenon was observed for such MARBs. To verify their electrochemical performance and biodegradability in living organisms, the authors injected the MARBs directly into mice. Such MARBs exhibited an initial discharge specific capacity of 25.6 mA h g^{-1} at a current rate of 1000 mA h g^{-1}, and a capacity retention of 69.1% even after 200 cycles at the same current rate (Figure 12n). When the MARBs had finished powering the biosensor, they completely disappeared after 10 weeks without surgical removal (Figure 12o), suggesting excellently biodegradable functionality. These satisfactory results provide impetus for more research leading to further applications of MARBs with biodegradable functionality.

4. Recent Advances in Integrated Systems Based on ARBs

As mentioned in Section 3, another effective strategy for achieving multifunctional ARBs is to integrate other functional devices with different configurations and working mechanisms. For the ARBs, its main role is to store and supply energy in the off-state and operation processes of electronics, separately. Currently, an exhausted battery would usually be recharged from the fixed grid when the stored energy runs out. To some extent this is inconvenient, especially in applications for wearable, miniature, and implantable electronic products. Therefore, the ARBs need to be integrated with devices that possess energy harvesting and energy conversion functions, to build energy systems that can self-charge. On the other hand, when a fully charged conventional ARB is used within such energy system, it is necessary to be plugged into the electronic component to power it. To simplify this procedure, the ARBs can be put to work immediately after integration with the electronics, which

requires integrating ARBs into energy utilizing devices. Such smart ARBs may have great potential and may better satisfy the needs of future electronics since they further facilitate the miniaturization of the full device. To date, related studies have been published on the integration of ARBs with energy harvesting and energy utilizing devices separately or simultaneously. The following section systematically summarizes these reports.

4.1. ARBs Integrated with Energy Harvesting Devices

Well-known energy harvesting devices include solar cells, nanogenerators, and thermoelectric devices.[233–235] They can capture solar energy, mechanical energy, and thermal energy, respectively, converting it into electricity. To date, the first two energy harvesting devices have been well integrated into ARBs in a single device. Solar energy is a renewable, widespread, abundant, and clean energy source. On the premise of making full use of solar energy, human beings would not have to be concerned about increasing energy demands and environmental problems with the conventional energy sources. However, the availability of solar energy is markedly affected by external conditions such as weather, climate, times, and area, thus accompanied by fluctuation and intermittence.[236,237] These limitations make them unsuitable for direct and continuous use in electronics. Accordingly, the concurrent harvesting and storage of solar energy is obviously desirable and indeed feasible. This efficient solution can not only avert the waste of solar energy but also provide stable energy output. The configurations and materials to be used in conventional ARBs are challenging and it is often even impossible to fabricate such an integrated single device. Therefore, it is requires to develop new generations of ARBs that are well compatible with solar cell modules to obtain the integration of the aforementioned two functions into one device.

Very recently, by combining blade coating with rolling assembly technologies, Niu and co-workers[238] fabricated an ultrathin all-in-one flexible planar ZIB. The excellent rate capacity and cyclic stability are superior to those of stacked and thick ZIBs, which may be related to the ultrathin features of the device that accelerate ionic transfer. Its unique and simple configuration can be customized and edited into arbitrary shapes. As an example, two such ZIB in series were made into the shape of a "panda paper-cut" as a power source to light up a red LED (**Figure 13**a), which indicates the good scope for compatibility or integration with other devices. Indeed, as depicted in Figure 13b, an integrated device that can harvest and store energy was built by integrating ultrathin flexible ZIB with perovskite solar cells (PSCs). Subsequently, the photo-charging curve is almost identical to the galvanostatic charging curve in the alternating photo-charging/galvanostatic discharging and GCD processes (Figure 13c), which suggests that this integrated device exhibits excellent self-charging capability through the solar cell. Nevertheless, the planar architecture is generally bulky and heavy, resulting in difficulties to use it in portable electronics. As stated above, fiber-shaped ARBs may have tremendous potential due to their lightweight and weaving properties for future smart clothing. Lately, their integration with energy harvesting devices was prosperously explored to obtain smart fiber-shaped ARBs with self-charging functionality.[239] Such fiber-shaped integrated devices can be readily woven into fabrics and textiles for wearable electronics, improving convenience, comfort, and living standards for human beings. As illustrated in Figure 13d, the fiber-shaped solar cells and ZIBs were woven into a photo-charging fabric with energy harvesting and storage capability by adopting an industrial shuttle-flying weaving technology. This bifunctional fabric can act as a power source at a current density of 1 mA for 2 h after it was charged at 6.4 V in the sunlight. In addition, its performance is almost impervious to the external environment even during deformation, movement, or during rainy days (Figure 13e). To prove the use of ZIBs for humans (Figure 13f), a body area sensor network consisting of a temperature sensor, a body-motion sensor, and a humidity sensor have been designed to monitor personal healthcare.

In addition to harvesting solar energy, mechanical energy as a random and ubiquitous resource can also be harvested and converted into electricity by nanogenerators (NGs). Wang et al.[240–244] have reported numerous pioneering researches works regarding this topic. Such mechanical energy is mainly generated by vibrations, waves, airflow, and motion. Similarly, they are featuring irregularities and intermittency and, thus, the power output would be unstable and the device applicable only to a limited range of applications in conventional electronics.[245,246] Therefore, they may better be integrated into batteries to store the generated energy by the NGs for later use. As an example, Zhi et al.[247] recently reported the integration of triboelectric nanogenerators (TENGs) into aqueous ZIBs to obtain self-powered integrated devices based on mechanical energy. As illustrated in Figure 13g, the TENGs and ZIBs were embedded in different pixels of a specially customized flexible 3D spacer fabric, to account for the different working principles of the two integrated modules. The obtained integrated device exhibited outstanding mechanical energy harvesting capacity from human motion, which is reflected in the generation of excellent V_{oc} and I_{sc} values of approximately 10–15 V and 3–4 μA, giving a maximum power output of up to ≈18.19 mW m^{-2}. The ZIB energy storage module displayed a specific capacity of up to 265 mAh g^{-1} and a stable cyclability over 1000 times with a capacity retention of 76.9%. More importantly, the ZIB increased its voltage from 0.9 to 1.28 V and then displayed a capacity of 10.9 μAh at a rate of 4 μA (Figure 13h). Evidence for the correct operation of the integrated device with mechanical energy harvesting and energy storage capacity was obtained by powering an electronic watch through the ZIB that had been charged via the TENG using a hand press (Figure 13i). In short, the designed 3D spacer fabric allows for the integration of two components with different working mechanisms. It is worth noting that Wang et al.[248] integrated a solar energy with a mechanical energy harvesting device to form a hybrid textile. It is expected that this pioneering work will be extended in future research, where ARBs may be promising candidates to be integrated into this kind of hybrid textile to store harvested solar and mechanical energy.

4.2. Integrated with Energy Utilizing Devices

Although multitudinous efforts have been devoted to the exploration and improvement of the electrochemical performance

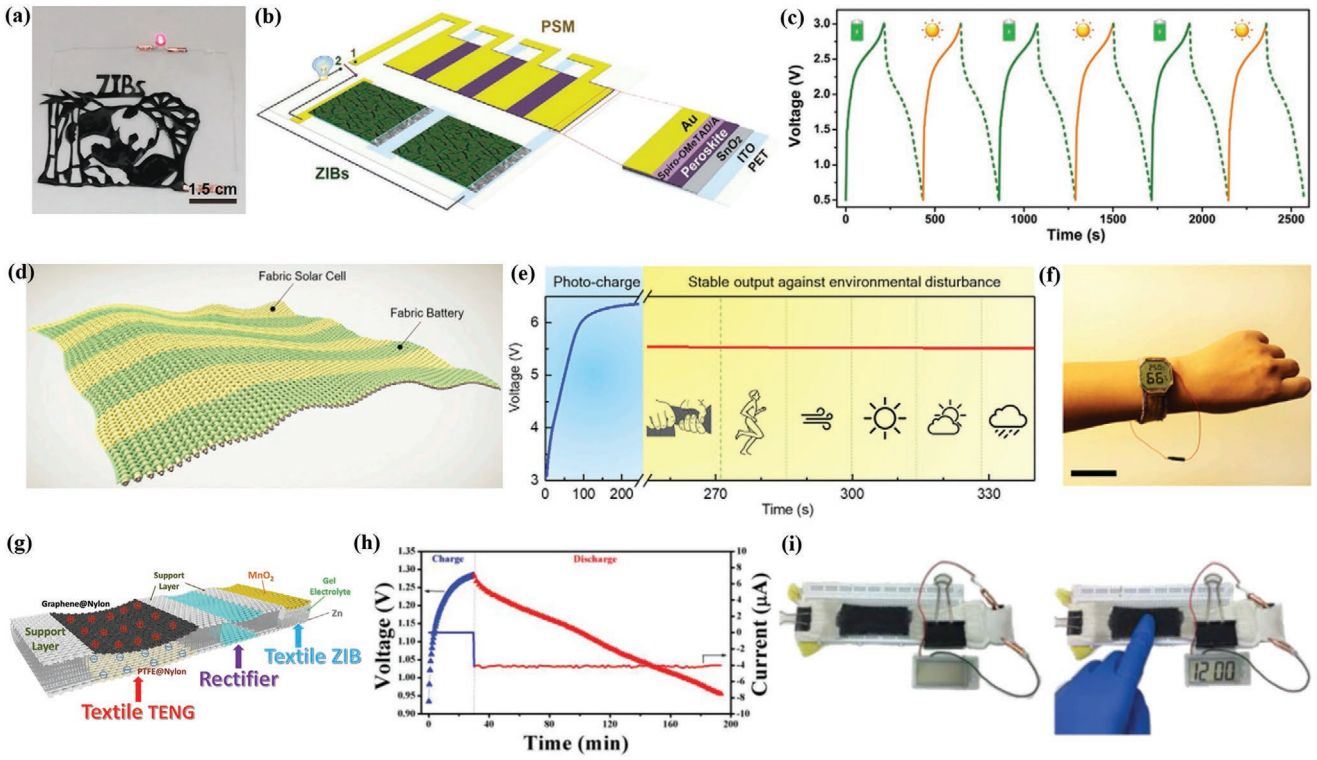

Figure 13. a) Photo of a "panda paper-cut" power supply light up a LED. b) Diagram of the PSM-ZIBs. c) Voltage–time curves of the PSM-ZIBs. Reproduced with permission.[238] Copyright 2021, Wiley-VCH. d) Schematic illustration of the photo-charging fabric. e) The photo-charging fabric offered stable voltage output under various environmental conditions. f) An example of the photo-charging fabric employed powering a temperature sensor and a humidity sensor. Reproduced with permission.[239] Copyright 2018, Elsevier. g) The schematic diagram of the fabric-based device with energy harvesting and storage ability. h) The charging/discharging characteristics of flexible ZIB charged by using TENG fabric as a power source through hand press. i) The flexible ZIB charged by the TENG through hand press powering an electronic watch. Reproduced with permission.[248] Copyright 2018, Wiley-VCH.

of ARBs, the usage for powering electronics is the final purpose, which at present carries the inconvenience of having to frequently insert and dismount the ARBs into and out of the respective electronic component. To more directly employ and manage stored energy, ARBs may be integrated into energy utilization systems such as various types of sensors to realize an all-in-one device with energy storage and energy utilization functionality.

Recently, Yao et al.[249] reported that an integrated system that can utilize stored energy directly was assembled by integrating a microbattery with a pressure sensor. First, an aqueous Ni@MnO_2||Zn microbattery was fabricated based on the active materials being deposited on a carbon nanotube film as an electrode and PVA as an electrolyte. Such microbattery exhibited a high specific capacity of 0.718 mAh cm^{-2} along with an energy density of 0.98 mW cm^{-2}. In addition, almost no loss of discharge specific capacity under extreme bending conditions was observed, which was explained by the excellent flexibility of the device (**Figure 14**a). Next, a thin PDMS was selected as a matrix to attach the microbattery and the pressure sensors to the opposite sides of the PDMS to form the final integrated device, as depicted in Figure 14b. Finally, the integrated miniaturized device exhibiting high flexibility and sensitivity was applied to monitor the human pulse and muscular activity. Figure 14c shows the real-time ΔI–t curves for measuring the human wrist artery, which contain sufficient information to deduce detailed clinical information from the measured wrist pulse. As shown in Figure 14d, the aforementioned fiber-shaped ZIB can be integrated with a strain sensor to be woven into a wearable fingertip.[220] The strain sensor directly responds depending on whether it is in a straight or bent state (Figure 14e), which constitutes evidence for the feasibility of the integration of energy storage devices with energy utilization systems in wearable devices. To customize the geometries of integrated electronics, advanced manufacturing technologies have been adopted. For example, Kim et al.[250] employed a combination of electrospinning, laser micromachining, and 3D printing techniques to create high-power aqueous ZIBs. As shown in Figure 14f, the ZIBs consist of a PANI-coated carbon fiber (CF) cathode and Zn anode. They can be assembled into various geometries, such as square, circular H- and ring shapes. Among them, cylindrical cells offered a superior rate capacity with discharge capacities of 162, 91, and 30 mAh g^{-1} at various rates of 1, 18, and 234 C, respectively (Figure 14g). Impressively, a ring-shaped ZIB was integrated with a photocell, a resistor (47 Ω), a transistor, and a red LED to obtain an integrated wearable photosensor, as illustrated in Figure 14h. Intriguingly, such integrated photosensor could switch on a red LED, when the photocell detects a certain level of darkness (Figure 14i), which constitutes a meaningful example of stored electrical energy being utilized immediately.

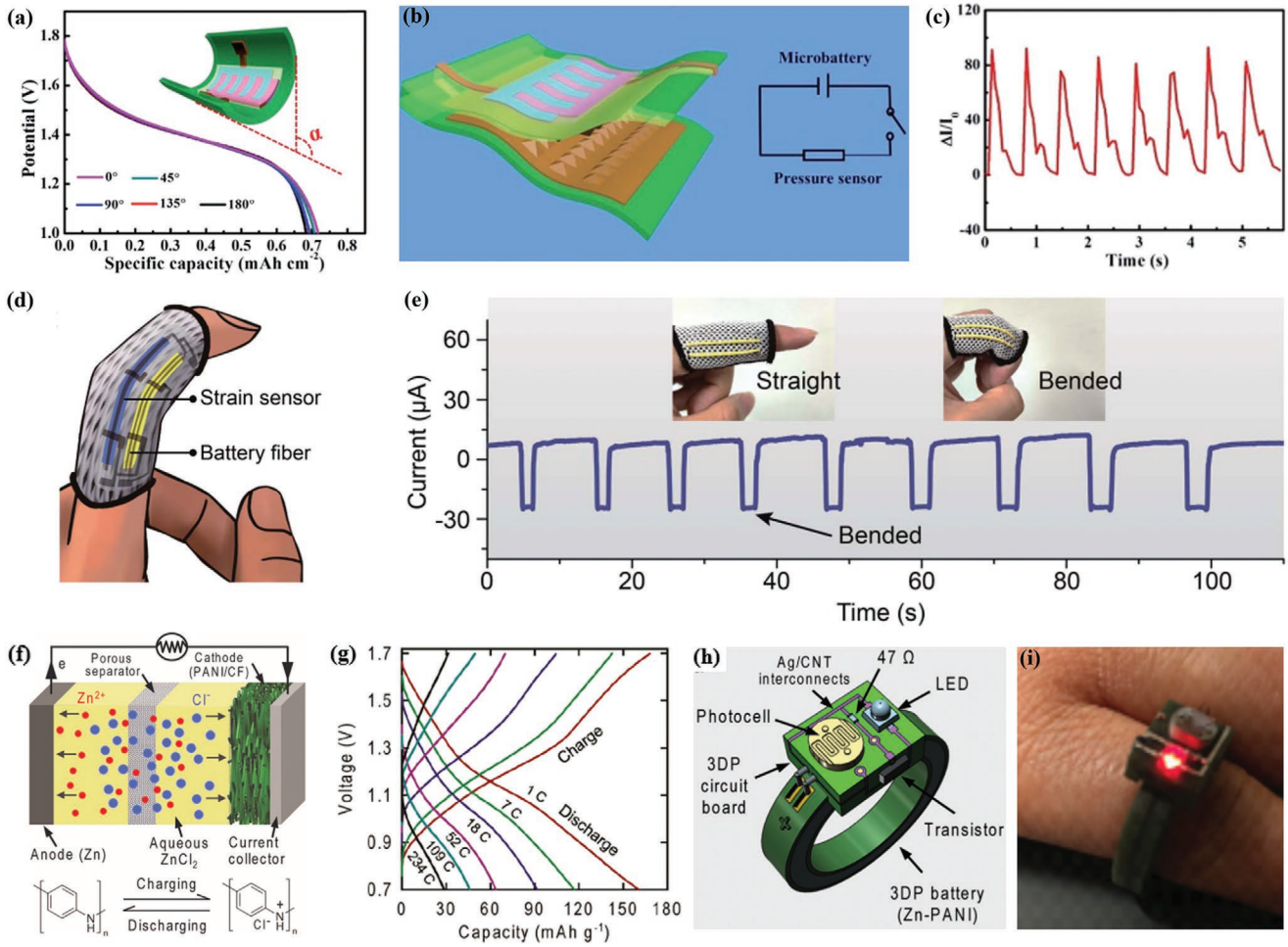

Figure 14. a) Discharge curves of the flexible microbattery at different bending degree. b) Schematic illustration of the microbattery-pressure sensor system. c) A microbattery-pressure sensor system for pulse detection. Reproduced with permission.[249] Copyright 2018, Royal Society of Chemistry. d) The illustration of a strain sensor fiber powered by battery fibers integrated in a fingertip. e) The current time curve of the strain sensor fiber with the increase of bending cycle. Reproduced with permission.[220] Copyright 2021, Royal Society of Chemistry. f) Schematic of ZIB configuration and electrochemical reaction mechanism of PANI. g) Rate performance of a cylindrical battery. h) Schematic diagram of a wearable photosensor with a ring battery and a 3D printed circuit board. i) Photo of the photosensor on a pinky finger. Reproduced with permission.[250] Copyright 2018, American Chemical Society.

4.3. Integration with Energy Harvesting and Energy Utilizing Devices

From the above studies, there is no doubt that the strategy of integration can improve the functionality of ARBs. However, this strategy may not be limited to the integration of only two components.[251–254] Extensive research and development efforts have shown that it is feasible to integrate ARBs with energy harvesting and energy utilization systems at the same time. Such integrated three module hybrid energy systems exhibit the capability of energy harvest, storage, and utilization, which may be regarded the optimum device for practical applications in flexible wearable electronics.

As illustrated in **Figure 15**a, Yao et al.[255] successfully assembled a fully solar-powered coaxial-fiber stretchable sensing system by integrating solar cells, a Zn-MnO_2 battery, and a stretchable strain sensor to simultaneously realize energy harvesting, storage, and utilization. More specifically, such an integrated system can be charged up at 1.8 V under sunlight irradiation in 784 s, followed by galvanostatic discharge at 1.0 V at different current densities, which proves its self-powering and energy storage capability (Figure 15b). To obtain evidence for the energy utilization functionality, this coaxial fiber-shaped integrated device was used to detect back motions in real-time by employing fiber-shaped Zn-MnO_2 batteries to power fibrous strain sensors, as illustrated in Figure 15c. Therefore, such highly compact 1D fiber-shaped integrated architectures not only exhibit reduced the size but also increased energy efficiency and flexibility, which lays the foundation for the construction of optimal devices that can be integrated into fabrics or textiles. Electronic textiles/fabrics may be useful components to realize the application of wearable electronics in many fields such as health monitoring and artificial intelligence. Peng et al.[256] proposed recently that deoxyribonucleic acid (DNA) as an active material can be electrophoretically deposited onto Ag-based fibrous substrates. Consequently, they were

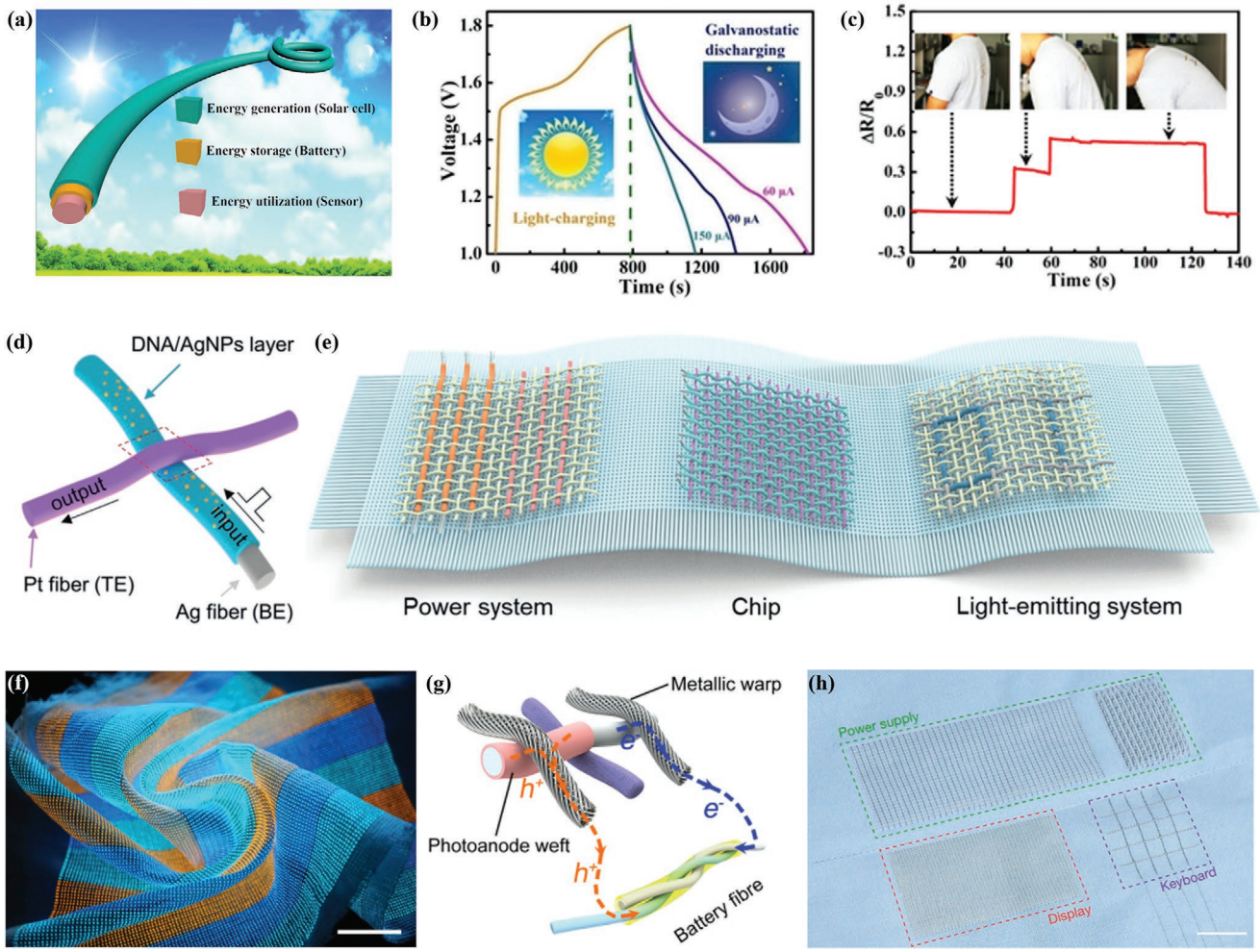

Figure 15. a) Schematic of the fully solar-powered stretchable sensing system. b) Light-charging and galvanostatic discharge curves of the stretchable battery. c) The change of relative resistance with time. Reproduced with permission.[255] Copyright 2019, Elsevier. d) Textile chip made of DNA-bridged memristor cross-bar arrays. e) Schematic illustration of textile-type integrated with diverse modules. Reproduced with permission.[256] Copyright 2020, Wiley-VCH. f) Photo of a functional multicolor display textile under various deformations. g) Schematic mechanism of the energy harvesting and storage component. h) Photo of an integrated textile system. Reproduced with permission.[257] Copyright 2021, Springer Nature.

used to interlace Pt-based fibrous substrates with each other to be woven into textiles, as shown in Figure 15d. Such textile chips act as memristors, offering better memristive performances than organic memristors. This may well be ascribed to the unique double helix chain with biological compatibility and the reasonable ionic conductivity of DNA allowing an ultra-low operation voltage of 0.3 V, high switching speed of 20 ns, and low power consumption of 100 pW. It is suggested that in future research, photovoltaic fibers and fiber-shaped batteries could be integrated by weaving it into the textile power source. Furthermore, light-emitting modules to build wearable information processing devices with energy harvesting, storage, and utilization capability may be integrated in this way as well (Figure 15e). Information from the human pulse may be recorded and further displayed by memristors and light-emitting modules in such an integrated device. Although electronic textiles/fabrics with power supplying and sensing functions have been achieved, their large-area displays need to be improved significantly to facilitate the communication between humans and devices to improve the practicality of such applications. Recently, Peng et al.[257] reported a textile display of 6 m x 25 cm size, which contains 5×10^5 electroluminescent units with a spacing of about 800 microns. As shown in Figure 15f, the textile display was woven using electric field-driven devices based on zinc sulfide phosphors (ZnS), while copper and manganese doping allowed controlling their color. It should be noted that, unlike in OLED devices, ZnS phosphor can be dispersed in an insulating polymer matrix by applying alternating electrical fields on the polymer matrix. Subsequently, the resulting device can be used to be woven into the textile together with a power supply that exhibits both power generation and storage capability (Figure 15g), and contains a keyboard to form a multifunctional integrated textile systems with a real-time communication tool, as illustrated in Figure 15h. Considering such progress, it is anticipated that future research may deal with the integration of more functionalities into flexible and breathable smart textiles that can withstand repeated washing for their wide application as

future wearable electronics in communication technology, navigation, and medical care.

5. Conclusions and Outlook

In summary, conventional aqueous rechargeable batteries (ARBs) cannot satisfy the ever-growing demands of novel portable, wearable and micro electronic devices. It is imperative to develop multi-functional ARBs (MARBs) for high-performance energy storage and conversion systems. Apart from the basic energy storage mechanism, other additional functionalities have been introduced into ARBs. Here, in this comprehensive review, numerous recent research and development efforts have been presented that are devoted to the exploitation of multifunctional features in MARBs. Two major design principles have been highlighted that can endow additional functionality to ARBs: i) the incorporation of functional materials into ARBs with compressible/stretchable, self-healing, self-charging, self-protective, electrochromic, low temperature resistance, photodetection, shape memory, luminescence, or biodegradable capability into one of the active materials, current collector, electrolyte, separator, substrate or packaging material; ii) integration of ARBs with a functional device having energy harvesting (e.g., solar cells and nanogenerators) and/or energy utilization (e.g., sensors) functionality in a single device. More specifically, the stretchable/compressible, shape-memory, and biodegradable functionalities can be obtained by mainly modifying the current collector, substrate, or packaging material. The self-healing, low temperature resistive, and self-protection functionalities can be obtained by mainly modifying the electrolyte or separator, whereas the electrochromic, self-charging, photodetection, and luminescent functionalities can be obtained by modifying the active materials. The integration strategy enables the ARBs to form self-powering and energy utilizing systems. In this review, we have illustrated the state-of-the-art of MARBs in terms of the smart module preparation, the device configuration design, evaluation of the electrochemical performance, and assessment of the multifunctionality. These reported studies clearly indicated that MARBs exhibiting both energy storage capability and other smart functions possess unlimited potential for applications in the next generation of portable and wearable electronics.

Despite vigorous development in recent years, we believe that the exploration of MARBs in terms of performance and practicality may still be in its infancy. There may be several bottlenecks to be overcome in further research development studies, which requires optimizing and modifying the modules of MARBs to accelerate their development and lead to the next research stage. Currently, metal-based current collectors and substrates are the most commonly used in MARBs, whereas their heavy nature may significantly reduce the inherent energy density of the whole device system. In contrast, recent carbon-based nanomaterials such as carbon cloth, carbon film, and carbon fiber exhibit lightweight, soft, and elastic properties, but their electrical conductivity is lower than that of their metallic counterparts. Therefore, metal-coated carbon-based current collectors and substrates may be prepared by electrodeposition, dyeing methods, or even electroless deposition to maintain both their metallic and flexible character. Conventional active materials are mainly inorganics, especially those containing heavy metal ions, that may raise safety concerns and increase costs when applied to wearable devices. Replacing them with flexible organics having similar functions is a promising choice for future research. For the electrolyte and separator, the further development of high- and multi-performance electrolytes and separators to play the dual role of both facilitating ionic transport and preventing short circuits is urgently needed to achieve MARBs with more than two functions. Developing innovative packaging materials and technologies, such as fully biobased films and 3D printing packages, are highly desired to meet the demands of lightweight and permeability of portable and wearable devices. In addition, several knowledge gaps and technical problems remain to be overcome to expand the application scope of MARBs. As illustrated in **Figure 16**, the following challenges and strategies should be tackled and followed most urgently.

1. Introduction of more functional materials into ARBs: There may be no doubt that the development of novel functional materials is an effective strategy to create new functionalities in ARBs. Nevertheless, the development of such novel functional materials currently outpaces their development, selection and integration into ARBs. From the large number of functional materials existing, only a small number have been tested for endowing multifunctional behavior to ARBs. Consequently, according to their characteristics, more suitable functional materials may be chosen for the corresponding components in ARBs. For instance, the combination of certain thermoelectric materials with ARBs may lead to self-charging functionality that can convert heat into electricity that can be stored in ARBs.[258,259] Furthermore, the combination of bio-materials with self-healing and biocompatible properties may be an indispensable prerequisite for the development of implantable ARBs.[260] Similarly, waterproof ARBs prepared by nature-inspired superhydrophobic materials may well prevent sweat corrosion from the human body.[261,262] In addition, well-known luminescent materials based on organic macromolecular or supramolecular materials need also to be considered since they may be well suited to fabricate photoluminescent or electroluminescent ARBs.[263,264]
2. Regulation and balance in the performance: The common strategy of only pursuing the improvement of the versatility and functionality of ARBs may not be advisable, if their essential electrochemical properties are ignored. By introducing novel functionalities into ARBs, it is crucial to assess the impact on the original electrochemical performance, which often significantly declines. In several instances, combined energy storage and smart functional materials in MARBs may not have reached their maximum potential in terms of a balanced performance. There are possible limitations by undesirable phenomena of incompatibility or even exclusion between the selected two types of material. As an example, there may be a trade-off between the energy density and stretchability due to the mechanical property mismatch between the utilization of rigid electroactive materials and soft elastic substrates.[265] For future studies, innovations in

Figure 16. Schematic diagram of main challenges of MARBs.

device configuration and the choice of novel functional materials may be effective measures to circumvent this trade-off and optimize the overall performance.

3. Development of more functionalities in MARBs: Despite the complication of this approach, constructing ARBs with smaller sizes and more functionalities may be necessary to satisfy the ever-growing demands of modern electronics industry. Smart MARBs with two or more functionalities seem to be desirable for reducing the amount of electronic devices necessary, which may draw more attention from the consumers. In future research, a promising approach to realize this purpose is the simultaneous introduction of diverse functional materials to produce ARBs with more smart properties.[100,266] Furthermore, apart from the integration with solar cells, nanogenerators, and sensors, other functional systems such as electrochemical actuators[267,268] and biomedical devices[269] may also be integrated into ARBs to achieve efficient energy storage and conversion.
4. Formulation of standards in performance evaluation: To date, one of the most urgent tasks that remain to be addressed is the requirement for establishing a unified standard to evaluate the performance of MARBs. However, this is a formidable challenge because it involves several research and development fields and disciplines. As an example, there may exist two different materials or two different strategies that can give the ARBs the same novel functionalities, but the comparison of their functionalities seems arbitrary due to distinct working mechanisms, testing conditions, and application environments. As another example, the degree of deformation of ARBs is generally tested qualitatively rather than quantitatively, which appears to be inaccurate especially for miniature and fiber-shaped devices, enabling it impossible to make a fair comparison of deformability. Therefore, in combination with interdisciplinary characteristics, it is necessary to work and agree on the establishment of uniform criteria for evaluating the functionalities and properties of ARBs, including various electrochemical performance parameters, the smart capabilities, and many more. Laying out uniform assessment standards on a solid foundation is an indispensable prerequisite to achieve industrialization and commercialization of MARBs.
5. Exploration of the working mechanisms: As a matter of fact, the research on the basic mechanisms of electrochemical reactions and smart properties in MARBs has never ceased. However, the presented characterization methods and means in most of the available publications are often conventional, rather approximate and superficial, which prevents more in-depth understanding of the underlying mechanisms. To further reveal and better understand the underlying mechanisms, it is necessary to trace the changes in the structure, composition, and morphology of the material and their correlations. Furthermore, the subassembly of the different components of MARBs should be studied in real-time and in situ during operation. A promising option may be the use of advanced in-situ/operando visualization and characterization techniques, such as in situ XRD, FTIR, SEM, and TEM, to monitor the dynamic evolutions inside the components of MARBs during operation.[270,271] Another strategy that has to be mentioned is the option to perform theoretical calculations and simulations to gain theoretical support for a deeper understanding of the structure–performance relationships of functional molecules for the design of novel device configurations.[272,273] Consequently, combining both strategies, in situ characterization during operation and theoretical predictions will most likely provide vital insights into the working mechanism of MARBs for a better guidance of their performance optimization and development directions.
6. Achieving satisfactory wearability: Another vitally promising research direction for future MARBs is to successfully establish or improve the techniques to weave them into fabrics or clothes for achieving good wearability. It is expected that this strategy has the potential to profoundly reshape large parts of the human lifestyle. For this purpose, MARBs are needed that exhibit wearable characteristics comparable to normal clothes, namely feature tailorability, washability, comfortability, breathability, permeability, and aesthetics besides flexibility and stretchability.[274–276] Compared with the planar configuration counterpart, fiber-shaped MARBs have shown the greater potential to be woven into wearable electronic fabrics and textiles on a large scale by adopting cutting-edge industrial knitting technologies. This may be due to the fact that such fibers are very similar to the texture of yarn and wool, and can thus be woven into clothing more easily.[277,278] However, it should be noticed that current fiber-shaped MARBs need to be further optimized to coat them with gel electrolyte and/or elastomers for packaging purposes.
7. Focusing on the market demand: Although this review presented here is concerned with the technological aspects of the current MARB developments, it has to be stated that the strongest driving force for the vigorous future development of MARBs may be the economic market demands. As summarized above, scientists mainly focus on the exploration of various MARBs, while less attention is paid to market conditions,

potentially affecting and restricting the developmental directions of MARBs in the long term. With that in mind, scientists should timely change their ideas and communicate with governments and market leaders, to obtain more input that focuses on the market in terms of scale, demands, segments and other factors. Considering such aspects may further accelerate the development of MARBS to reach the ultimate and common goal, which is their market commercialization. With the advent of the electronic information age (e.g., 5G and Internet of Things),[279,280] more attention may be paid to the application requirements in implantable medical devices, uninterruptible power supplies, unmanned vehicles for aerospace applications, and other operation scenarios for further developing suitable MARBs in future research.

8. Shift to commercial application: At the current stage, most of the MARBs are still in the research and development phase and are mainly produced and investigated in the laboratory. Promoting lab-made devices into industry products involves considering their manufacturing scalability. Therefore, a primary consideration for scientists and engineers should probably be the up-scaling, feasibility of mass production, safety concerns, cost issues, and environmental impact to ultimately achieve commercialization. Moreover, the specific metrics of different equipment and usage scenarios should be formulated to judge whether certain MARBs can be used as a commercial device. These specific metrics are mainly reflected as follows: A) Degree of stretching/compression, number of stretching/compression cycles, and capacity retention for stretchable/compressible MARBs; B) number of self-healing cycles and capacity retention rate for self-healing MARBs; C) degree of coloration, specific capacity, voltage, and light transmittance for electrochromic MARBs; D) minimum operating temperature, specific capacity and cycle stability at this temperature for low temperature resistive MARBs; E) critical temperature for self-protecting MARBs; F) self-powering rate and energy conversion efficiency for self-charging MARBs; G) photoelectric responsive sensitivity for photodetecting MARBs; H) shape recovery time for shape memory MARBs; and I) biodegradation rate for biodegradable MARBs. For assessing the relationship between the electrochemical capability and the additional functionality integrated into MARBs, we propose the following equation:

$$B = \frac{1}{2}E + \sum_{n}^{1}\frac{1}{2n}F \quad (1)$$

where B represent the total performance parameter of a model MARB, E the electrochemical capability, n the maximum number of additional functions, and F the additional functional capability.

Although a large amount of challenges involved with the development of future MARBs still remain in terms of electrochemical performances, smart behaviors, and practicalities, we believe that plenty of excellent research work will emerge to eventually solve the above-mentioned challenges in the near future. In summary, the application of MARBs in all kinds of electronics will have a bright future since they can not only serve as power sources but also contribute to smart functionalities.

Acknowledgements

L.L. and Q.C.Z. contributed equally to this work. This work was supported by the Southeast University (Start-up grant 3206002103A1, 9S06001803, and 1106002103), the National Natural Science Foundation of China (51420105003 and 11525415), the financial supports from the Science and Technology Project of Jiangxi Province (20192BCD40017), the Singapore Ministry of Education Academic Research Fund Tier 2 (MOE2019-T2-2-127 and MOE-T2EP50120-0002), A*STAR under AME IRG (A2083c0062), A*STAR under IAF-ICP (I2001E0067 (IAF-ICP)-P2.1), the Singapore Ministry of Education Academic Research Fund Tier 1 (RG90/19 and RG73/19), and the Singapore National Research Foundation Competitive Research Program (NRF-CRP18-2017-02).

Conflict of Interest

The authors declare no conflict of interest.

Keywords

aqueous electrolytes, functional materials, integrated systems, multifunctionality, rechargeable batteries

Received: June 6, 2021
Revised: July 28, 2021
Published online: October 24, 2021

[1] M. Armand, J.-M. Tarascon, *Nature* **2008**, *451*, 652.
[2] D. Larcher, J.-M. Tarascon, *Nat. Chem.* **2015**, *7*, 19.
[3] C. Schubert, *Nature* **2011**, *474*, 531.
[4] X. Jia, C. Liu, Z. G. Neale, J. Yang, G. Cao, *Chem. Rev.* **2020**, *120*, 7795.
[5] K. S. Kang, Y. S. Meng, J. Breger, C. P. Grey, G. Ceder, *Science* **2006**, *311*, 977.
[6] M. Li, J. Lu, Z. Chen, K. Amine, *Adv. Mater.* **2018**, *30*, 1800561.
[7] M. S. Whittingham, *Chem. Rev.* **2004**, *104*, 4271.
[8] J.-M. Tarascon, *Nature* **2001**, *414*, 359.
[9] G. Fang, J. Zhou, A. Pan, S. Liang, *ACS Energy Lett.* **2018**, *3*, 2480.
[10] P. K. Nayak, L. Yang, W. Brehm, P. Adelhelm, *Angew. Chem., Int. Ed.* **2018**, *57*, 102.
[11] Y. Feng, M. Xu, T. He, B. Chen, F. Gu, L. Zu, R. Meng, J. Yang, *Adv. Mater.* **2021**, *33*, 2007262.
[12] T. Hosaka, K. Kubota, A. Shahul Hameed, S. Komaba, *Chem. Rev.* **2020**, *120*, 6358.
[13] D. Chao, W. Zhou, F. Xie, C. Ye, H. Li, M. Jaroniec, S.-Z. Qiao, *Sci. Adv.* **2020**, *6*, eaba4098.
[14] H. Zhang, X. Liu, H. Li, I. Hasa, S. Passerini, *Angew. Chem., Int. Ed.* **2021**, *60*, 598.
[15] F. Wan, X. Zhou, Y. Lu, Z. Niu, J. Chen, *ACS Energy Lett.* **2020**, *5*, 3569.
[16] G. Liang, F. Mo, X. Ji, C. Zhi, *Nat. Rev. Mater.* **2021**, *6*, 109.
[17] D. G. Kwabi, Y. Ji, M. J. Aziz, *Chem. Rev.* **2020**, *120*, 6467.
[18] S. Cai, X. Chu, C. Liu, H. Lai, H. Chen, Y. Jiang, F. Guo, Z. Xu, C. Wang, C. Gao, *Adv. Mater.* **2021**, *33*, 2007470.
[19] Z. Liu, Y. Huang, Y. Huang, Q. Yang, X. Li, Z. Huang, C. Zhi, *Chem. Soc. Rev.* **2020**, *49*, 180.
[20] Z. Tie, Z. Niu, *Angew. Chem., Int. Ed.* **2020**, *59*, 21293.
[21] A. Ramanujapuram, G. Yushin, *Angew. Chem., Int. Ed.* **2018**, *8*, 1802624.
[22] H. Long, W. Zeng, H. Wang, M. Qian, Y. Liang, Z. Wang, *Adv. Sci.* **2018**, *5*, 1700634.

[23] T. Liu, X. Cheng, H. Yu, H. Zhu, N. Peng, R. Zheng, J. Zhang, M. Shui, Y. Cui, J. Shu, *Energy Storage Mater.* **2019**, *18*, 68.
[24] D. Chen, M. Lu, D. Cai, H. Yang, W. Han, *J. Energy Chem.* **2021**, *54*, 712.
[25] H. Liu, J.-G. Wang, Z. You, C. Wei, F. Kang, B. Wei, *Mater. Today* **2021**, *42*, 73.
[26] D.-J. Yoo, M. Heeney, F. Glöcklhofer, J. W. Choi, *Nat. Commun.* **2021**, *12*, 2386.
[27] Y. Liu, G. He, H. Jiang, I. P. Parkin, P. R. Shearing, D. J. L. Brett, *Adv. Funct. Mater.* **2021**, *31*, 2010445.
[28] F. Chen, Z. Y. Leong, H. Y. Yang, *Energy Storage Mater.* **2017**, *7*, 189.
[29] W.-J. Song, S. Lee, G. Song, S. Park, *ACS Energy Lett.* **2019**, *4*, 177.
[30] X. Li, Z. Du, Z. Song, B. Li, L. Wu, Q. Liu, H. Zhang, W. Li, *Adv. Funct. Mater.* **2018**, *28*, 1800599.
[31] S. Pan, J. Ren, X. Fang, H. Peng, *Adv. Energy Mater.* **2016**, *6*, 1501867.
[32] F. Mo, G. Liang, Z. Huang, H. Li, D. Wang, C. Zhi, *Adv. Mater.* **2020**, *32*, 1902151.
[33] Y. Zhai, Y. Li, H. Zhang, D. Yu, Z. Zhu, J. Sun, S. Dong, *ACS Appl. Mater. Interfaces* **2019**, *11*, 28072.
[34] Z. Chen, X. Li, D. Wang, Q.i Yang, L. Ma, Z. Huang, G. Liang, A. Chen, Y. Guo, B. Dong, X. Huang, C. Yang, C. Zhi, *Energy Environ. Sci.* **2021**, *14*, 3492.
[35] H.-W. Zhu, J. Ge, Y.-C. Peng, H.-Y. Zhao, L.-A. Shi, S.-H. Yu, *Nano Res.* **2018**, *11*, 1554.
[36] Z. Pan, J. Yang, W. Zang, Z. Kou, C. Wang, X. Ding, C. Guan, T. Xiong, H. Chen, Q. Zhang, Y. Zhong, M. Liu, L. Xing, Y. Qiu, W. Li, C. Yan, Y. Zhang, J. Wang, *Energy Storage Mater.* **2019**, *23*, 375.
[37] D. Wang, L. Wang, G. Liang, H. Li, Z. Liu, Z. Tang, J. Liang, C. Zhi, *ACS Nano* **2019**, *13*, 10643.
[38] F. Wang, J. Tseng, Z. Liu, P. Zhang, G. Wang, G. Chen, W. Wu, M. Yu, Y. Wu, X. Feng, *Adv. Mater.* **2020**, *32*, 2000287.
[39] C. Li, Q. Zhang, J. Sun, T. Li, S. E. , Z. Zhu, B. He, Z. Zhou, Q. Li, Y. Yao, *ACS Energy Lett.* **2018**, *3*, 2761.
[40] Z. Wang, F. Mo, L. Ma, Q. Yang, G. Liang, Z. Liu, H. Li, N. Li, H. Zhang, C. Zhi, *ACS Appl. Mater. Interfaces* **2018**, *10*, 44527.
[41] Z.-H. Lin, W.-S. Hsu, A. Preet, L.-H. Yeh, Y.-H. C. , Y.-P. Pao, S.-F. Lin, S. Lee, J.-C. Fan, L. Wang, Y.-P. Chiu, B.-S. Yip, T.-E. Lin, *Nano Energy* **2021**, *79*, 105440.
[42] X. Chen, H. Lin, J. Deng, Y. Zhang, X. Sun, P. Chen, X. Fang, Z. Zhang, G. Guan, H. Peng, *Adv. Mater.* **2014**, *26*, 8126.
[43] P. Yang, P. Sun, W. Mai, *Mater. Today* **2015**, *19*, 394.
[44] Z. Wang, X. Wang, S. Cong, F. Geng, Z. Zhao, *Mater. Sci. Eng. R* **2020**, *140*, 100524.
[45] R. Giannuzzi, R. Scarfiello, T. Sibillano, C. Nobile, V. Grillo, C. Giannini, P. D. Cozzoli, M. Manca, *Nano Energy* **2017**, *41*, 634.
[46] D. Qiu, J. Wu, L. Liang, H. Zhang, H. Cao, W. Yong, T. Tian, J. Gao, F. Zhuge, J. Nanosci, *Nanotechnology* **2018**, *18*, 7502.
[47] J. Z. Chen, W. Y. Ko, Y. C. Yen, P. H. Chen, K. J. Lin, *ACS Nano* **2012**, *6*, 6633.
[48] H. Yang, J. H. Yu, H. J. Seo, R. H. Jeong, J. H. Boo, *Appl. Surf. Sci.* **2018**, *461*, 88.
[49] P. H. Yang, Y. Ding, Z. Y. Lin, Z. W. Chen, Y. Z. Li, P. F. Qiang, M. Ebrahimi, W. J. Mai, C. P. Wong, Z. L. Wang, *Nano Lett.* **2014**, *14*, 731.
[50] H. S. Peng, X. M. Sun, F. J. Cai, X. L. Chen, Y. C. Zhu, G. P. Liao, D. Y. Chen, Q. W. Li, Y. F. Lu, Y. T. Zhu, Q. X. Jia, *Nat. Nanotechnol.* **2009**, *4*, 738.
[51] S. Zhen, J. Xu, B. Lu, S. Zhang, L. Zhao, J. Li, *Electrochim. Acta* **2014**, *146*, 666.
[52] R. J. Mortimer, *Chem. Soc. Rev.* **1997**, *26*, 147.
[53] M. Lahav, M. E. van der Boom, *Adv. Mater.* **2018**, *30*, 1706641.
[54] J. Chen, Z. Wang, Z. Chen, S. Cong, Z. Zhao, *Nano Lett.* **2020**, *20*, 1915.
[55] F. H. L. Koppens, T. Mueller, P. Avouris, A. C. Ferrari, M. S. Vitiello, M. Polini, *Nat. Nanotechnol.* **2014**, *9*, 780.
[56] S. S. Gu, Z. Lou, L. D. Li, Z. J. Chen, X. D. Ma, G. Z. Shen, *Nano Res.* **2016**, *9*, 424.
[57] M. Zhu, Y. Huang, Y. Huang, Z. Pei, Q. Xue, H. Li, H. Geng, C. Zhi, *Adv. Funct. Mater.* **2016**, *26*, 4481.
[58] Z. Jin, Q. Zhou, Y. Chen, P. Mao, H. Li, H. Liu, J. Wang, Y. Li, *Adv. Mater.* **2016**, *28*, 3697.
[59] L. W. Sang, M. Y. Liao, M. Sumiya, *Sensors* **2013**, *13*, 10482.
[60] X. Wang, B. Liu, R. Liu, Q. Wang, X. Hou, D. Chen, R. Wang, G. Shen, *Angew. Chem.* **2014**, *126*, 1880.
[61] S. Cai, X. Xu, W. Yang, J. Chen, X. Fang, *Adv. Mater.* **2019**, *31*, 1808138.
[62] F. Teng, K. Hu, W. Ouyang, X. Fang, *Adv. Mater.* **2018**, *30*, 1706262.
[63] B. D. Boruah, A. Mathieson, B. Wen, C. Jo, F. Deschler, M. D. Volder, *Nano Lett.* **2020**, *20*, 5967.
[64] Z. Tie, L. Liu, S. Deng, D. Zhao, Z. Niu, *Angew. Chem., Int. Ed.* **2020**, *59*, 4920.
[65] M. Li, J. Meng, Q. Li, M. Huang, X. Liu, K. A. Owusu, Z. Liu, L. Mai, *Adv. Funct. Mater.* **2018**, *28*, 1802016.
[66] M. Li, Q. He, Z. Li, Q. Li, Y. Zhang, J. Meng, X. Liu, S. Li, B. Wu, L. Chen, Z. Liu, W. Luo, C. Han, L. Mai, *Adv. Energy Mater.* **2019**, *9*, 1901469.
[67] L. Hu, Y. Cui, *Energy Environ. Sci.* **2012**, *5*, 6423.
[68] H. Cao, F. Wan, L. Zhang, X. Dai, S. Huang, L. Liu, Z. Niu, *J. Mater. Chem. A* **2019**, *7*, 11734.
[69] C. Chen, J. Song, S. Zhu, Y. Li, Y. Kuang, J. Wan, D. Kirsch, L. Xu, Y. Wang, T. Gao, Y. Wang, H. Huang, W. Gan, A. Gong, T. Li, J. Xie, L. Hu, *Chem* **2018**, *4*, 544.
[70] X. Gui, J. Wei, K. Wang, A. Cao, H. Zhu, Y. Jia, Q. Shu, D. Wu, *Adv. Mater.* **2010**, *22*, 617.
[71] C. Xu, Z. Li, C. Yang, P. Zou, B. Xie, Z. Lin, Z. Zhang, B. Li, F. Kang, C.-P. Wong, *Adv. Mater.* **2016**, *28*, 4105.
[72] X. Gong, Q. Yang, C. Zhi, P. S. Lee, *Adv. Energy Mater.* **2020**, *11*, 2003308.
[73] T. Lv, Y. Yao, N. Li, T. Chen, *Angew. Chem.* **2016**, *128*, 9337.
[74] N. Bowden, S. Brittain, A. G. Evans, J. W. Hutchinson, G. M. Whitesides, *Nature* **1998**, *393*, 146.
[75] Z. F. Liu, S. Fang, F. A. Moura, J. N. Ding, N. Jiang, J. Di, M. Zhang, X. Lepró, D. S. Galvão, C. S. Haines, N. Y. Yuan, S. G. Yin, D. W. Lee, R. Wang, H. Y. Wang, W. Lv, C. Dong, R. C. Zhang, M. J. Chen, Q. Yin, Y. T. Chong, R. Zhang, X. Wang, M. D. Lima, R. Ovalle-Robles, D. Qian, H. Lu, R. H. Baughman, *Science* **2015**, *349*, 400.
[76] Y. Zhang, S. Xu, H. Fu, J. Lee, J. Su, K.-C. Hwang, J. A. Rogers, Y. Huang, *Soft Matter* **2013**, *9*, 8062.
[77] W. Liu, Z. Chen, G. Zhou, Y. Sun, H. R. Lee, C. Liu, H. Yao, Z. Bao, Y. Cui, *Adv. Mater.* **2016**, *28*, 3578.
[78] C. Choi, J. M. Lee, S. H. Kim, S. J. Kim, J. Di, R. H. Baughman, *Nano Lett.* **2016**, *16*, 7677.
[79] L. Suo, O. Borodin, T. Gao, M. Olguin, J. Ho, X. Fan, C. Luo, C. Wang, K. Xu, *Science* **2015**, *350*, 938.
[80] A. Ramanujapuram, G. Yushin, *Adv. Energy Mater.* **2018**, *8*, 1802624.
[81] C. Chakkaravarthy, A. K. A. Waheed, H. V. K. Udupa, *J. Power Sources* **1981**, *6*, 203.
[82] X. Li, L. Ma, Y. Zhao, Q. Yang, D. Wang, Z. Huang, G. Liang, F. Mo, Z. Liu, C. Zhi, *Mater. Today Energy* **2019**, *14*, 100361.
[83] Q. Zhao, M. J. Zachman, W. A. Sadat, J. Zheng, L. F. Kourkoutis, L. Archer, *Sci. Adv.* **2018**, *4*, eaau8131.
[84] Y. Yamada, K. Furukawa, K. Sodeyama, K. Kikuchi, M. Yaegashi, Y. Tateyama, A. Yamada, *J. Am. Chem. Soc.* **2014**, *136*, 5039.
[85] T. Sun, H. Du, S. Zheng, J. Shi, Z. Tao, *Adv. Funct. Mater.* **2021**, *31*, 2010127.
[86] L. Yan, J. Huang, Z. Guo, X. Dong, Z. Wang, Y. Wang, *ACS Energy Lett.* **2020**, *5*, 685.

[87] T. Sun, X. Yuan, K. Wang, S. Zheng, J. Shi, Q. Zhang, W. Cai, J. Liang, Z. Tao, *J. Mater. Chem. A* **2021**, *9*, 7042.
[88] Y. Zhao, Z. C. , F. Mo, D. Wang, Y. Guo, Z. Liu, X. Li, Q. Li, G. Liang, C. Zhi, *Adv. Sci.* **2021**, *8*, 2002590.
[89] X. Cheng, J. Pan, Y. Zhao, M. Liao, H. Peng, *Adv. Energy Mater.* **2018**, *8*, 1702184.
[90] F. Mo, G. Liang, Q. Meng, Z. Liu, H. Li, J. Fan, C. Zhi, *Energy Environ. Sci.* **2019**, *12*, 706.
[91] F. Chen, D. Zhou, J. Wang, T. Li, X. Zhou, T. Gan, S. Handschuh-Wang, X. Zhou, *Angew. Chem.* **2018**, *130*, 6678.
[92] M. Chen, J. Chen, W. Zhou, X. Han, Y. Yao, C.-P. Wong, *Adv. Mater.* **2021**, *33*, 2007559.
[93] S. Huang, F. Wan, S. Bi, J. Zhu, Z. Niu, J. Chen, *Angew. Chem., Int. Ed.* **2019**, *58*, 4313.
[94] L. Han, K. Liu, M. Wang, K. Wang, L. Fang, H. Chen, J. Zhou, X. Lu, *Adv. Funct. Mater.* **2018**, *28*, 1704195.
[95] H. Gao, Z. Zhao, Y. Cai, J. Zhou, W. Hua, L. Chen, L. Wang, J. Zhang, D. Han, M. Liu, L. Jiang, *Nat. Commun.* **2017**, *8*, 15911.
[96] X. Liu, D. Wu, H. Wang, Q. Wang, *Adv. Mater.* **2014**, *26*, 4370.
[97] J. A. Neal, D. Mozhdehi, Z. B. Guan, *J. Am. Chem. Soc.* **2015**, *137*, 4846.
[98] C. Wang, H. Wu, Z. Chen, M. T. McDowell, Y. Cui, Z. Bao, *Nat. Chem.* **2013**, *5*, 1042.
[99] Y. Huang, M. Zhong, Y. Huang, M. Zhu, Z. Pei, Z. Wang, Q. Xue, X. Xie, C. Zhi, *Nat. Commun.* **2015**, *6*, 10310.
[100] G. Liang, Z. Liu, F. Mo, Z. Tang, H. Li, Z. Wang, V. Sarangi, A. Pramanick, J. Fan, C. Zhi, *Light: Sci. Appl.* **2018**, *7*, 102.
[101] D. J. Phillips, M. I. Gibson, *Chem. Commun.* **2012**, *48*, 1054.
[102] H. H. Ko, Z. X. Zhang, Y. L. Chueh, E. Saiz, A. Javey, *Angew. Chem., Int. Ed.* **2010**, *49*, 616.
[103] J. S. Scarpa, D. D. Mueller, I. M. Klotz, *J. Am. Chem. Soc.* **1967**, *89*, 6024.
[104] F. Mo, H. Li, Z. Pei, G. Liang, L. Ma, Q. Yang, D. Wang, Y. Huang, C. Zhi, *Sci. Bull.* **2018**, *63*, 1077.
[105] Q. Cheng, Z. Song, T. Ma, B. B. Smith, R. Tang, H. Yu, H. Jiang, C. K. Chan, *Nano Lett.* **2013**, *13*, 4969.
[106] Z. Song, T. Ma, R. Tang, Q. Cheng, X. Wang, D. Krishnaraju, R. Panat, C. K. Chan, H. Yu, H. Jiang, *Nat. Commun.* **2014**, *5*, 3140.
[107] Q. Zhang, J. Sun, Z. Pan, J. Zhang, J. Zhao, X. Wang, C. Zhang, Y. Yao, W. Lu, Q. Li, Y. Zhang, Z. Zhang, *Nano Energy* **2017**, *39*, 219.
[108] Z. Niu, H. Dong, B. Zhu, J. Li, H. H. Hng, W. Zhou, X. Chen, S. Xie, *Adv. Mater.* **2013**, *25*, 1058.
[109] K. Guo, N. Yu, Z. Hou, L. Hu, Y. Ma, H. Li, T. Zhai, *J. Mater. Chem. A* **2017**, *5*, 16.
[110] Z. G. Wei, R. Sandstrom, S. Miyazaki, *J. Mater. Sci.* **1998**, *33*, 3743.
[111] L. Sun, W. M. Huang, Z. Ding, Y. Zhao, C. C. Wang, H. Purnawali, C. Tang, *Mater. Des.* **2012**, *33*, 577.
[112] Y. Heo, H. A. Sodano, *Adv. Funct. Mater.* **2014**, *24*, 5261.
[113] Y. Xia, Y. He, F. Zhang, Y. Liu, J. Leng, *Adv. Mater.* **2021**, *33*, 2000713.
[114] J. Deng, Y. Zhang, Y. Zhao, P. Chen, X. Cheng, H. Peng, *Angew. Chem., Int. Ed.* **2015**, *54*, 15419.
[115] M. Kaltenbrunner, G. Kettlgruber, C. Siket, R. Schwödiauer, S. Bauer, *Adv. Mater.* **2010**, *22*, 2065.
[116] W. Song, S. Yoo, G. Song, S. Lee, M. Kong, J. Rim, U. Jeong, S. Park, *Batteries Supercaps* **2019**, *2*, 181.
[117] Y. Huang, Y. Huang, M. Zhu, W. Meng, Z. Pei, C. Liu, H. Hu, C. Zhi, *ACS Nano* **2015**, *9*, 6242.
[118] R. Guo, J. Chen, B. Yang, L. Liu, L. Su, B. Shen, X. Yan, *Adv. Funct. Mater.* **2017**, *27*, 1702394.
[119] Z. Yang, L. Li, Y. Luo, R. He, L. Qiu, H. Lin, H. Peng, *J. Mater. Chem. A* **2013**, *1*, 954.
[120] Z. Yang, J. Deng, H. Sun, J. Ren, S. Pan, H. Peng, *Adv. Mater.* **2014**, *26*, 7038.
[121] R. Wang, M. Yao, Z. Niu, *InfoMat* **2020**, *2*, 113.
[122] Y. Zhou, H. Qi, J. Yang, Z. Bo, F. Huang, M. S. Islam, X. Lu, L. Dai, R. Amal, C. H. Wang, Z. Han, *Energy Environ. Sci.* **2021**, *14*, 1854.
[123] C. Chen, J. Cao, Q. Lu, X. Wang, L. Song, Z. Niu, J. Chen, *Adv. Funct. Mater.* **2017**, *27*, 1604639.
[124] Y. Huang, S. V. Kershaw, Z. Wang, Z. Pei, J. Liu, Y. Huang, H. Li, M. Zhu, A. L. Rogach, C. Zhi, *Small* **2016**, *12*, 3393.
[125] W. Guo, X. Xue, S. Wang, C. Lin, Z. L. Wang, *Nano Lett.* **2012**, *12*, 2520.
[126] A. Ramadoss, B. Saravanakumar, S. W. Lee, Y.-S. Kim, S. J. Kim, Z. L. Wang, *ACS Nano* **2015**, *9*, 4337.
[127] P. Hiralal, S. Imaizumi, H. E. Unalan, H. Matsumoto, M. Minagawa, M. Rouvala, A. Tanioka, G. A. J. Amaratunga, *ACS Nano* **2010**, *4*, 2730.
[128] G. Sun, H. Yang, G. Zhang, J. Gao, X. Jin, Y. Zhao, L. Jiang, L. Qu, *Energy Environ. Sci.* **2018**, *11*, 3367.
[129] S. Qu, Z. Song, J. Liu, Y. Li, Y. Kou, C. Ma, X. Han, Y. Deng, N. Zhao, W. Hu, C. Zhong, *Nano Energy* **2017**, *39*, 101.
[130] Q. Liu, Y. Wang, L. Dai, J. Yao, *Adv. Mater.* **2016**, *28*, 3000.
[131] M. K. Hota, Q. Jiang, Z. Wang, Z. L. Wang, K. N. Salama, H. N. Alshareef, *Adv. Mater.* **2019**, *31*, 1807450.
[132] S. Zheng, H. Wang, P. Das, Y. Zhang, Y. Cao, J. Ma, S. Liu, Z.-S. Wu, *Adv. Mater.* **2021**, *33*, 2005449.
[133] G. Sun, X. Zhang, R. Lin, J. Yang, H. Zhang, P. Chen, *Angew. Chem., Int. Ed.* **2015**, *54*, 4651.
[134] L. Liu, Y. Yu, C. Yan, K. Li, Z. Zheng, *Nat. Commun.* **2015**, *6*, 7260.
[135] K. Wang, Q. Meng, Y. Zhang, Z. Wei, M. Miao, *Adv. Mater.* **2013**, *25*, 1494.
[136] Q. Meng, H. Wu, Y. Meng, K. Xie, Z. Wei, Z. Guo, *Adv. Mater.* **2014**, *26*, 4100.
[137] Q. Zhang, W. Xu, J. Sun, Z. Pan, J. Zhao, X. Wang, J. Zhang, P. Man, J. Guo, Z. Zhou, B. He, Z. Zhang, Q. Li, Y. Zhang, L. Xu, Y. Yao, *Nano Lett.* **2017**, *17*, 7552.
[138] J. Han, C. Xu, J. Zhang, N. Xu, Y. Xiong, X. Cao, Y. Liang, L. Zheng, J. Sun, J. Zhai, Q. Sun, Z. L. Wang, *ACS Nano* **2021**, *15*, 1597.
[139] Z. Gao, P. Liu, X. Fu, L. Xu, Y. Zuo, B. Zhang, X. Sun, H. Peng, *J. Mater. Chem. A* **2019**, *7*, 14447.
[140] D. G. Mackanic, T.-H. Chang, Z. Huang, Y. Cui, Z. Bao, *Chem. Soc. Rev.* **2020**, *49*, 4466.
[141] H. Gwon, J. Hong, H. Kim, D.-H. Seo, S. Jeonb, K. Kang, *Energy Environ. Sci.* **2014**, *7*, 538.
[142] X. Peng, L. Peng, C. Wu, Y. Xie, *Chem. Soc. Rev.* **2014**, *43*, 3303.
[143] X. Wang, J. Gao, Z. Cheng, N. Chen, L. Qu, *Angew. Chem., Int. Ed.* **2016**, *55*, 14643.
[144] G. Nyström1, A. Marais1, E. Karabulut1, L. Wågberg1, Y. Cui, M. M. Hamedi, *Nat. Commun.* **2015**, *6*, 7259.
[145] M. Zhang, H. Mei, P. Chang, L. Cheng, *J. Mater. Chem. A* **2020**, *8*, 10670.
[146] D. Kong, Y. Wang, S. Huang, B. Zhang, Y. V. Lim, G. J. Sim, P. V. Alvarado, Q. Ge, H. Y. Yang, *ACS Nano* **2020**, *14*, 9675.
[147] L. Ma, S. Chen, Z. Pei, Y. Huang, G. Liang, F. Mo, Q. Yang, J. Su, Y. Gao, J. A. Zapien, C. Zhi, *ACS Nano* **2018**, *12*, 1949.
[148] M. Shin, W.-J. Song, H. B. Son, S. Yoo, S. Kim, G. Song, N.-S. Choi, S. Park, *Adv. Energy Mater.* **2018**, *8*, 1801025.
[149] C. Yan, X. Wang, M. Cui, J. Wang, W. Kang, C. Y. Foo, P. S. Lee, *Adv. Energy Mater.* **2014**, *4*, 1301396.
[150] R. Kumar, J. Shin, L. Yin, J.-M. You, Y. S. Meng, J. Wang, *Adv. Energy Mater.* **2017**, *7*, 1602096.
[151] Y. Xu, Y. Zhang, Z. Guo, J. Ren, Y. Wang, H. Peng, *Angew. Chem., Int. Ed.* **2015**, *54*, 15390.
[152] H. Li, Z. Liu, G. Liang, Y. Huang, Y. Huang, M. Zhu, Z. Pei, Q. Xue, Z. Tang, Y. Wang, B. Li, C. Zhi, *ACS Nano* **2018**, *12*, 3140.
[153] A. M. Zamarayeva, A. E. Ostfeld, M. Wang, J. K. Duey, I. D. B. P. Lechêne, G. Davies, D. A. Steingart, A. C. Arias, *Sci. Adv.* **2017**, *3*, e1602051.

[154] Y. Xu, Y. Zhao, J. Ren, Y. Zhang, H. Peng, *Angew. Chem., Int. Ed.* **2016**, *55*, 7979.
[155] J. Liu, M. Hua, J. Wang, N. Nie, Y. Wang, Y. Wangd, J. Zhang, Y. Huang, *Nano Energy* **2019**, *58*, 338.
[156] Y. Wang, J. Liu, Y. Feng, N. Nie, M. Hu, J. Wang, G. Pan, J. Zhang, Y. Huang, *Chem. Commun.* **2020**, *56*, 4793.
[157] Y. Chen, X. Wu, Y. Feng, J. Gao, Y. Huang, W. Gan, Q. Yuan, *Carbon* **2020**, *166*, 64.
[158] D. Y. Wu, S. Meure, D. Solomon, *Prog. Polym. Sci.* **2008**, *33*, 479.
[159] M. Q. Zhang, M. Z. Rong, *J. Polym. Sci., Part B: Polym. Phys.* **2012**, *50*, 229.
[160] X. X. Chen, M. A. Dam, K. Ono, A. Mal, H. B. Shen, S. R. Nutt, K. Sheran, F. Wudl, *Science* **2002**, *295*, 1698.
[161] B. K. Ahn, D. W. Lee, J. N. Israelachvili, J. H. Waite, *Nat. Mater.* **2014**, *13*, 867.
[162] Y. Zhao, Y. Zhang, H. Sun, X. Dong, J. Cao, L. Wang, Y. Xu, J. Ren, Y. Hwang, I. H. Son, X. Huang, Y. Wang, H. Peng, *Angew. Chem., Int. Ed.* **2016**, *55*, 14384.
[163] S. S. Soni, K. B. Fadadu, A. Gibaud, *Langmuir* **2012**, *28*, 751.
[164] J. Zhao, K. K. Sonigara, J. Li, J. Zhang, B. Chen, J. Zhang, S. S. Soni, X. Zhou, G. Cui, L. Chen, *Angew. Chem., Int. Ed.* **2017**, *56*, 7871.
[165] Y. Huang, J. Liu, J. Wang, M. Hu, F. Mo, G. Liang, C. Zhi, *Angew. Chem., Int. Ed.* **2018**, *57*, 9810.
[166] J.-P. Zhang, X.-C. Huang, X.-M. Chen, *Chem. Soc. Rev.* **2009**, *38*, 2385.
[167] C. Lu, M. Zhang, D. Tang, X. Yan, Z. Zhang, Z. Zhou, B. Song, H. Wang, X. Li, S. Yin, H. Sepehrpour, P. J. Stang, *J. Am. Chem. Soc.* **2018**, *140*, 7674.
[168] Z. Ji, H. Wang, Z. Chen, P. Wang, J. Liu, J. Wang, M. Hu, J. Fei, N. Nie, Y. Huang, *Energy Storage Mater.* **2020**, *28*, 334.
[169] S. K. Deb, *Appl. Opt.* **1969**, *8*, 192.
[170] J. Zhao, Y. Tian, Z. Wang, S. Cong, D. Zhou, Q. Zhang, M. Yang, W. Zhang, F. Geng, Z. Zhao, *Angew. Chem., Int. Ed.* **2016**, *55*, 7161.
[171] D. Wei, M. R. Scherer, C. Bower, P. Andrew, T. Ryhanen, U. Steiner, *Nano Lett.* **2012**, *12*, 1857.
[172] L. Zhang, D. Chao, P. Yang, L. Weber, J. Li, T. Kraus, H. J. Fan, *Adv. Energy Mater.* **2020**, *10*, 2000142.
[173] W. Zhang, H. Li, M. Al-Hussein, A. Y. Elezzabi, *Adv. Optical Mater.* **2020**, *8*, 1901224.
[174] J. Wang, J. Liu, M. Hu, J. Zeng, Y. Mu, Y. Guo, J. Yu, X. Ma, Y. Qiu, Y. Huang, *J. Mater. Chem. A* **2018**, *6*, 11113.
[175] X. Xia, Z. Ku, D. Zhou, Y. Zhong, Y. Zhang, Y. Wang, M. J. Huang, J. Tu, H. J. Fan, *Mater. Horiz.* **2016**, *3*, 588.
[176] W. Zhang, H. Li, W. W. Yu, A. Y. Elezzabi, *Light: Sci. Appl.* **2020**, *9*, 121.
[177] H. Li, L. McRae, C. J. Firby, A. Y. Elezzabi, *Adv. Mater.* **2019**, *31*, 1807065.
[178] Y. Tian, W. Zhang, S. Cong, Y. Zheng, F. Geng, Z. Zhao, *Adv. Funct. Mater.* **2015**, *25*, 5833.
[179] T. Koketsu, J. Ma, B. J. Morgan, M. Body, C. Legein, W. Dachraoui, M. Giannini, A. Demortière, M. Salanne, F. Dardoize, H. Groult, O. J. Borkiewicz, K. W. Chapman, P. Strasser, D. Dambournet, *Nat. Mater.* **2017**, *16*, 1142.
[180] F. Wan, L. Zhang, X. Dai, X. Wang, Z. Niu, J. Chen, *Nat. Commun.* **2018**, *9*, 1656.
[181] H. Li, C. J. Firby, A. Y. Elezzabi, *Joule* **2019**, *3*, 2268.
[182] H. Li, W. Zhang, A. Y. Elezzabi, *Adv. Mater.* **2020**, *32*, 2003574.
[183] J. Wang, L. Zhang, L. Yu, Z. Jiao, H. Xie, X. W. Lou, X. W. Sun, *Nat. Commun.* **2014**, *5*, 4921.
[184] S. Chen, Y. Zhang, H. Geng, Y. Yang, X. Rui, C. C. Li, *J. Power Sources* **2019**, *441*, 227192.
[185] T. He, Y. Ye, H. Li, S. Weng, Q. Zhang, M. Li, T. Liu, J. Cheng, X. Wang, J. Lu, B. Wang, *Mater. Today* **2021**, *43*, 53.
[186] T. He, S. Weng, Y. Ye, J. Cheng, X. Wang, X. Wang, B. Wang, *Energy Storage Mater.* **2021**, *38*, 389.
[187] L. Suo, F. Han, X. Fan, H. Liu, K. Xu, C. Wang, *J. Mater. Chem. A* **2016**, *4*, 6639.
[188] A. Tron, S. Jeong, Y. D. Park, J. Mun, *ACS Sustainable Chem. Eng.* **2019**, *7*, 14531.
[189] Z. Chen, X. Li, D. Wang, Q. Yang, L. Ma, Z. Huang, G. Liang, A. Chen, Y. Guo, B. Dong, X. Huang, C. Yang, C. Zhi, *Energy Environ. Sci.* **2021**, *14*, 3492.
[190] H. Wang, Z. Chen, Z. Ji, P. Wang, J. Wang, W. Ling, Y. Huang, *Mater. Today Energy* **2021**, *19*, 100577.
[191] H. Wang, H. Zhang, Y. Cheng, K. Feng, X. Li, H. Zhang, *Electrochim. Acta* **2018**, *278*, 279.
[192] Q. Yang, F. Mo, Z. Liu, L. Ma, X. Li, D. Fang, S. Chen, S. Zhang, C. Zhi, *Adv. Mater.* **2019**, *31*, 1901521.
[193] M. Zhu, X. Wang, H. Tang, J. Wang, Q. Hao, L. Liu, Y. Li, K. Zhang, O. G. Schmidt, *Adv. Funct. Mater.* **2020**, *30*, 1907218.
[194] D. P. Leonard, Z. Wei, G. Chen, F. Du, X. Ji, *ACS Energy Lett.* **2018**, *3*, 373.
[195] L. Jiang, Y. Lu, C. Zhao, L. Liu, J. Zhang, Q. Zhang, X. Shen, J. Zhao, X. Yu, H. Li, X. Huang, L. Chen, Y.-S. Hu, *Nat. Energy* **2019**, *4*, 495.
[196] G. Zhu, K. Wen, W. Lv, X. Zhou, Y. Liang, F. Yang, Z. Chen, M. Zou, J. Li, Y. Zhang, W. He, *J. Power Sources* **2015**, *300*, 29.
[197] Q. Nian, J. Wang, S. Liu, T. Sun, S. Zheng, Y. Zhang, Z. Tao, J. Chen, *Angew. Chem., Int. Ed.* **2019**, *58*, 16994.
[198] J. Chen, J. Vatamanu, L. Xing, O. Borodin, H. Chen, X. Guan, X. Liu, K. Xu, W. Li, *Adv. Energy Mater.* **2020**, *10*, 1902654.
[199] N. Chang, T. Li, R. Li, S. Wang, Y. Yin, H. Zhang, X. Li, *Energy Environ. Sci.* **2020**, *13*, 3527.
[200] Q. Zhang, Y. Ma, Y. Lu, L. Li, F. Wan, K. Zhang, J. Chen, *Nat. Commun.* **2020**, *11*, 4463.
[201] F. Yue, Z. Tie, S. Deng, S. Wang, M. Yang, Z. Niu, *Angew. Chem., Int. Ed.* **2021**, *60*, 13882.
[202] H. Jiang, W. Shin, L. Ma, J. J. Hong, Z. Wei, Y. Liu, S. Zhang, X. Wu, Y. Xu, Q. Guo, M. A. Subramanian, W. F. Stickle, T. Wu, J. Lu, X. Ji, *Adv. Energy Mater.* **2020**, *10*, 2000968.
[203] C. Strietzel, M. Sterby, H. Huang, M. Strømme, R. Emanuelsson, M. Sjödin, *Angew. Chem., Int. Ed.* **2020**, *59*, 9631.
[204] Z. Guo, J. Huang, X. Dong, Y. Xia, L. Yan, Z. Wang, Y. Wang, *Nat. Commun.* **2020**, *11*, 959.
[205] F. Mo, G. Liang, D. Wang, Z. Tang, H. Li, C. Zhi, *EcoMat* **2019**, *1*, e12008.
[206] Y. Zhao, L. Ma, Y. Zhu, P. Qin, H. Li, F. Mo, D. Wang, G. Liang, Q. Yang, W. Liu, C. Zhi, *ACS Nano* **2019**, *13*, 7270.
[207] Y. Li, J. Fu, C. Zhong, T. Wu, Z. Chen, W. Hu, K. Amine, J. Lu, *Adv. Energy Mater.* **2019**, *9*, 1802605.
[208] Z. Chen, P. C. Hsu, J. Lopez, Y. Li, J. W. F. To, N. Liu, C. Wang, S. C. Andrews, J. Liu, Y. Cui, Z. Bao, *Nat. Energy* **2016**, *1*, 15009.
[209] J. Zhu, M. Yao, S. Huang, J. Tian, Z. Niu, *Angew. Chem., Int. Ed.* **2020**, *59*, 16480.
[210] P. Yang, C. Feng, Y. Liu, T. Cheng, X. Yang, H. Liu, K. Liu, H. J. Fan, *Adv. Energy Mater.* **2020**, *10*, 2002898.
[211] B. D. Boruah, A. Mathieson, S. K. Park, X. Zhang, B. Wen, L. Tan, A. Boies, M. D. Volder, *Adv. Energy Mater.* **2021**, *11*, 2100115.
[212] Z. Fang, Y. Zhang, X. Hu, X. Fu, L. Dai, D. Yu, *Angew. Chem., Int. Ed.* **2019**, *58*, 9248.
[213] B. D. Boruah, A. Mathieson, B. Wen, S. Feldmann, W. M. Dose, M. D. Volder, *Energy Environ. Sci.* **2020**, *13*, 2414.
[214] S. Ahmad, C. George, D. J. Beesley, J. J. Baumberg, M. D. Volder, *Nano Lett.* **2018**, *18*, 1856.
[215] A. Paolella, C. Faure, G. Bertoni, S. Marras, A. Guerfi, A. Darwiche, P. Hovington, B. Commarieu, Z. Wang, M. Prato, M. Colombo, S. Monaco, W. Zhu, Z. Feng, A. Vijh, C. George, G. P. Demopoulos, M. Armand, K. Zaghib, *Nat. Commun.* **2017**, *8*, 14643.

[216] Y. Zhang, F. Wan, S. Huang, S. Wang, Z. Niu, J. Chen, *Nat. Commun.* **2020**, *11*, 2199.
[217] L. Wang, K.-W. Huang, J. Chen, J. Zheng, *Sci. Adv.* **2019**, *5*, eaax4279.
[218] Y. Liu, Q. Li, K. Ma, G. Yang, C. Wang, *ACS Nano* **2019**, *13*, 12081.
[219] K. Zhu, T. Wu, K. Huang, *Adv. Energy Mater.* **2019**, *9*, 1901968.
[220] M. Liao, J. Wang, L. Ye, H. Sun, P. Li, C. Wang, C. Tang, X. Cheng, B. Wang, H. Peng, *J. Mater. Chem. A* **2021**, *9*, 6811.
[221] X. Xie, Z. Fang, M. Yang, F. Zhu, D. Yu, *Adv. Funct. Mater.* **2021**, *31*, 2007942.
[222] H. Sun, X. You, J. Deng, X. L. Chen, Z. B. Yang, P. N. Chen, X. Fang, H. S. Peng, *Angew. Chem., Int. Ed.* **2014**, *53*, 6664.
[223] M. Chen, Y. Yang, D. Chen, H. Wang, *Chin. Chem. Lett.* **2018**, *29*, 564.
[224] Z. T. Zhang, X. L. Chen, P. N. Chen, G. Z. Guan, L. B. Qiu, H. J. Lin, Z. B. Yang, W. Y. Bai, Y. F. Luo, H. S. Peng, *Adv. Mater.* **2014**, *26*, 466.
[225] N. A. Kyeremateng, T. Brousse, D. Pech, *Nat. Nanotechnol.* **2017**, *12*, 7.
[226] J. Chmiola, C. Largeot, P. L. Taberna, P. Simon, Y. Gogotsi, *Science* **2010**, *328*, 480.
[227] H. Y. Shi, Y. J. Ye, K. Liu, Y. Song, X. Sun, *Angew. Chem., Int. Ed.* **2018**, *130*, 16597.
[228] T. Barman, A. R. Pal, *ACS Appl. Mater. Interfaces* **2015**, *7*, 2166.
[229] S. Bi, F. Wan, S. Huang, X. Wang, Z. Niu, *ChemElectroChem* **2019**, *6*, 3933.
[230] H. Jung, Y.-U. Kim, M.-S. Sung, Y. Hwa, G. Jeong, G.-B. Kim, H.-J. Sohn, *J. Mater. Chem.* **2011**, *21*, 11213.
[231] Z. Wang, Z. Ruan, Z. Liu, Y. Wang, Z. Tang, H. Li, M. Zhu, T. F. Hung, J. Liu, Z. Shi, C. Zhi, *J. Mater. Chem. A* **2018**, *6*, 8549.
[232] M. Zhu, Z. Wang, H. Li, Y. Xiong, Z. Liu, Z. Tang, Y. Huang, A. L. Rogach, C. Zhi, *Energy Environ. Sci.* **2018**, *11*, 2414.
[233] S. Yun, Y. Qin, A. R. Uhl, N. Vlachopoulos, M. Yin, D. Li, X. Han, A. Hagfeldt, *Energy Environ. Sci.* **2018**, *11*, 476.
[234] Y. Song, N. Wang, Y. Wang, R. Zhang, H. Olin, Y. Yang, *Adv. Energy Mater.* **2020**, *10*, 2002756.
[235] B. Poudel, Q. Hao, Y. Ma, Y. Lan, A. Minnich, B. Yu, X. Yan, D. Wang, A. Muto, D. Vashaee, X. Chen, J. Liu, M. S. Dresselhaus, G. Chen, Z. Ren, *Science* **2008**, *320*, 634.
[236] A. Hagfeldt, G. Boschloo, L. Sun, L. Kloo, H. Pettersson, *Chem. Rev.* **2010**, *110*, 6595.
[237] Z. S. Chai, N. N. Zhang, P. Sun, Y. Huang, C. X. Zhao, H. J. Fan, X. Fan, W. J. Mai, *ACS Nano* **2016**, *10*, 9201.
[238] M. Yao, Z. Yuan, S. Li, T. He, R. Wang, M. Yuan, Z. Niu, *Adv. Mater.* **2021**, *33*, 2008140.
[239] N. Zhang, F. Huang, S. Zhao, X. Lv, Y. Zhou, S. Xiang, S. Xu, Y. Li, G. Chen, C. Tao, Y. Nie, J. Chen, X. Fan, *Matter* **2020**, *2*, 1260.
[240] Z. L. Wang, J. H. Song, *Science* **2006**, *312*, 242.
[241] X. Wang, J. Song, J. Liu, Z. L. Wang, *Science* **2007**, *316*, 102.
[242] Y.-F. Lin, J. Song, Y. Ding, S.-Y. Lu, Z. L. Wang, *Adv. Mater.* **2008**, *20*, 3127.
[243] M.-P. Lu, J. Song, M.-Y. Lu, M.-T. Chen, Y. Gao, L.-J. Chen, Z. L. Wang, *Nano Lett.* **2009**, *9*, 1223.
[244] F.-R. Fan, Z.-Q. Tian, Z. L. Wang, *Nano Energy* **2012**, *1*, 328.
[245] C. Yan, Y. Gao, S. Zhao, S. Zhang, Y. Zhou, W. Deng, Z. Li, G. Jiang, L. Jin, G. Tian, T. Yang, X. Chu, D. Xiong, Z. Wang, Y. Li, W. Yang, J. Chen, *Nano Energy* **2020**, *67*, 104235.
[246] F. Hu, Q. Cai, F. Liao, M. Shao, S.-T. Lee, *Small* **2015**, *11*, 5611.
[247] Z. Wang, Z. Ruan, W. S. Ng, H. Li, Z. Tang, Z. Liu, Y. Wang, H. Hu, C. Zhi, *Small Methods* **2018**, *2*, 1800150.
[248] J. Chen, Y. Huang, N. Zhang, H. Zou, R. Liu, C. Tao, X. Fan, Z. L. Wang, *Nat. Energy* **2016**, 16138.
[249] B. He, Q. Zhang, L. Li, J. Sun, P. Man, Z. Zhou, Q. Li, J. Guo, L. Xie, C. Li, X. Wang, J. Zhao, T. Zhang, Y. Yao, *J. Mater. Chem. A* **2018**, *6*, 14594.
[250] C. Kim, B. Y. Ahn, T.-S. Wei, Y. Jo, S. Jeong, Y. Choi, I.-D. Kim, J. A. Lewis, *ACS Nano* **2018**, *12*, 11838.
[251] X. Wang, B. Liu, R. Liu, Q. Wang, X. Hou, D. Chen, R. Wang, G. Shen, *Angew. Chem., Int. Ed.* **2014**, *126*, 1880.
[252] Y. Fu, H. Wu, S. Ye, X. Cai, X. Yu, S. Hou, H. Kafafy, D. Zou, *Energy Environ. Sci.* **2013**, *6*, 805.
[253] K. Dong, Y. C. Wang, J. Deng, Y. Dai, S. L. Zhang, H. Zou, B. Gu, B. Sun, Z. L. Wang, *ACS Nano* **2017**, *11*, 9490.
[254] Z. Wen, M. H. Yeh, H. Guo, J. Wang, Y. Zi, W. Xu, J. Deng, L. Zhu, X. Wang, C. Hu, L. Zhu, X. Sun, Z. L. Wang, *Sci. Adv.* **2016**, *2*, e1600097.
[255] Q. Zhang, L. Li, H. Li, L. Tang, B. He, C. Li, Z. Pan, Z. Zhou, Q. Lia, J. Sun, L. Wei, X. Fan, T. Zhang, Y. Yao, *Nano Energy* **2019**, *60*, 267.
[256] X. Xu, X. Zhou, T. Wang, X. Shi, Y. Liu, Y. Zuo, L. Xu, M. Wang, X. Hu, X. Yang, J. Chen, X. Yang, L. Chen, P. Chen, H. Peng, *Angew. Chem., Int. Ed.* **2020**, *59*, 12762.
[257] X. Shi, Y. Zuo, P. Zhai, J. Shen, Y. Yang, Z. Gao, M. Liao, J. Wu, J. Wang, X. Xu, Q. Tong, B. Zhang, B. Wang, X. Sun, L. Zhang, Q. Pei, D. Jin, P. Chen, H. Peng, *Nature* **2021**, *591*, 240.
[258] L. Zhang, X.-L. Shi, Y.-L. Yang, Z.-G. Chen, *Mater. Today* **2021**, *46*, 62.
[259] X.-L. Shi, J. Zou, Z.-G. Chen, *Chem. Rev.* **2020**, *120*, 7399.
[260] T. Mei, C. Wang, M. Liao, J. Li, L. Wang, C. Tang, X. Sun, B. Wang, H. Peng, *J. Mater. Chem. A* **2021**, *9*, 10104.
[261] K. Liu, Y. Tian, L. Jiang, *Prog. Mater. Sci.* **2013**, *58*, 503.
[262] M. Liu, S. Wang, L. Jiang, *Nat. Rev. Mater.* **2017**, *2*, 17036.
[263] R. Hu, N. L. C. Leung, B. Z. Tang, *Chem. Soc. Rev.* **2014**, *43*, 4494.
[264] J. Li, J. Wang, H. Li, N. Song, D. Wang, B. Z. Tang, *Chem. Soc. Rev.* **2020**, *49*, 1144.
[265] Y. Xie, Y. Liu, Y. Zhao, Y. H. Tsang, S. P. Lau, H. Huang, Y. Chai, *J. Mater. Chem. A* **2014**, *2*, 9142.
[266] H. Li, T. Lv, H. Sun, G. Qian, N. Li, Y. Yao, T. Chen, *Nat. Commun.* **2019**, *10*, 536.
[267] D. Chen, Q. Pei, *Chem. Rev.* **2017**, *117*, 11239.
[268] W. A. D. M. Jayathilaka, K. Qi, Y. Qin, A. Chinnappan, W. Serrano-García, C. Baskar, H. Wang, J. He, S. Cui, S. W. Thomas, S. Ramakrishna, *Adv. Mater.* **2019**, *31*, 1805921.
[269] Y. Zhang, J. Ding, B. Qi, W. Tao, J. Wang, C. Zhao, H. Peng, J. Shi, *Adv. Funct. Mater.* **2019**, *29*, 1902834.
[270] J. Chen, D. H. C. Chua, P. S. Lee, *Small Methods* **2020**, *4*, 1900648.
[271] J. Pu, C. Zhong, J. Liu, Z. Wang, D. Chao, *Energy Environ. Sci.* **2021**, *14*, 3872.
[272] L. Zhang, Y. Hou, *Adv. Energy Mater.* **2021**, *11*, 2003823.
[273] P. Tan, W. Kong, Z. Shao, M. Liu, M. Ni, *Prog. Energy Combust. Sci.* **2017**, *62*, 155.
[274] Z. M. Lin, J. Yang, X. S. Li, Y. F. Wu, W. Wei, J. Liu, J. Chen, J. Yang, *Adv. Funct. Mater.* **2018**, *28*, 1704112.
[275] T. L. Andrew, L. Zhang, N. Cheng, M. Baima, J. J. Kim, L. Allison, S. Hoxie, *Acc. Chem. Res.* **2018**, *51*, 850.
[276] G. Chen, Y. Li, M. Bick, J. Chen, *Chem. Rev.* **2020**, *120*, 3668.
[277] J. Shi, S. Liu, L. Zhang, B. Yang, L. Shu, Y. Yang, M. Ren, Y. Wang, J. Chen, W. Chen, Y. Chai, X. Tao, *Adv. Mater.* **2020**, *32*, 1901958.
[278] W. Ma, Y. Zhang, S. Pan, Y. Cheng, Z. Shao, H. Xiang, G. Chen, L. Zhu, W. Weng, H. Bai, M. Zhu, *Chem. Soc. Rev.* **2021**, *50*, 7009.
[279] R. Arshad, S. Zahoor, M. A. Shah, A. Wahid, H. Yu, *IEEE Access* **2017**, *5*, 15667.
[280] V. Ilderem, *Nat. Electron.* **2020**, *3*, 5.

Lei Li received his Ph.D. degree under the supervision of Prof. Mei-Jin Lin in organic chemistry from Fuzhou University in 2019. Nowadays, he works as a post-doctoral fellow in the research group of Prof. Li-Tao Sun at Southeast University. His research focuses on the organic functional materials for energy storage devices, mainly including non-aqueous and aqueous rechargeable batteries.

Qichong Zhang received his Ph.D. degree in condensed matter physics from Tongji University in 2017. He was a research fellow with the School of Electrical and Electronic Engineering, Nanyang Technological University, Singapore, from 2018 to 2021. He is currently a full professor with Key Laboratory of Multifunctional Nanomaterials and Smart Systems, Suzhou Institute of Nano-Tech and Nano-Bionics, Chinese Academy of Sciences. His main research interests focus on electrochemical nanomaterials and fiber-shaped functional device design.

Lei Wei received his B.E. degree in electrical engineering from Wuhan University of Technology in 2005 and his Ph.D. degree in photonics engineering from the Technical University of Denmark in 2010. Then, he joined the Research Laboratory of Electronics at the Massachusetts Institute of Technology as a postdoctoral associate. In September 2014, he joined the School of Electrical and Electronic Engineering at Nanyang Technological University in Singapore as a Nanyang assistant professor. In August 2019, he was promoted to associate professor. His main research interests are fiber-based optoelectronic devices, novel multi-functional fiber structures, and in-fiber energy generation and storage.